THERMAL EFFECTS IN STELLAR PULSATIONS

By

WILLIAM DEAN PESNELL

A DISSERTATION PRESENTED TO THE GRADUATE SCHOOL
OF THE UNIVERSITY OF FLORIDA
IN PARTIAL FULFILLMENT OF THE REQUIREMENTS
FOR THE DEGREE OF DOCTOR OF PHILOSOPHY

UNIVERSITY OF FLORIDA

1983

ACKNOWLEDGEMENTS

I would like to thank Dr. J. Robert Buchler for his assistance during the past four years as well as his great patience. In addition, I would like to thank A. N. Cox for insight into the physical nature of stellar pulsations and Dr. Oded Regev for useful suggestions and discussions.

Several other people have assisted in parts of the work. They include Dr. Robert Coldwell, who assisted in the writing of the programs that are included and Sharon Bullivant, who demonstrated the use of the word processor. I would also like to thank Marie Jose Goupil for reading the rough drafts of the manuscript.

Some of the computations in this work were performed at the Los Alamos National Laboratory, Los Alamos, New Mexico, while I was a Summer Graduate Research Assistant there in the summer of 1982. The bulk of the computations were done at the University of Florida, primarily under the MUSIC subsystem, for which I am grateful.

TABLE OF CONTENTS

Abstract of Dissertation Presented to the Graduate School
of the University of Florida in Partial Fulfillment of the
Requirements for the Degree of Doctor of Philosophy

THERMAL EFFECTS IN STELLAR PULSATIONS

By

WILLIAM DEAN PESNELL

AUGUST 1983

Chairman: Dr. Jean Robert Buchler
Major Department: Physics

A Sturm-Liouville operator, embedded in the linearized radial pulsation equations, is used to analyze the thermal effects of stellar pulsations. Asymptotic expansions are utilized to demonstrate the nature of these eigenfunctions and to define the thermal response time of a stellar model. The eigenvalues and eigenvectors for models of a Cepheid and Beta Cephei variable are given showing the differences in the two classes of variables. The time scales introduced agree with earlier ones in their common use of predicting the location of possible driving zones. In addition, a way of displaying the temperature variations in the hydrogen ionization zone without the customary "spike" is demonstrated, and a new class of pulsations, called "sudden" modes, is introduced.

CHAPTER I

INTRODUCTION

The use of time scales to interpret phenomena found in stars has been a favorite tool in astrophysics, (see Cox and Giuli 1968; Saio and Wheeler 1982; and Shibahashi and Osaki 1981). Primarily, they are used to simplify the governing equations by ignoring time dependences that are much longer or averaging those that are much shorter than the subject under study. Examples of this include the suppression of hydrodynamic and possibly thermal phenomena when examining nuclear evolution (Iben 1965), nuclear evolution effects in stellar pulsations (Christy 1966), and hydrodynamic phenomena when studying thermal flashes (Henyey and Ulrich 1972). These time scales arise by recasting the various relationships into non-dimensional forms and defining the factors multiplying the time derivatives as position dependent time scales. This produces a good approximation for the discussion of some attributes of pulsations.

However, we have been using asymptotic formulations to study stellar pulsations (Buchler 1978), and when we attempted to include the outer layers (Buchler and Regev 1982a), it was found necessary to understand the thermal structure in a more quantitative way. Other authors have found modes that are dominated by thermal effects (Wood

1976; King 1980; and Saio and Wheeler 1982) which have been called "strange modes." In this work, a mathematical formalism for studying modes with these characteristics is given.

We shall clarify what the thermal response of a star is and show effects in pulsations that result. A Sturm-Liouville operator, embedded in the linear, non-adiabatic radial pulsation equations, is used to give what will be called the thermal eigenfunctions of a star. It will be shown that under physically realistic assumptions, the eigenvalues are real and represent decays back to the initial state, here assumed to be one of thermal equilibrium.

Asymptotic forms for the eigenvalues and eigenfunctions are shown, and several realistic models have their spectra calculated. A discussion of the physical requirements for the quasi-adiabatic approximation for the stability coefficient is given, along with a way of evaluating it without the introduction of cutoffs in the integration variable. The lowest order pulsation operator is shown to have a more complicated structure than the simple adiabatic operator, when the outer layers are included. This operator, and the accompanying stability coefficient, are derived for a general star and compared to earlier work. A new class of modes, dominated by thermal effects, is shown to exist.

CHAPTER II

BACKGROUND

The theoretical study of stellar pulsations can be divided into several general areas. First is the adiabatic wave equation and the discovery that the periods predicted by this theory agree with observations (Ledoux and Walraven 1958; Cox, J.P. 1980). Here the entire star is assumed to react faster via an acoustic process than thermally, implying that stellar pulsations are basically sound waves propagating in the envelope. In much of a star's mass, adiabaticity is a very good assumption and the periods calculated will be correct as long as this is true. The stability analysis of an adiabatic mode uses the quasi-adiabatic approximation (Ledoux and Walraven 1958; Ledoux 1965), although the integrals must have a cutoff introduced to prevent the outer layers from dominating the result. These calculations demonstrate that the quasi-adiabatic interior would damp any oscillations unless an active source of driving was present. Several authors (Cox 1960 and 1958; Zhevakin 1963 and his earlier papers) showed that the thermodynamic work derivable from the ionization of once ionized helium could provide the necessary driving for the classical Cepheid variables. This driving mechanism requires that some of the star be non-adiabatic and a finely tuned relationship between the location in the star of the

ionization zone and the transition from adiabatic to non-adiabatic behavior be satisfied. Predictions of this theory are narrow instability strips in the H-R diagram (Cox, J.P. 1980), with sharply defined blue edges where the evolving star first becomes unstable.

Other classes of stars are driven by similar mechanisms. Both radial and non-radial oscillations in the ZZ Ceti variables are driven by hydrogen ionization (Starrfield et al. 1982; Winget, Saio and Robinson 1982). Hot white dwarfs, in particular PG1159-035, have been shown to be unstable to radial pulsations in Starrfield, Cox and Hodson (1980), and this analysis has been extended in Starrfield et al. (1983), to include non-radial motion and to show the driving is due to the ionization of carbon and oxygen. Variables such as the RR Lyrae, BL Herculae, δ Scuti and W Virginis classes, are driven primarily by helium ionization although hydrogen does participate in the destabilization (Cox, J.P. 1980).

Once the destabilizing mechanism was known, computer codes were developed that followed the nonlinear behavior of pulsating stars (Christy 1964; King et al. 1964), and reproduced many observed features of the Cepheid and RR Lyrae variables. Details such as the asymmetry of the light and velocity curves and the phase shift of the luminosity maximum with respect to the radius minimum were explained using large (and expensive) codes. A number of new problems arose from this work, two major ones being the mass discrepancy in Cepheids (Cox, A. N. 1980a) and the lack of driving in Beta Cephei variables (Osaki 1982; Lesh and Aizenman 1978). In the attempt to understand these difficulties, fully non-adiabatic, but linear, stability analyses were developed (Baker and

Kippenhahn 1962; Castor 1971; and Saio, Winget, and Robinson 1983). These analyses have the advantages of being much easier to use and less expensive than the nonlinear codes. They are easily modified to include more physics, such as convection (see, for example, Baker and Gough 1979).

The linear analysis shows only whether a given model is self-exciting or damping. An unstable model in the linear regime is a candidate for further study in a hydrodynamic code. However, the use of the linear, non-adiabatic eigenvectors in a perturbation expansion is limited due to their non-periodic nature. To understand how non-linearities affect an oscillation, without using a hydrodynamic computer code, a purely real spectrum of eigenvalues is required in first order. The adiabatic eigenfrequencies satisfy this requirement, but treat the outer layers in an extremely poor fashion.

As the bulk of the star is quasi-adiabatic, Buchler (1978) developed a formalism using two-time asymptotic techniques modeled after Cole (1968) and Kuzmak (1959). This method links the linear analysis with the nonlinear calculations by providing a consistent expansion in powers of the amplitude (Buchler and Perdang 1979). The requirement of periodicity is inherent in an expansion of this type, but the payoff is the capability to study a pulsation amplitude as it starts at an initial value and evolves to a final state. Additional problems that can be studied include modal selection, mode switching, and the feedback of the pulsation on the thermal evolution of the star, all of which are open questions in this field (Regev and Buchler 1981; Simon, Cox and Hodson 1980).

In the simplest version of the theory, the quasi-adiabatic results are recovered in the zero amplitude limit, but at the cost of introducing a cutoff in the integrals. When this was done, it became obvious that these layers were being incorrectly treated and that a more reliable method needed to be developed. A straightforward way of including these layers was presented in Buchler and Regev (1982a), where the structure of the eigenvectors was determined by the condition of constant luminosity above the cutoff point in the model. While giving good results for stars of the Beta Cephei class (Pesnell, Regev and Buchler 1982), cooler stars, like Cepheids, were not treated much better than with the simpler adiabatic approximation. The present work was undertaken to quantify the thermal behavior of pulsations. The results presented are encouraging and explain or clarify several phenomena found in stellar pulsations.

CHAPTER III

THEORY

The structure and evolution of stars is governed by a set of four equations: the conservation of momentum, energy, and mass, and a flux equation. Other relationships are constituitive, such as the equation of state, opacity (see Appendix A), and nuclear energy generation rates. Written in a Lagrangian form which uses the interior mass as the independent variable, these equations are (see Clayton 1968, ch. 6; Appendix B below)

$$\frac{\partial r^3}{\partial m} = 4\pi\rho \tag{3-1}$$

$$\frac{d^2 r}{d t^2} = -\frac{Gm}{r^2} - 4\pi r^2 \frac{\partial P}{\partial m} \equiv g(r,S) \tag{3-2}$$

$$T \frac{d S}{d t} = q(\rho,T) - \frac{\partial L}{\partial m} \equiv T\, k(r,S) \tag{3-3}$$

$$L(m) = -(4\pi r^2)^2 \frac{ac}{3\kappa} \frac{\partial T^4}{\partial m} \tag{3-4}$$

The symbols are defined here to be

m = mass beneath the point of interest

r = radius from the center of the star to this point

ρ = density

T = temperature

P = pressure, $P = P(\rho,T)$

S = entropy, $S = S(\rho,T)$

L = luminous flux

κ = opacity, $\kappa = \kappa(\rho,T)$

q = nuclear energy generation rate, $q = q(\rho,T)$.

We have assumed radiative heat transfer in the diffusion approximation and that all constitutive quantities are given by analytic expressions.

To study this system, the equations are solved with all time derivatives set to zero to find an initial model in hydrostatic and thermal equilibrium. The equations are then linearized in r and S and combined to give two operator equations with two unknowns, δr and δS. Written in operator form these are

$$\frac{d^2\delta r}{dt^2} = \left(\frac{\partial g}{\partial r}\right)_S \cdot \delta r + \left(\frac{\partial g}{\partial S}\right)_r \cdot \delta S \equiv - A\cdot\delta r - B\cdot\delta S \qquad (3\text{-}5)$$

$$\frac{d\,\delta S}{dt} = \left(\frac{\partial k}{\partial r}\right)_S \cdot \delta r + \left(\frac{\partial k}{\partial S}\right)_r \cdot \delta S \equiv C\cdot\delta r + D\cdot\delta S. \qquad (3\text{-}6)$$

It is well known that, with the appropriate boundary conditions, the A operator is of the Sturm-Liouville class and yields a symmetric matrix operator (Castor 1971; Buchler and Regev 1982b).

The operator A is the adiabatic pulsation operator ($\delta S=0$) which can be written as (see Cox, J. P. 1980)

$$\frac{d}{dr}\left\{\Gamma_1 P\rho r^4\left[\frac{d}{dr}\frac{\delta r}{r}\right]\right\} + \left\{r^3\frac{d}{dr}\left[(3\Gamma_1-4)P\right] - \rho r^4\frac{d^2}{dt^2}\right\}\frac{\delta r}{r} = 0$$

and in the Schrodinger form of this equation (Morse and Feshbach 1953, ch. 6), the new independent variable has the dimensions of time and represents the acoustic travel time from a point in the star to the surface and is given by

$$t_{acous}(r) = \int_r^{R_*} dr\left[\frac{\Gamma_1(r)\ P(r)}{\rho(r)}\right]^{1/2} = \int_r^{R_*} dr/c(r) \quad (3\text{-}7)$$

where $c(r)$ is the local adiabatic sound speed and R_* is the equilibrium radius of the star. The fundamental radial pulsation period is roughly given by $t_{acous}(R_{core})$, the sound travel time from the core to the surface. As the acoustic time corresponds to the time for a dynamic response to occur, $t_{acous}(r)$ can be identfied as the dynamic time scale as a function of position in a star.

The nice properties of A come from the fact that it is of second order in the spatial derivatives (the time dependence is assumed to be $\exp(\ i\omega t\ )$). Looking at the D operator, the same second order derivatives are present. We now show that there is a representation where D has the same properties as A, and a natural definition of the thermal time scale will result.

CHAPTER IV

THE THERMAL OPERATOR

For an optically thick medium, the thermal operator D can be written in a continuum form as

$$T \frac{d\ \delta S}{d\ t} = q(\rho_{eq}, T_{eq})\ q_T \frac{\delta S}{C_v} - \frac{d}{d\ m}\left[L_{eq}(m)(4 - \kappa_T) \frac{\delta S}{C_v} + L_{eq}(m)\left(\frac{d\ lnT}{d\ m}\right)^{-1} \frac{d\ \delta S/C_v}{d\ m}\right]. \tag{4-1}$$

Here $q_T = \left(\frac{\partial \ln q}{\partial \ln T}\right)_\rho$, $\frac{d\ L_{eq}}{d\ m} = q(\rho_{eq}, T_{eq})$, i.e. an initial model in thermal balance, $\kappa_T = \left(\frac{\partial \ln \kappa}{\partial \ln T}\right)_\rho$, $C_v = \left(\frac{\partial\ U}{\partial\ T}\right)_\rho$, and all derivatives are evaluated at the equilibrium densities and temperature. This form for D has been linearized at constant density (radius) and is strictly valid at points deep in the star so that $\tau \gg 1$.

We assume a time dependence of the form $\exp(-\sigma t)$, and note that the operator is of second order in the spatial derivative. Therefore, an integrating factor, μ, exists that transforms D into a self-adjoint operator. This factor can be written as

$$\mu(m) = e^{\int_{m_0}^{m} (4 - \kappa_T) \frac{d\ lnT}{d\ m}\, dm} \tag{4-2}$$

where m_0 is a reference mass, here chosen to be m_{core}, the mass of the

core where nuclear burning occurs. Defining a new eigenvector as $\xi = \delta S/C_v$ and $\lambda = \frac{d \ln L_{eq}}{d m}$, equation 4-1 becomes

$$\frac{\mu T}{L_{eq}} C_v \sigma \xi = \left[\lambda(4 - \kappa_T - q_T) - \frac{d \kappa_T}{d m}\right]\xi + \frac{d}{d m}\left[\mu\left(\frac{d \ln T}{d m}\right)^{-1}\frac{d \xi}{d m}\right] \tag{4-3}$$

Appropriate boundary conditions (which make 4-3 self-adjoint) are

$$\frac{d \delta L/L}{d m} \equiv a\, \xi(m_*) + b \frac{d\xi}{dm}(m_*) = 0 \tag{4-4a}$$

and

$$\xi(m_0) = 0. \tag{4-4b}$$

The surface boundary condition (4-4a) is equivalent to the assumption that at the surface there is no radiation incident from the outside (Castor 1971). In this form, 4-4a shows that the thermal readjustment time of the outer surface is infinitely short. As the weight function on the left-hand side is positive definite, and the function multiplying the derivative on the right-hand side is negative definite, 4-4 is of the Sturm-Liouville class of operators (Boyce and DiPrima 1969, ch. 11). Comparing 4-3 to the standard Sturm-Liouville equation, since $-\mu\left(\frac{d \ln T}{d m}\right)^{-1} > 0$ and $\mu T C_v/L_{eq} > 0$, all eigenvalues are real and positive. With each eigenvalue σ_n is associated an eigenvector ξ_n whose number of nodes corresponds to the numeric position of the $\{\sigma_n\}$ in an increasing ordering of the eigenvalues starting with σ_0. In addition,

the eigenvectors are non-degenerate, orthogonal with respect to the weight function $\mu C_v T / L_{eq}$, and can be normalized so that (m_* is the total mass of the star)

$$\int_0^{m_*} \mu\, T\, C_v\, \xi_i\, \xi_j \frac{dm}{L_{eq}} = \delta_{ij}.$$

Due to their Sturm-Liouville character, these eigenvectors form a complete set for describing the δS readjustment in a star. In combination with the adiabatic radial wave functions (Cox, J. P. 1980), a complete set for describing spherically symmetric disturbances of a star is found, provided that equations 3-1 through 3-4 are always valid.

To understand the structure of the eigenvectors, the approximation of neglecting nuclear burning can be made. This reduces the equation to a version suitable for discussing thermal effects in a stellar envelope. Without nuclear burning the initial luminosity is constant and the analysis is halted at a mass (m_{core}) outside the region where this assumption is not valid. As the structure of the ξ_n's will show, this is equivalent to assuming we are looking at "short" thermal time scales that do not probe the core. Radial stellar pulsations are an envelope phenomenon, so this assumption is justified.

Neglecting nuclear burning and defining L_* to be the static luminosity entering the envelope from below, equation 4-3 becomes

$$\sigma \frac{\mu\, T}{L_*} C_v \xi_n = -\mu \frac{d\, \kappa_T}{d\, m} \xi_n + \frac{d}{d\, m}\left[\mu \left(\frac{d\, \ln T}{d\, m}\right)^{-1} \frac{d\, \xi_n}{d\, m}\right]. \qquad (4\text{-}5)$$

Following Ledoux and Pekeris (1941), we multiply eq. 4-5 by ξ_n and

integrate over the interval $m_0 = m_{core} \leq m \leq m_*$. A self-adjoint system satisfies a minimum principle and any well behaved eigenvector can be used to estimate the lowest eigenvalue, σ_0. Choosing $\xi_0(m) = 1$ for all m, this estimate is

$$\sigma_0 = - L_* \frac{\int_{m_0}^{m_*} \mu(m) \frac{d \kappa_T}{d m} dm}{\int_{m_0}^{m_*} \mu T C_v dm} \equiv - L_* \frac{\int_{m_0}^{m_*} \mu \frac{d \kappa_T}{d m} dm}{\langle U \rangle} . \qquad (4\text{-}6)$$

If the thermal time is defined as the reciprocal of σ_0, this gives the overall thermal time of the envelope as

$$t_{th} = - \frac{\langle U \rangle}{L_* \int_{m_0}^{m_*} \mu \frac{d \kappa_T}{d m} dm} . \qquad (4\text{-}7)$$

There is an apparent mathematical inconsistency with this expression. When the opacity derivative, κ_T, is constant in the envelope, the thermal time is undefined. However, comparing 4-6 to the expression for the adiabatic radial pulsation fundamental frequency (Ledoux 1965),

$$\omega_0 = \frac{\int_0^{m_*} 4\pi r^2 \frac{d}{d m} \left[(3 \Gamma_1 - 4) P \right] dm}{\int_0^{m_*} r^2 dm}$$

they have the same form only if $\frac{d P}{d m} = 0$, so that the formula for t_{th} is incomplete. If $\frac{d P}{d m} = 0$ and $\frac{d \Gamma_1}{d m} = 0$, then $\omega_0 = 0$, but the variations of P are large in a star, varying many orders of magnitude, while Γ_1 can vary only from 1 to 5/3 and the neglect of the pressure

derivative would not be correct. The inclusion of nuclear burning in 4-7 remedies this situation and the net thermal time for the star is then

$$t_{th,nuc} = \frac{\langle U \rangle}{L_* \int_0^{m_*} \mu \left[\lambda(4 - \kappa_T - q_T) - \frac{d\,\kappa_T}{d\,m} \right] dm} \qquad (4\text{-}7')$$

which allows for the luminosity variations and shows that the apparent infinite value of t_{th} from 4-7 when κ_T is constant in the star is not real. The term allowing for nuclear burning will always give a finite value for $t_{th,nuc}$. When κ_T is constant in the envelope, the assumed form of ξ is a poor approximation and gives an unrealistic result. The positivity of $t_{th,nuc}$ is difficult to guarantee, but a simple case would require that $4 - \kappa_T - q_T > 0$, $\frac{d\,\ln L}{d\,m} > 0$, and $\frac{d\,\kappa_T}{d\,m} < 0$, all of which can be satisfied in most of a star's mass, although in some nuclear burning regions, q_T can be much greater than zero, and the opacity variations are discussed below. The inclusion of nuclear burning as it relates to stability of stellar models is discussed in Hansen (1978) and Gabriel (1972). In this work, this area will not be discussed as the simplifications that result from the neglect of the core make the interpretation of the results easier.

The opacity is of the Kramers' form ($\kappa_T \sim -3.5 < 0$) near the surface but inside the ionization zones. Near the core, electron scattering will dominate, ($\kappa_T \dashrightarrow 0$), so that κ_T decreases going outward in the star. Therefore, except in a small region near the ionization zones, t_{th} will have only positive contributions in the integral. The mass of the ionization zones is small compared to the total mass of a star, so that the negative contributions to the integral

will not cause a negative overall time scale. In addition, each point in the star is weighted by the ratio

$$\mu(m) \sim \left(\frac{T(m)}{T(m_0)}\right)^4 - \kappa_T(m)$$

which gives the interior regions far more importance than the outer layers, further reducing the influence of the negative portions of the integrand. Physically t_{th} represents the time necessary to remove the μ weighted internal energy $\langle U \rangle$ by the radiative luminosity present, allowing for the position (and therefore temperature) dependence of the opacity derivative.

Another thermal time can be found from equation 3-3 as the time necessary to remove the material thermal energy at the static luminosity present in the envelope. Writing this in a integral form (Saio, Winget and Robinson 1983) yields

$$t_{th,p} = \int_{m_0}^{m_*} T\, C_v\, dm/L_*. \qquad (4\text{-}8)$$

Comparing the two definitions, there are several differences. The value $t_{th,p}$ is counting only the thermal energy in the matter that makes up the star. In equation 4-7, the formula emphasizes the radiation ($\mu \sim T^4$) and the method of energy transport, as well as giving the interior stellar regions more weight than the outer layers. These differences are minor and are overshadowed by a major shortcoming of t_{th}. The definition in 4-8 can be generalized to calculate a thermal time as a function of mass by replacing the lower limit in the integral

by the desired mass. Values for $t_{th,p}$ found are always positive and can be interpreted as time scales. However, when the same technique is done with t_{th}, the value returned is not positive definite due to the ionization zones near the surface. Mathematically, this generalization means that $\xi(m') = 1$, $m'>m$ and $\xi(m') = 0$, $m'<m$, a Heaviside step function at m. The derivatives of ξ in 4-5 will yield delta functions at m, adding contributions to t_{th} that are not easily understood. To alleviate these difficulties, t_{th} shall be redefined in terms of the independent variable that results from analyzing eq. 4-3 by standard asymptotic methods.

Asymptotic Expansions

Following the technique outlined in Morse and Feshbach (1953, ch. 6) we make the substitutions:

$$y(x) = \left[-\mu^2 \frac{TC_v}{L_*} \left(\frac{d\ \ln T}{d\ m}\right)^{-1} \right]^{1/4} \xi,$$

$$x = \frac{1}{J} \int_{m_0}^{m} \left[-\frac{TC_v}{L_*} \frac{d\ \ln T}{d\ m} \right]^{1/2} dm\ ,$$

$$J = \int_{m_0}^{m_*} \left[-\frac{TC_v}{L_*} \frac{d\ \ln T}{d\ m} \right]^{1/2} dm\ ,$$

$$k^2 = J^2\sigma\ ,$$

and

$$w(x) = \frac{1}{\left[-\mu^2 \left(\frac{d\ \ln T}{d\ m}\right)^{-1} TC_v\right]^{1/4}} \frac{d^2 \left[-\mu^2 \left(\frac{d\ \ln T}{d\ m}\right)^{-1} TC_v \right]^{1/4}}{d\ x^2} - \frac{J^2}{\pi^2} \frac{L_*}{TC_v} \frac{d\ \kappa_T}{d\ m}\ ;$$

to transform eq. 4-3 to

$$\frac{d^2 y}{d x^2} + (k^2 - w(x)) y = 0. \qquad (4\text{-}9)$$

The units of J are $(\text{time})^{1/2}$, so a natural definition of the overall thermal time of a stellar envelope is

$$t_{th} = J^2. \qquad (4\text{-}10)$$

We note that the integrating factor μ does not appear in this definition. As μ is an artificial quantity introduced for mathematical convenience, this is physically appealing.

From the equilibrium model (B-4 in Appendix B below) there is a relationship between L_* and dlnT/dm. Inserting this into eq. 4-10 gives

$$t_{th} = \left[\int_{m_0}^{m_*} \left(\frac{3 C_v \kappa}{(4\pi r^2)^2 a c T^3} \right)^{1/2} dm \right]^2 \qquad (4\text{-}11a)$$

or, using the continuity equation (3-1), $R_0 = r(m_0)$ and $R_* = r(m_*)$,

$$t_{th} = \left[\int_{R_0}^{R_*} \left(\frac{3 C_v \kappa}{a c T^3} \right)^{1/2} \rho \, dr \right]^2. \qquad (4\text{-}11b)$$

This definition shows the effect of both the internal energy that must be dissipated and the method of dissipation. Rewriting 4-11(b) in a slightly different way

$$t_{th} = \left[\int_{R_0}^{R_*} \left(\frac{3 \kappa T C_v}{c \; aT^4} \right)^{1/2} \rho \, dr \right]^2 \qquad (4\text{-}11c)$$

or, defining $U_{gas} = T\, C_v$,

$$t_{th} = \frac{3}{c}\left[\int_{R_0}^{R_*} (\kappa\rho \frac{U_{gas}}{U_{rad}})^{1/2}\, dr\right]^2 \qquad (4\text{-}12)$$

we have a interesting definition for t_{th}. The photon diffusion length is present ($1/\kappa\rho$), so increasing the optical thickness increases the relaxation time. The 3/c term can be interpreted as the diffusion velocity of the photon; however, this is dicussed below. From the ratio of internal energies, it is seen that in the central regions where this ratio is large, the contributions to t_{th} increase. Near the surface, where the density and opacity approach zero and the temperature becomes constant, the radiation dominates and the integrand becomes small.

If the approximation of a monatomic ideal gas with black body radiation is made, a simple relationship exists for the ratio U_{gas}/U_{rad}. Defining n to be the reciprocal of the mean molecular weight (or the molar density in moles/gr), the pressure of the gas can be written as

$$P = P_{gas} + P_{rad} = nR\rho T + \frac{a}{3} T^4,$$

or, introducing β (Chandrasekhar 1967,ch. 6),

$$P_{gas} = \beta P \text{ and } P_{rad} = (1-\beta)P.$$

The internal energy of the gas can be written as

$$U = U_{gas} + U_{rad} = \frac{3}{2} nRT + aT^4/\rho,$$

so that

$$U_{gas} = \frac{3}{2} P_{gas}/\rho = \frac{3}{2} \beta P/\rho$$

and

$$U_{rad} = 3P_{rad}/\rho = (1-\beta)P/\rho.$$

With these assumptions, the ratio becomes

$$U_{gas}/U_{rad} = 1/2\, \beta/(1 - \beta).$$

This mixture has a thermal time given by

$$t_{th} = \frac{3}{2c} \left\{ \int_0^{R_*} \left[\kappa\rho\, \beta/(1-\beta) \right]^{1/2} dr \right\}^2. \qquad (4\text{-}13)$$

If β is constant in the envelope

$$t_{th} = \frac{3}{2c} \frac{\beta}{1 - \beta} \left[\int_0^{R_*} (\kappa\rho)^{1/2} dr \right]^2. \qquad (4\text{-}14)$$

Here we see that the thermal time is a diffusion length

$$l = \left[\int_{R_0}^{R_*} (\kappa\rho)^{1/2} \, dr \right]^2 \qquad (4\text{-}15)$$

divided by a diffusion velocity

$$v = c \, \frac{2}{3} \, (1 - \beta)/\beta, \qquad (4\text{-}16)$$

where c is the speed of light in vacuo.

The diffusion velocity must be less than c; therefore, the value of β must be greater than 0.4. This formula shows that in stars where β is of order 1, the thermal times are large as it takes a long time for a photon to move through the material. In a star that is radiation dominated, the thermal time is short as the photons can move freely through the envelope. These interpretations are qualitative, depending on the assumed nature of U_{gas}. They are suitable for estimating whether a star undergoes adiabatic pulsations or moves in some way that shows large thermal effects. A star with a very tenuous envelope, and therefore small β, would be expected to show large thermal effects. Stars of this type include the R Corona Borealis class (King 1980; Saio and Wheeler 1982), as well as α Cygnus (Lucy 1976; Pesnell 1981).

Returning to the original form of t_{th}, a position dependent time scale can be defined by replacing the lower limit by the desired radius. The resultant formula represents the thermal travel time from that point to the surface and can be written as

$$t_{th}(r) = \left[\int_{r}^{R_*} \left(\frac{3 \kappa C_v}{a c T^3} \right)^{1/2} \rho \, dr \right]^2. \qquad (4\text{-}17)$$

In figure 4-1, we compare this thermal time with $t_{th,p}$, also generalized to a position dependent form as discussed above (Cox, J.P. 1980; Saio, Winget, and Robinson 1983). The time scales are plotted versus the logarithm of temperature (with the surface of the star at the left of the diagram) for a model of BW Vulpeculae and in figure 4-2, for a generic Cepheid, discussed in chapter 5. Except for the constant separation, it is readily seen that the two functions agree quite well in the interior but diverge from one another at the surface. This effect is a consequence of $t_{th,p}$ containing only the material thermal energy, which for a hot star is quite considerable and the drop to zero at the surface is due only to the integral formulation for $t_{th,p}$. In the equation for t_{th}, the method of energy transport reduces to the grey atmosphere approximation at the surface, and the thermal time must therefore approach zero more smoothly for any class of star.

This disagreement does not change the normal use of the thermal time. Several classes of variable stars are driven by ionization zones, including Cepheids (Cox, J.P. 1980) and ZZ Ceti (Starrfield et al. 1982; Winget, Saio, and Robinson 1982). For this driving mechanism to function, the ionization zone must coincide with the point in the star where the transition from (quasi-)adiabatic (constant entropy) motion to highly non-adiabatic (constant luminosity) motion occurs (Cox and Whitney 1958). This transition zone is found at the radius, R_{tr}, where $t_{th,p}(R_{tr}) \sim \Pi_0$, the thermal time is of the same order as the

period of the pulsation. The expression for t_{th} is derived from a frequency, and the location of this region would be where $\sigma(R_{tr}) = t_{th}(R_{tr})^{-1} \sim \omega_0 = 2\pi/\Pi_0$, which is analagous to critical damping.

The constant separation in the figures is approximately 2π; so both formulations predict the same location for the transition zone, provided this region is below the atmosphere.

Asymptotic Thermal Eigenfunctions

Once the normalized coordinate has been defined, the asymptotic forms for the eigenvalues and eigenfunctions of eq. 4-9 can be calculated. Here, asymptotic implies that $k^2 = J^2 \sigma \gg w(x)$, for all values of x considered. Due to the surface effects, this is not a good assumption, but an important feature in the eigenfunctions can be seen in this approximation; so, it is discussed.

The asymptotic form of eq. 4-9 is the harmonic oscillator and has boundary conditions

$$a'y(1) + b' \frac{d\,y}{d\,x}(1) = 0 \qquad (4\text{-}18a)$$

and

$$y(0) = 0 \qquad (4\text{-}18b)$$

where a' and b' are a and b from eq. 4-4 transformed to the x coordinate system. Assuming $y(x) = A \sin(kx + \delta)$ replaces the outer boundary

condition by a transcendental equation of the form

$$\tan(k + \delta) = b'/a' \, k \qquad (4\text{-}19)$$

In the limit $k \gg 1$, this equation has roots that correspond to half-integer multiples of π (Butkov 1968, ch. 9), $k = (\frac{n}{2} + 1) \pi$, $\sigma = ((\frac{n}{2} + 1) \pi)^2/J^2$, and we shall let $\delta = 0$.

The physical eigenvector can be found from the asymptotic expression as

$$\xi_n(x) = y_n(x) \; / \; \left[- \mu^2 \frac{TC_v}{L_*} \left(\frac{d \ln T}{d m} \right)^{-1} \right]^{1/4}. \qquad (4\text{-}20)$$

In Figure 4-3, we plot the x variations for the Beta Cephei model. For log(T)<5.7, the shape of the eigenvector is determined solely by the denominator in 4-20. In this star the integrating factor decreases outward and the net effect is an eigenvector that peaks at the surface. (Figures 4-4 and 4-5). The minimum in μ at log(T)~4.6 is due to a maximum in κ_T at that temperature caused by the second ionization stage of helium. The shoulder in y at this temperature is also from this minimum.

Moving to a Cepheid model, the situation changes considerably. In Figure 4-6, the thermal coordinate is plotted, and we see that x~1 until log(T) >4.5, well interior to the hydrogen ionization zone. When the asymptotic (n=10) eigenvector is plotted (Figure 4-7), a large peak occurs at log(T)=3.9. This variation cannot be due to the cosine term in 4-20 as the argument is essentially 1.0; so, this feature must be due to

the denominator, whose major variations come from the integrating factor. A large minimum in μ can be seen in Figure 4-8, where the logarithm of μ is plotted. This minimum corresponds to the maximum in ξ and is caused by the large positive value for κ_T in the cool side of the hydrogen ionization zone. The integrating factor has a temperature dependence of roughly $T^{4 - \kappa_T}$, and in regions where $\kappa_T > 4$, μ increases outward instead of decreasing as it does elsewhere. This structure corresponds to the peak in the temperature eigenvector in a standard linear, non-adiabatic pulsational stability analysis. As the numeric results will demonstrate, any ionization zone will cause a local peaking of the eigenvector, but a region where $\kappa_T > 4$ causes an effect that is best removed when calculating thermal effects in these stars, and plotting the resultant eigenvectors. There are secondary minima in μ at log(T)~4.2 and 4.7 due to the ionization stages of helium. Any effects these have on the eigenvector y (Figure 4-7) are completely hidden by the peak from the hydrogen.

However, it is not true that $k^2 = J^2\sigma \gg w(x)$ everywhere. At the surface, $T \rightarrow T_0$ and $\kappa \rightarrow 0$, so that w(x) increases outward. While the interpretation of the "bumps" in the eigenfunctions as maxima in κ_T will be valid in the actual numeric results, the frequencies and eigenfunctions are not accurately represented in these expressions. With this knowledge in hand we now move on to solving the equations numerically and show the thermal modes for several stars.

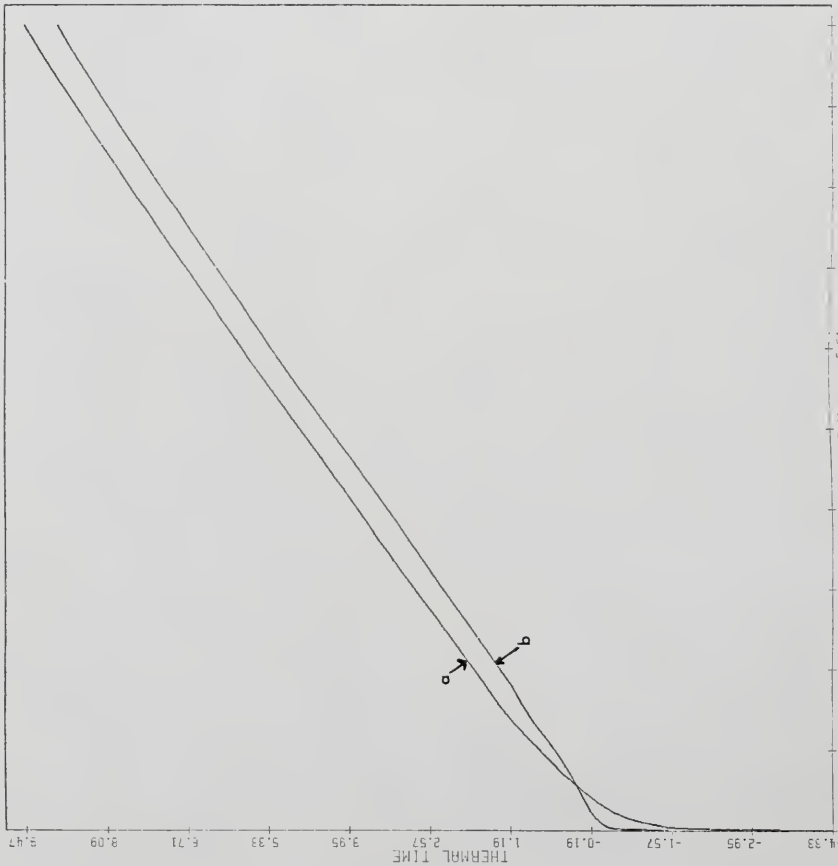

Figure 4-1: The logarithm of the thermal time versus log(T) for the BW Vulpeculae model. The curve labelled a is t_{th} and that labelled b is $t_{th,p}$.

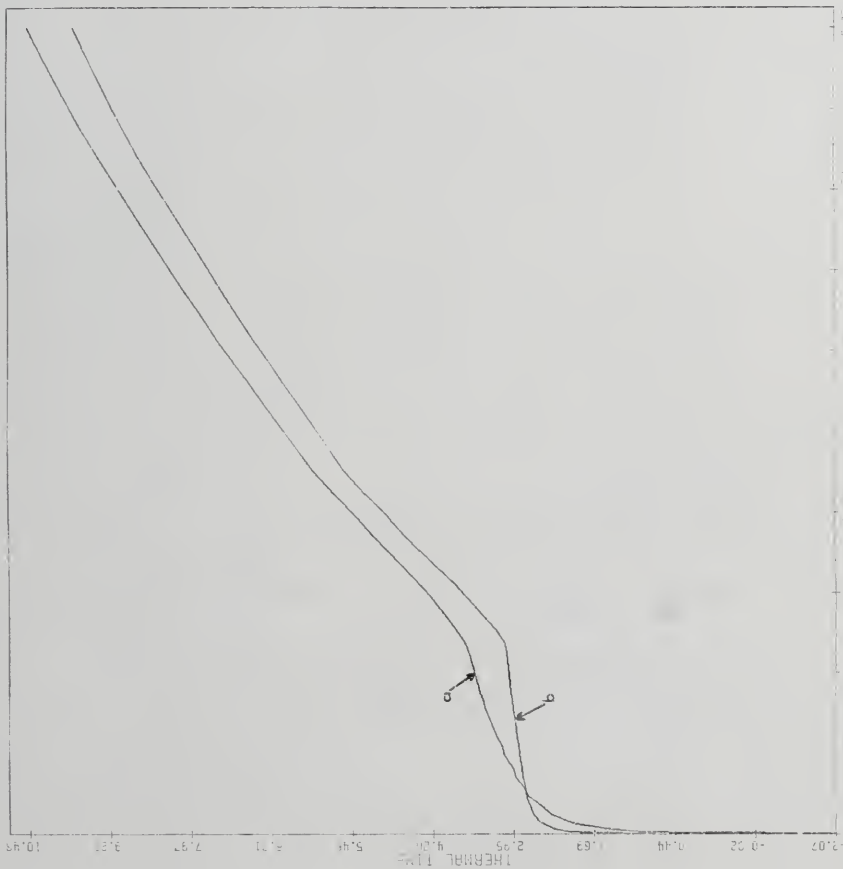

Figure 4-2: The logarithm of the thermal time versus log(T) for the Cepheid model. The curve labelled a is t_{th} and that labelled b is $t_{th,p}$.

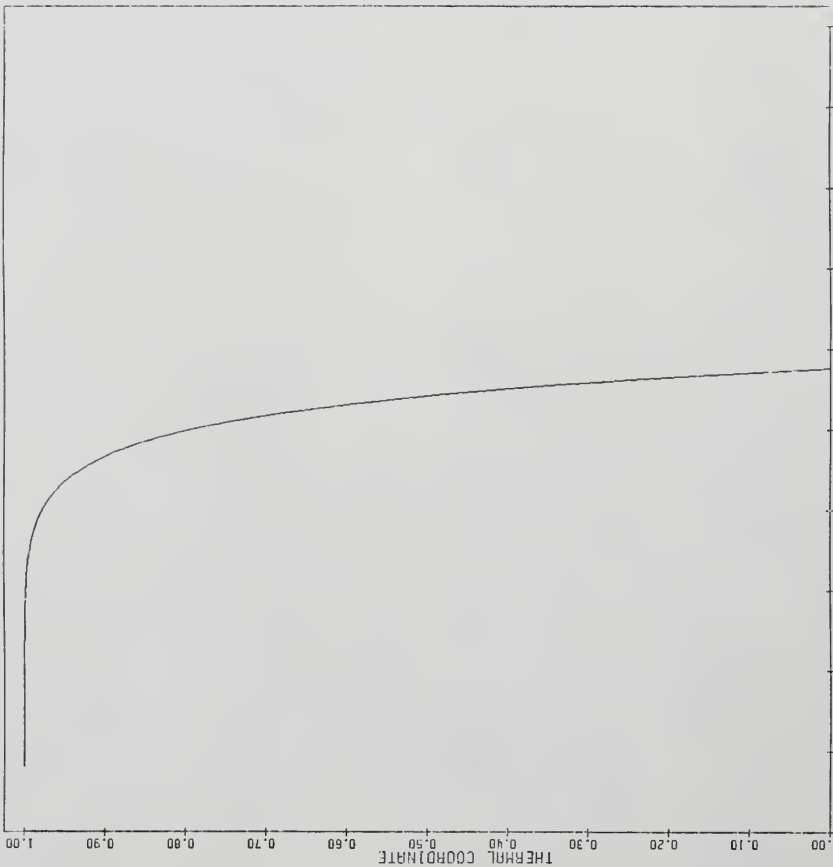

Figure 4-3: Normalized thermal coordinate versus log(T) for BW Vulpeculae.

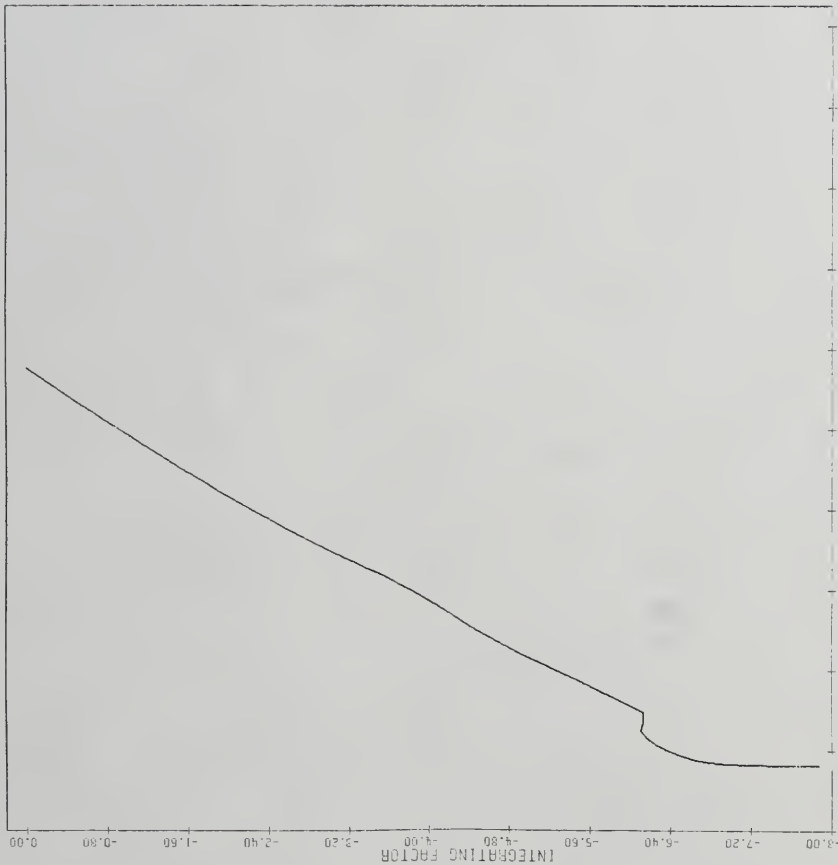

Figure 4-4: Logarithm of the integrating factor versus log(T) for the BW Vulpeculae model.

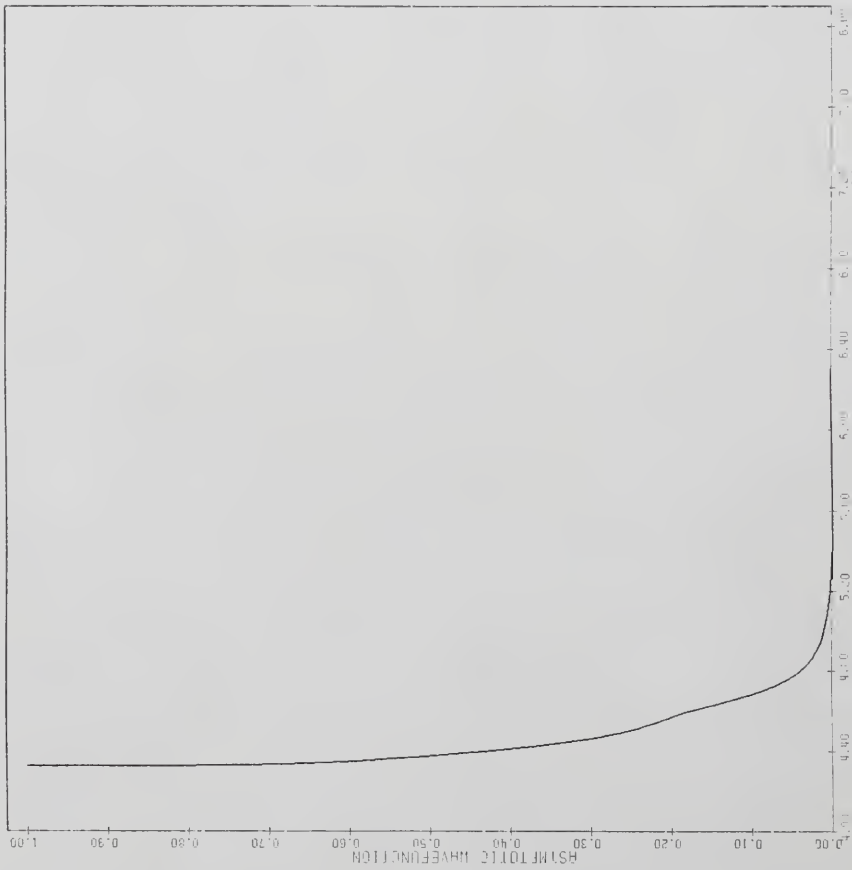

Figure 4-5: The asymptotic (n=10) wavefunction versus log(T) for the BW Vulpeculae model.

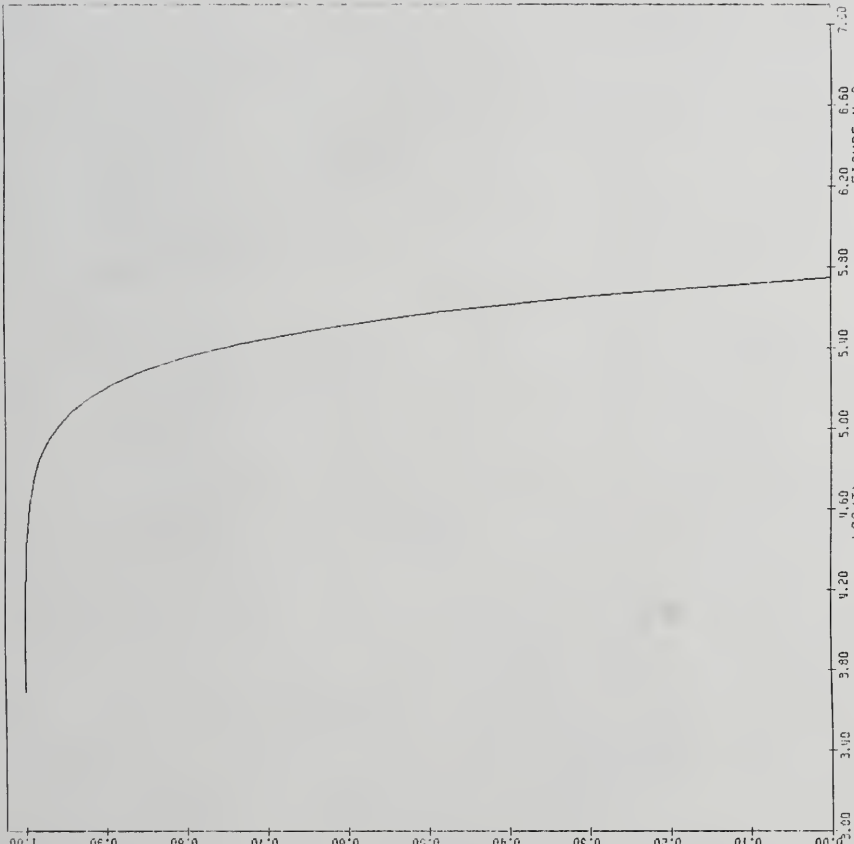

Figure 4-6: The normalized thermal coordinate versus log(T) for the Cepheid model.

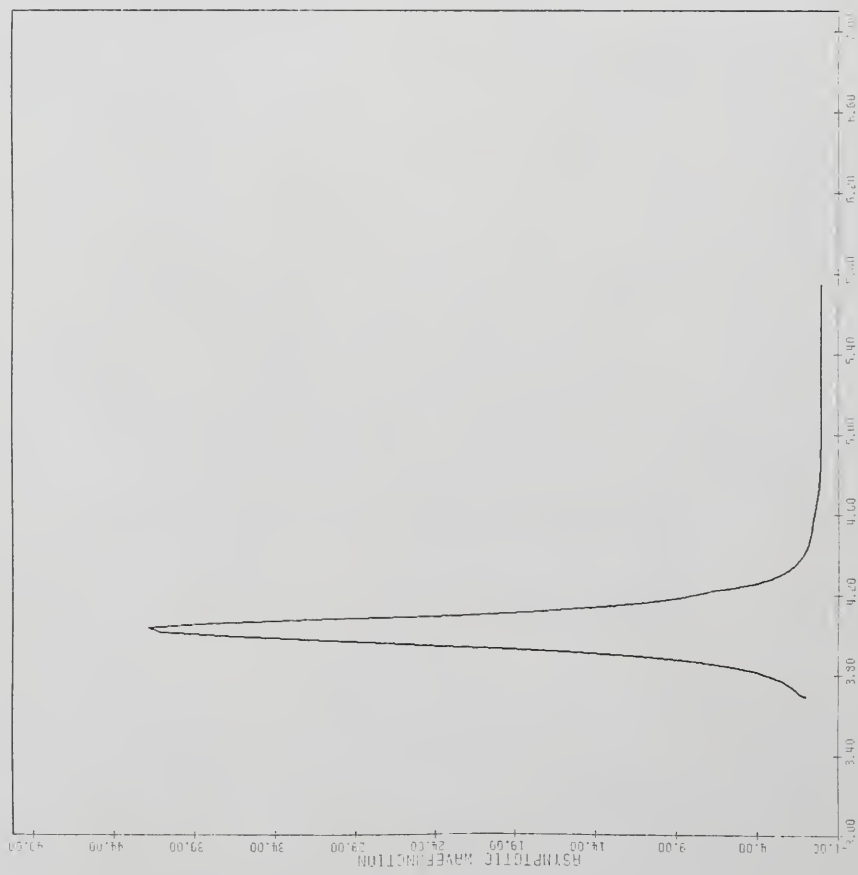

Figure 4-7: The asymptotic (n=10) wavefunction versus log(T) for the Cepheid model.

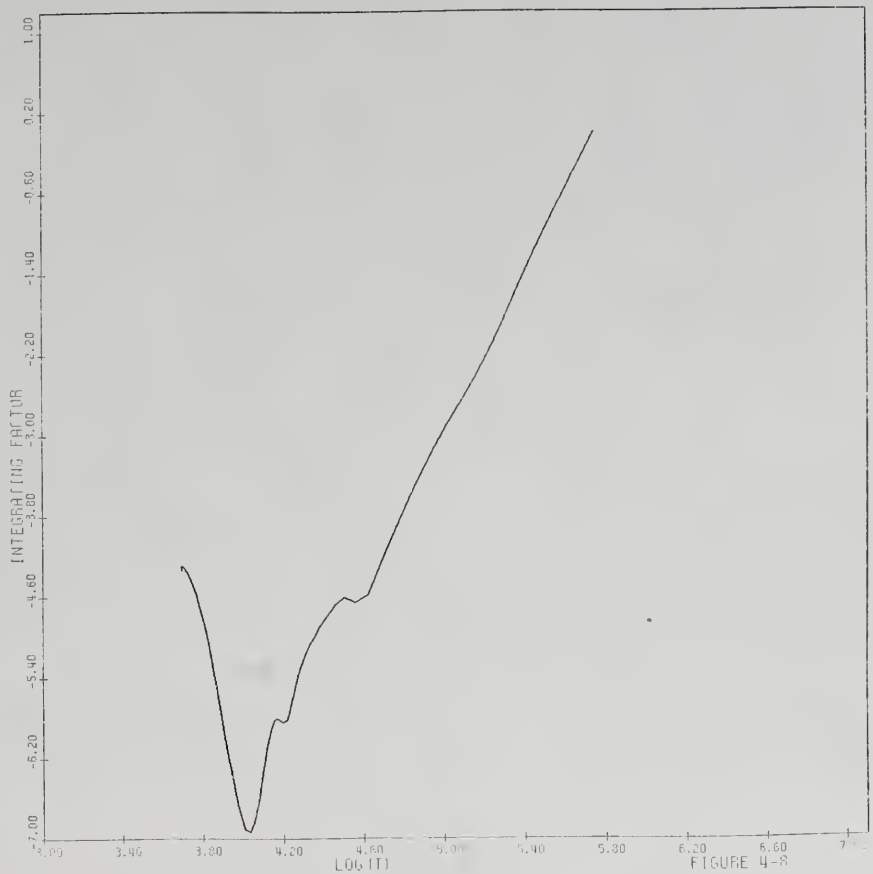

Figure 4-8: The logarithm of the integrating factor versus log(T) for the Cepheid.

CHAPTER V

NUMERIC RESULTS

In this section the eigenvalues and eigenvectors for two stellar models will be discussed. In each case, the initial model was found by using the model builder described in Appendix B, with mass, luminosity, effective temperature, and composition appropriate to the class of star the model represents. One model is of BW Vulpeculae, a hot supergiant of the Beta Cephei class of variables, and the other is a generic Cepheid.

To find the matrix operator, equations 3-3 and 3-4 are differentiated at constant radius (density) and written in a form resembling that of Castor (1971):

$$T \frac{d\ \delta S}{d\ t} = AK2 \cdot (T\delta S). \qquad (5\text{-}1)$$

Although the matrix AK2 is not symmetric, it is tridiagonal and a numeric analog of the integrating factor does exist (Wilkinson 1965). Applying this transformation to AK2 yields the D operator as a real, symmetric, tridiagonal matrix. The diagonal transformation matrix is defined as

$$\mu^{1/2}(1) = 1$$

$$\mu^{1/2}(I) = \mu^{1/2}(I-1)\left[\, AK2(I-1,3)/AK2(I,1)\,\right]^{1/2},\quad I=2,N,$$

and the matrix D is found by using $\mu^{1/2}$ as a similarity transformation

$$D = \mu^{1/2}\, AK2\, \mu^{-1/2}$$

so that the spectrum of D is identical to that of AK2. In a convective region of a star, one procedure is to neglect the Lagrangian perturbation of the convective flux (Saio, Winget and Robinson 1983). This will have no direct effect on the definition of $\mu^{1/2}$ as the two matrix elements, AK2(I-1,3) and AK2(I,1), are multiplied by the same fraction of the luminosity being carried by the radiation. Any gross features of $\mu^{1/2}$, such as peaks in ionization regions, will still be present in a model where convection is permitted, although they may be extended over a larger region due to the smaller temperature gradient. The transformation has one side benefit, the matrices analogous to AG2 and AK1 in Castor (1971), are much closer in magnitude to the elements of the symmetric matrices A and D and have smaller variations as a function of position in the model, resulting in better numeric accuracy.

Real eigenvalues are guaranteed by the symmetric, tridiagonal form of the matrix operator (Ralston 1967). For negative definite eigenvalues (representing decays) the diagonal elements must be negative. This can be seen in a simple example.

A negative diagonal element means that increasing the entropy (temperature) in a zone increases the luminous flux out of the zone

more than it decreases the flux entering it. This stabilizes the zone as the additional energy is lost and the temperature decays to its initial value. A simple example can be used if the luminosity gradient had a local relationship. Equation 5-1 would then be written as

$$\frac{d\ S}{d\ t} = -a(S - S_0)$$

so that

$$S(t) - S_0 = S_0 e^{-at}$$

If $a>0$, the entropy decays, but if $a<0$ the entropy increases. The latter situation is possible in a nuclear burning core but not in the envelope.

To preserve the Sturm-Liouville character of the continuum operator in 4-5 in the matrix operator, the off-diagonal elements must be positive. This condition is composed of two separate requirements. The luminosity exiting a zone must increase if the temperature of the zone above is decreased, and the luminosity entering a zone must also increase if the temperature of the zone below is increased. Both of these are easily satisfied if the opacity is independent of temperature or decreases with temperature, ($\kappa_T \leq 0$). From the form of the continuum operator (4-5), only if $\kappa_T > 4$ can violations of these conditions occur and these regions are precisely where the interpolation formulae for the luminosity are essential. In the initial model the temperature ratio is not allowed to exceed a given number in the ionization zones. This process limits the variation of the opacity as

well and raises the upper bound for positive matrix elements. A first order expansion of the super-diagonal matrix element shows that for

$$\kappa_T < 1/\ln(T(I-1)/T(I)) \sim 17 ,$$

these matrix elements are always positive. We have never found any negative off-diagonal matrix elements in any calculated envelope model. This process also limits the variations of the matrix elements so that the sum of the off-diagonal elements is less than the diagonal elements, permitting the use of Geschgorin's Theorem (Wilkinson 1965).

The boundary conditions are incorporated into the matrix operator by giving certain elements of the matrix special functional forms. Assuming the outer surface to be radiative and given by the grey atmosphere formula is equivalent to assuming that this surface has an infinitely short thermal response time. Therefore, the analytic form of this boundary condition is that of eq. 4-4, even though the diffusion approximation is not very accurate here. For numeric computations this expression is unsuitable, as it is valid at a point exterior to the actual surface of a model, and we have assumed that the exiting luminosity is given by

$$L(N+1) = 4\pi\sigma R^2(N+1) T_{eff}^4 \frac{3}{4} (\tau + \frac{2}{3})$$

When this formula is linearized and inserted into the operator equation, the outer equation reduces to one of first order and closes the system. The inner boundary condition is $\delta S/C_v \dashrightarrow 0$ and is included by zeroing

any elements in the matrix that refer to $\delta S/C_v(0)$. Again, this reduces the appropriate equation (here the innermost zone) to one of first order.

As the thermal time of the outer surface is zero, and the overall thermal time ($\sim \sigma_0^{-1}$) is normally longer than a pulsation period, the spectrum of D must contain eigenvalues which bracket the radial fundamental adiabatic pulsation frequency. Here is the information that we seek regarding the transition zone. All parts of a star that can relax faster through a thermal process than acoustically will move in a highly non-adiabatic fashion. These regions of a star will be called the "sudden" regions and correspond, in some stars (see below), to the outer layers where $\frac{d\ \delta L/L}{d\ m} = 0$ in a fully non-adiabatic stability analysis. The inner regions of a star have thermal response times longer than the fundamental period ($\sigma < \omega_0$) and are referred to as quasi-adiabatic.

Eigenvalues for this matrix can be found by a variety of means. For the low order modes iterating on the outer boundary condition is possible (Castor 1971), but the structure of the high order modes is such that this method fails. A general eigenvalue routine (Smith et al. 1976) is used to find all eigenvalues of D and the necessary eigenvectors are found by standard Gaussian back substitution. The eigenvectors of D and AK2 are related by the same similarity transformation as the matrices and the more desirable set can be calculated, depending on the effective temperature (T_{eff}), of the star under study. If $T_{eff} > 15{,}000$ K, then the hydrogen ionization zone is absent and the ξ_n's give a good representation of the thermal modes. When $T_{eff} < 15{,}000$ K, this ionization zone causes a spike to be present

in ξ_n as shown in the section on asymptotic eigenvectors in Chapter 4. To remove this feature, the eigenvectors of D are calculated and displayed. This results in a much clearer picture of what is occurring in the surface regions of the star.

We cannot look at the long decay rate modes as we have removed the core and the effect it has on the eigenvectors. The lower modes can have significant amplitude in the core, but the higher modes are effectively isolated from the core even more so than the radial pulsation modes. This causes the difficulty noted earlier, the number of nodes in a calculated eigenvector is no longer an indicator of it's position in the spectrum; the size of the numbers causes the computer to underflow and the interior portion of the eigenvector is set to zero! Physically, this implies that the exterior can react to perturbations on much shorter time scales than the interior. However, the outer layers are linked quite strongly to the interior through the low order modes. When a heat pulse is inserted at the base of the envelope, the entire model is affected. The outer layers react to maintain thermal balance with the new luminosity from the heat pulse. The eigenfunctions of the diffusion equation exhibit an infinite propagation velocity for perturbations (Morse and Feshbach 1953, ch. 7), causing this behavior. The asymptotic eigenfunctions are trigonometric with an amplitude that increases outward and we can therefore speak of the thermal time of a point in the star as the reciprocal of the largest eigenvalue whose eigenvector has significant amplitude at that position. This may seem ambiguous, but as thermal modes can be used to expand the pulsation equations in the thermal times, this identification will enable us to study the thermal

effects in an oscillation. In particular, the quasi-adiabatic stability coefficient and pulsations that are dominated by thermal effects can be defined.

Concentrating on those modes with have eigenvalues comparable to that of the radial fundamental pulsation frequency, we now examine two stellar models.

BW Vulpeculae

The physical parameters for this star are plotted in Figure 5-1 and the eigenfunctions $\delta r/r$, $\delta\rho/\rho$ and $\delta L/L$ for the radial, adiabatic, fundamental pulsation mode are shown in Figure 5-2. The results of a linear, non-adiabatic radial pulsation analysis (LNA) are shown in Table 5-1. To find a realistic model for this star, it was necessary to integrate into the nuclear burning core slightly, but the thermal modes discussed below are not altered by this.

The fundamental frequency (ω_0) is $3.9 * 10^{-4}$ sec^{-1}, and the four thermal eigenvectors with eigenfrequencies closest to this are plotted in Figure 5-3.

Important features are the cutoff near log(T)=5.2 and the two peaks. The peak near log(T)=4.6 is due to the second ionization of helium causing a local maximum in κ_T. At log(T)~5.1, a secondary peak associated with the first due to the use of the Rosseland mean opacity. The weighting function in this mean has a maximum at a temperature roughly four times that where the ionization occurs and causes a maximum in κ_T at this temperature. This peak has been studied by Stellingwerf

(1978) as well as Saio and Cox (1980), as a possible driving mechanism for these stars.

The luminosity variations ($\delta L/L$) for each mode are shown in Figure 5-4. Near the surface $\frac{d\ \delta L/L}{d\ m} = 0$, showing the domination of the short thermal times in this region. Moving inward (increasing the temperature), the luminosity variation starts to decrease at log(T)=5.0, oscillates due to the nodal structure of ξ , and drops to zero by log(T)=6.0. These modes are completely isolated from the nuclear burning core (log(T)>6.5) as stated earlier.

Figures 5-5 and 5-6 show the real and imaginary parts of the entropy variations as calculated from the LNA pulsational stability analysis. The peaks at log(T)=4.6 and 5.1 as well as a sharp cutoff above log(T)=5.3 can be seen in both components. Each feature has an analogy in the thermal eigenvectors in Figure 5-3. The modulus of the luminosity variations from this analysis is shown in Figure 5-7. The change from $\frac{d\ \delta L/L}{d\ m} = 0$ is present, albeit at a slightly higher temperature than in Figure 5-4. Some of this is due to contamination with low order thermal modes, but the significant amplitude in $\delta L/L$ (up to log(T)=6.0) is due to the adiabatic density fluctuations in this region.

This model shows that the shape of $\delta S/C_v$ in an LNA pulsational stability analysis is determined by the thermal modes of that star. As always, the model is stable and, at present, we do not find any new ways of destabilizing it. The structure of the eigenvectors serves to demonstrate and clarify the physical reasons behind a transition zone and the splitting of the star in two regions, adiabatic (log(T)>5.4) and

instantaneous thermal balance (or sudden) at log(T)<5.4. More interesting behavior can be seen when a model of a Cepheid variable is examined.

Cepheid model

This star is a generic Cepheid whose characteristics were obtained from A. N. Cox (1980a). The results of the LNA pulsational analysis and summary of the input data are found in Table 5-2. A graph of the physical parameters is found in Figure 5-8 and a graph of the adiabatic eigenvectors $\delta r/r$, $\delta\rho/\rho$ and $\delta L/L$ is shown in Figure 5-9. The model is unstable in the first three pulsation modes and corresponds to a model of the star DL Cassiopeiae. The results presented here are illustrated very nicely by this star and are similar to those of other Cepheids calculated.

In Figure 5-10 and 5-11 the four thermal modes that bracket the pulsation frequency ω_0, are plotted. These are the eigenvectors of AK2, and we see almost no detail (or the individual modes) due to the spike in the hydrogen ionization zone. The origin of this spike was discussed in the section on asymptotic eigenvectors, and as it eliminates any other features present, we choose to remove it from the eigenvectors. This is accomplished by using the eigenvectors of D, as shown in Figure 5-12. These vectors have the same eigenfrequencies as those in Figure 5-10, but much more detail can be seen. The bumps at log(T)=3.82 and 4.12 are due to the hydrogen ionization zone. They are the lower slopes of the spike, and the minimum at log(T)=4.0 is a result of modulation

effect of the integrating factor being a maximum at this point. The helium ionization zone is visible at log(T)=4.6 as an inverted peak, but the second peak at log(T)=5.1 is absent. From Figure 4-6, where the thermal coordinate for this star is plotted, we see that the value for x starts to drop away from one at this point. In the interpretation of features for log(T)<4.7, the neglect of the trigonometric function in ξ_n is valid, but interior to this, the actual nodal structure of ξ_n will start to dominate.

Examining the luminosity variations which correspond to Figure 5-12 (Figure 5-13), the driving mechanism responsible for destabilizing this star is visible (see below). To accentuate this, the variations for $\sigma \ll \omega_0$ are shown in Figure 5-14 and 5-15 and $\sigma > \omega_0$ in Figure 5-16 and 5-17. In the low frequency results, the luminosity looks much like that of BW Vul (Figure 5-4); increasing the frequency to those in Figure 5-16 and 5-17, the decrease in $\delta L/L$ near log(T)=4.6 has become larger than any other part of the vector. Here is the physical reason for the driving zone of this star.

For a star to be unstable in a pulsation mode, a region where $\frac{d\ \delta L/L}{d\ m} < 0$ must exist (Cox, J. P. 1980). This is seen if the work integral is writen in the form (Aizenman and Cox 1975; Buchler and Regev 1982b),

$$\frac{1}{L_*}\frac{d\ W}{d\ t} = \int_0^{m_*} (\Gamma_3 - 1)\ (\frac{\delta\rho}{\rho})^*\ (\frac{d\ \delta L/L}{d\ m})\ dm\ .$$

The quantity $\Gamma_3 - 1$ is always positive and for the fundamental mode $\frac{\delta\rho}{\rho} < 0$ (as $\frac{\delta r}{r}$ increases outward) (see Figure 5-2); thus, when

$\frac{d\ \delta L/L}{d\ m} > 0$ the star is stabilized and for $\frac{d\ \delta L/L}{d\ m} < 0$ the star is unstable. In the BW Vul model (Figure 5-7) $\frac{d\ \delta L/L}{dm}$ is zero in the atmosphere and $\delta L/L$ generally decreases with increasing temperature. The thermal modes have the same basic luminosity behavior (Figure 5-4), showing that this star is stable. In the Cepheid model, the pulsational $\delta L/L$ (Figure 5-26) shows a definite region near $\log(T) \sim 4.6$ where $\frac{d\ \delta L/L}{d\ m} < 0$. This outward decrease of $\delta L/L$ cannot be due to the adiabatic density fluctuations as they will always have $\delta L/L$ increasing outward. The thermal modes show a change in structure as the decay rate is increased through the value $\sigma \sim \omega$. The change in the shape of $\delta L/L$ in this region is the cause of the destabilization of the Cepheid. Calculations of the BW Vul model with $\sigma/\omega \ll 1$ and $\omega/\sigma \ll 1$ do not show the same change. Examining Figure 5-18 and 5-19 where the thermal modes with $\sigma/\omega \sim 10$, and Figures 5-20 and 5-21 where $\omega/\sigma \sim 10$, we do not see the same change in the structure of the thermal modes. This leads to the conclusion that the star's thermal structure prevents this type of driving mechanism from functioning.

The location of the transition zone in each model should be discussed as well. The BW Vul model shows a definite change from adiabaticity to sudden behavior at $\log(T)=5.2$. The Cepheid shows a less dramatic change, as the thermal eigenvectors do not show an extremely rapid cutoff at the transition. However, unlike BW Vul, the Cepheid has a region where $\frac{d\ \delta L/L}{d\ m} < 0$ that begins near the transition. Also, it would seem more difficult to establish a transition zone for this model as $\frac{d\ \delta L/L}{d\ m}$ is not zero until well above the helium ionization. In fact, the luminosity variations from the pulsation analysis (Figure 5-26) do

not have a vanishing derivative until above the hydrogen ionization zone. It is difficult to use the timescale arguments to locate the transition zone for such a model. The use of $\sigma \approx \omega_0$ to partition the thermal modes is, in this case, a fairly reliable way to locate this region. For $\sigma < \omega_0$, the thermal mode has a $\delta L/L$ vector that is, in general, increasing outward and has only a small dip in the helium ionization zone. When $\sigma > \omega_0$, $\delta L/L$ is dominated by this region, until $\sigma_n > \omega_0$, when the amplitude of the eigenvector $(\delta S/C_v)$ becomes small enough that the mode is isolated from that region of the star.

To see the benefits of the integrating factor, the real and imaginary parts of the LNA pulsational analysis are shown in Figures 5-22, 5-23, 5-24 and 5-25. In Figures 5-22 and 5-23, the eigenvectors of the AK2 matrix are shown, with the "spike" due to the hydrogen ionization zone dominating the graphs. When the eigenvectors of D are examined in Figures 5-24 and 5-25, the variations have been greatly reduced. In 5-22, $(\delta S/C_v)_{real}$ varies by two orders of magnitude and the imaginary part changes by almost three. The eigenvectors of D vary by less than one order of magnitude and the details of the helium ionization and other structures can be seen.

The eigenvectors shown in this section have some numeric noise that deserves comment. The system that is solved here is identical to that used in the LNA stability analysis, and any noise in the thermal modes is also present in that analysis. The "spikiness" of the eigenvectors present in Figure 5-14 can be eliminated by putting more zones in the model (here N=250) but this puts the eigenvalue routine at a loss for solutions. The envelope mass can be decreased, but at the expense of the

accuracy in the pulsation modes. The basic features of the thermal modes are well represented and accurately calculated. Interior of the transition zone, the adiabatic density fluctatiuons will overwhelm the small luminosity changes due to the entropy variations.

The optimal numeric solution to an eigenvalue problem is found when the matrix elements are approximately equal in magnitude. The transformation of the mechanical variable introduced by Castor (1971), $\delta r \rightarrow XO = \sqrt{DM2}\ \delta r$, does this for the adiabatic wave equation. In a model where the shell mass is a geometric progression increasing inward, this transformation is equivalent to each zone having the same acoustic traversal time. The sound speed is roughly proportional to the square root of the temperature and the thickness of the shell is roughly proportional to the mass; so, the integrand in 3-7 has equal contributions from each zone.

This transformation has the unfortunate side effect of decreasing the numeric niceness of the thermal operator, D. The thermal diffusion velocity (4-16) decreases as the sound speed increases. To optimize the matrix D, the mass of each zone should decrease inward, the opposite direction required of A. This tradeoff between the adiabatic and thermal operators will be important only if the mode is dominated by thermal effects. For quasi-adiabatic modes, the interior is dominated by the adiabatic density fluctuations and the inaccuracy in the thermal modes is unimportant. We are working on ways of circumventing this difficulty so that both operators are represented as accurately as possible.

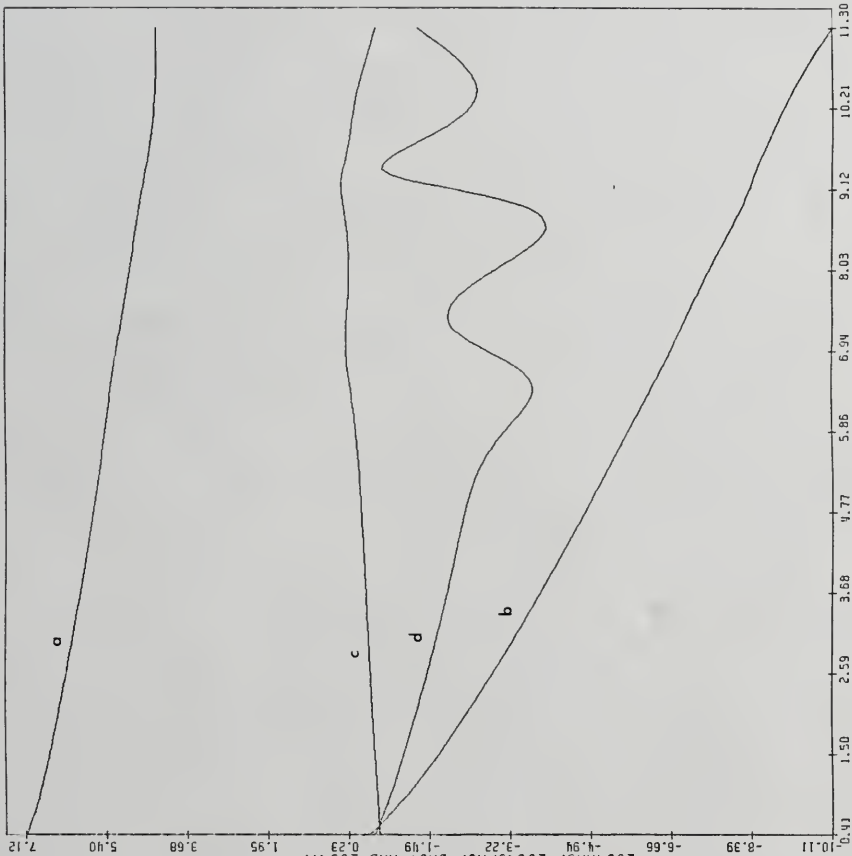

Figure 5-1: Physical parameters for BW Vulpeculae. Plotted versus the surface mass fraction are: (a) log(T), (b) log(ρ), (c) log(κ) and (d) κ_T.

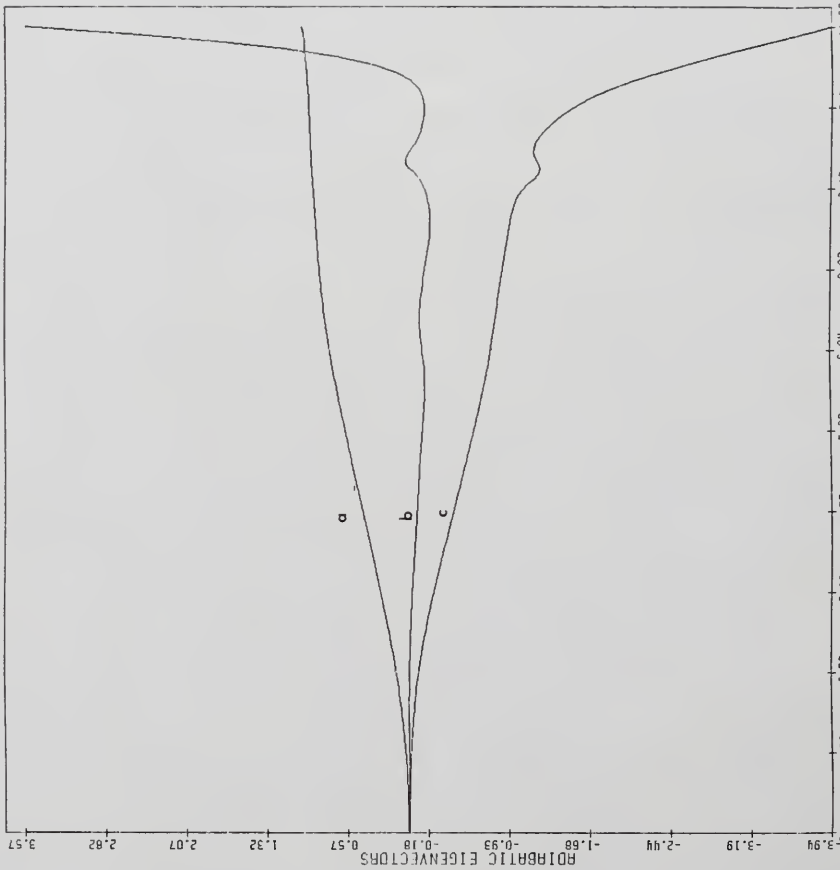

Figure 5-2: Radial adiabatic fundamental eigenvectors versus surface mass fraction for BW Vulpeculae: (a) $\delta r/r$, (b) $\delta\rho/\rho$, (c) $\delta L/L$.

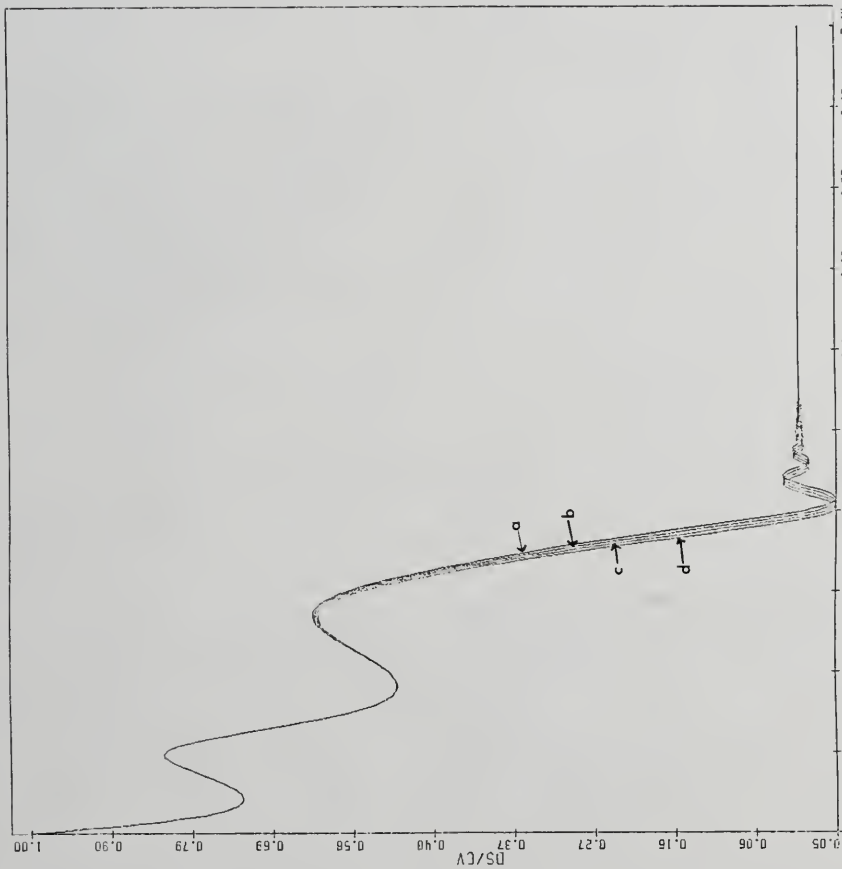

Figure 5-3: Thermal modes for BW Vulpeculae. The decay rate for each mode is: (a) -3.49(-4), (b) -3.89(-4), (c) -4.34(-4) and (d) -4.84(-4).

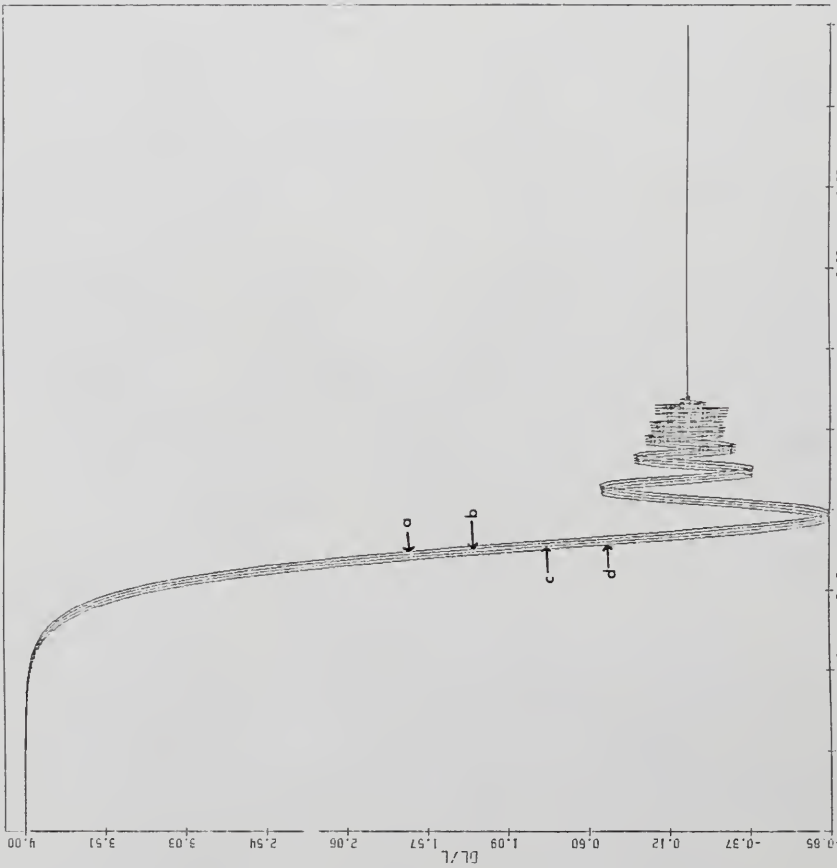

Figure 5-4: Luminosity variations associated with the thermal modes in Figure 5-3. The decay rates are: (a)-3.49(-4), (b)-3.89(-4), (c)-4.34(-4) and (d)-4.84(-4).

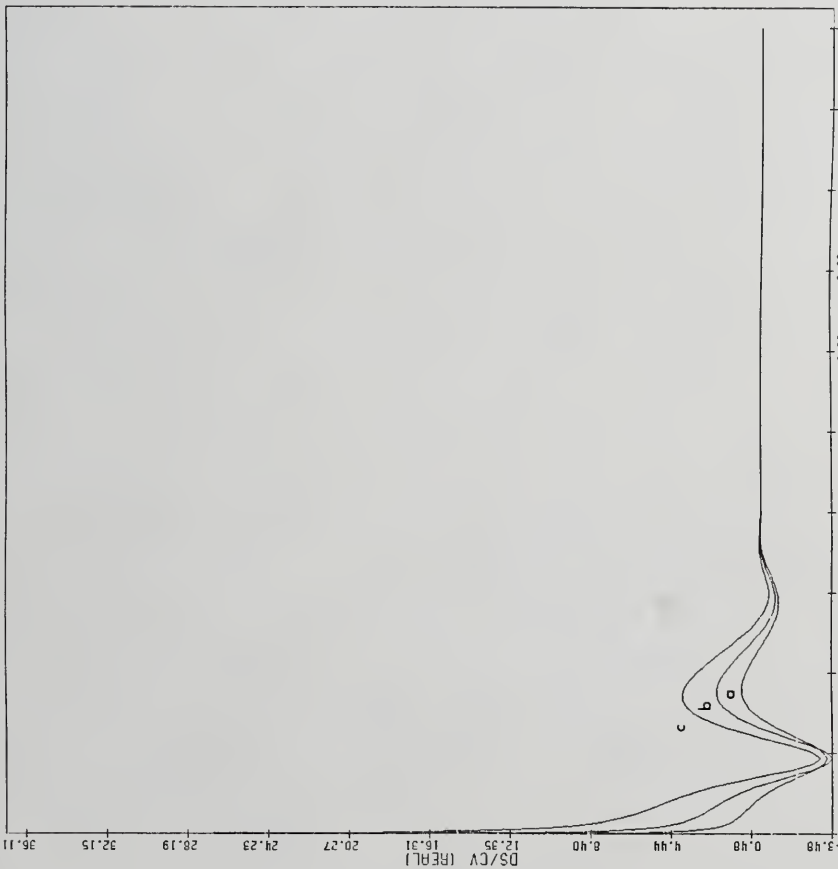

Figure 5-5: Real part of the pulsational $\delta S/C_v$ for BW Vulpeculae. Plotted versus log(T) are: (a) fundamental, (b) first overtone and (c) second overtone.

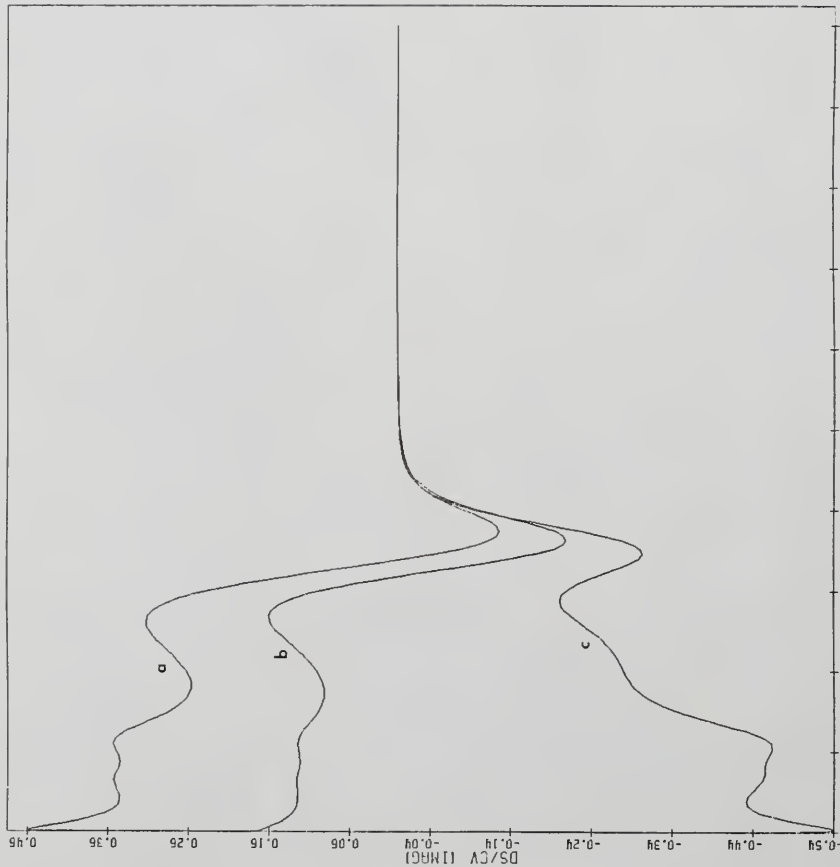

Figure 5-6: Imaginary part of the pulsational $\delta S/C_v$ for BW Vulpeculae. Plotted versus log(T) are: (a) fundamental, (b) first and second overtone (c).

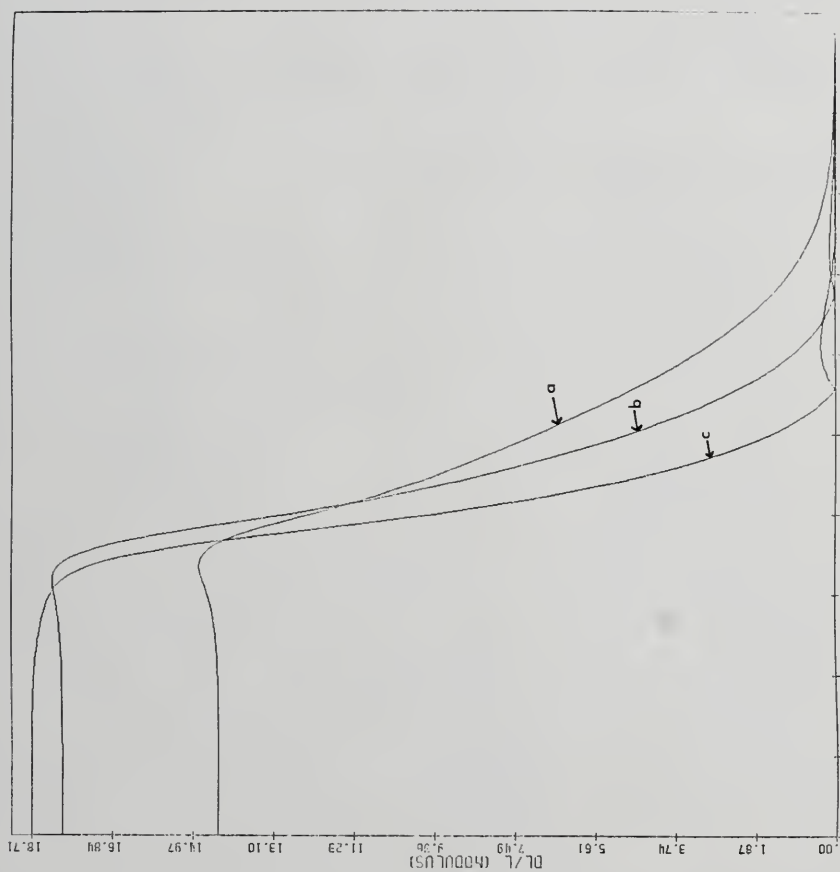

Figure 5-7: Modulus of the pulsational δL/L for the BW Vulpeculae model. Plotted versus log(T) are the: (a) fundamental, (b) first and (c) second overtone.

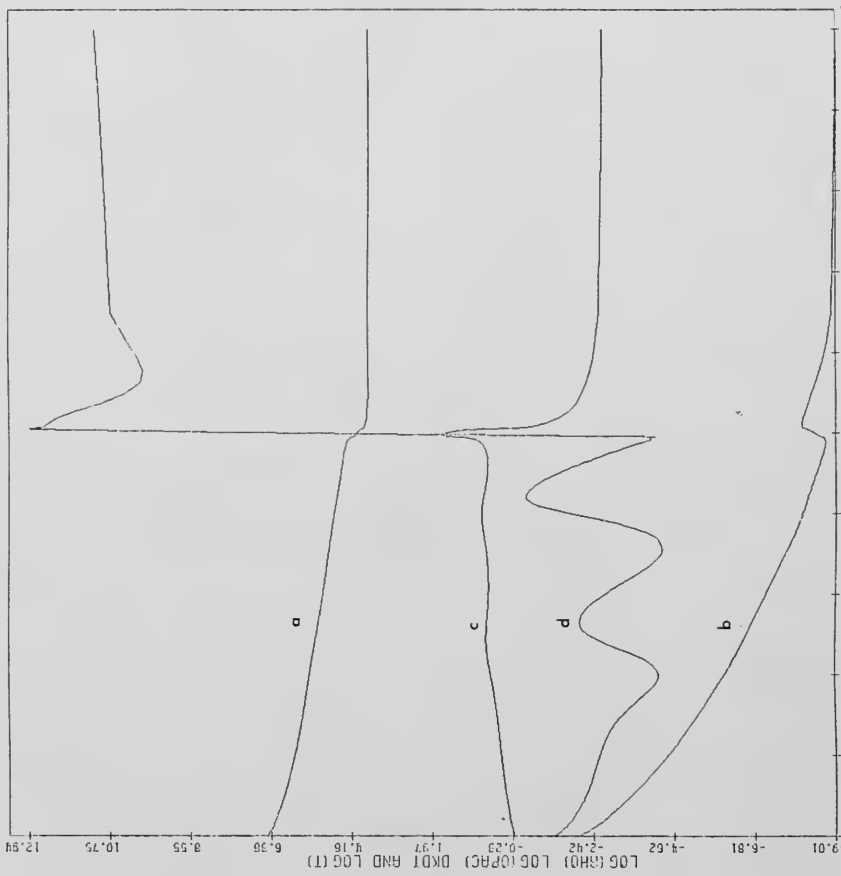

Figure 5-8: Physical parameters for the Cepheid model. Plotted versus the surface mass fraction are: (a) log(T), (b) log(ρ), (c) log(κ) and (d) κ_T.

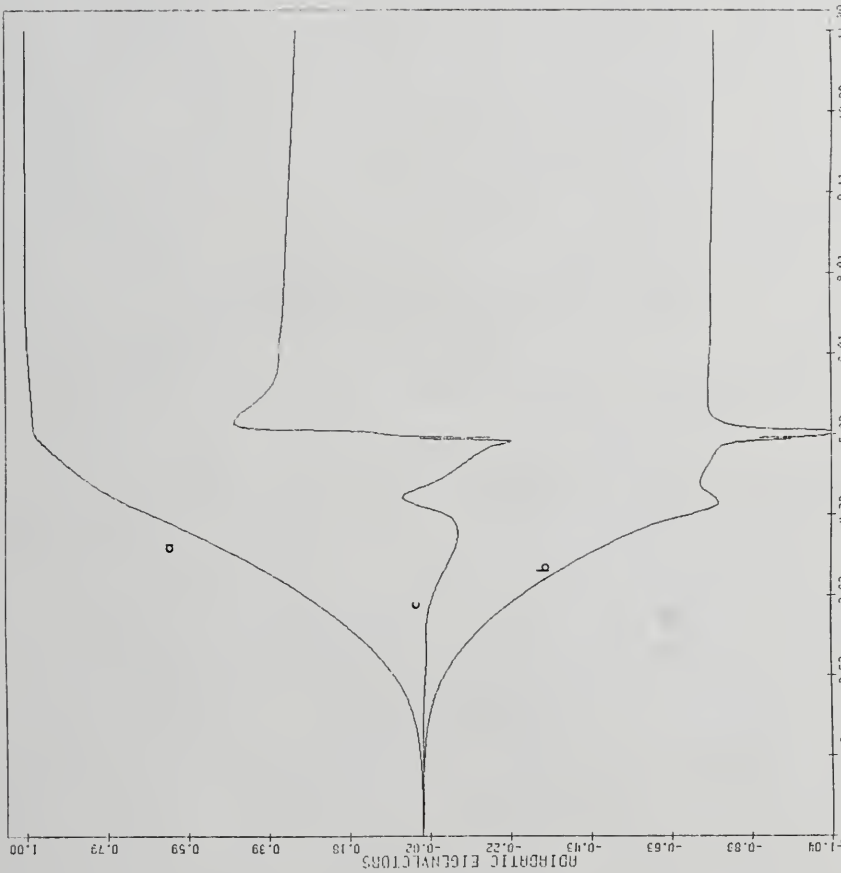

Figure 5-9: Radial adiabatic fundamental eigenvectors for the Cepheid model. Plotted versus surface mass fraction are (a) $\delta r/r$, (b) $\delta\rho/\rho$ and (c) $\delta L/L$.

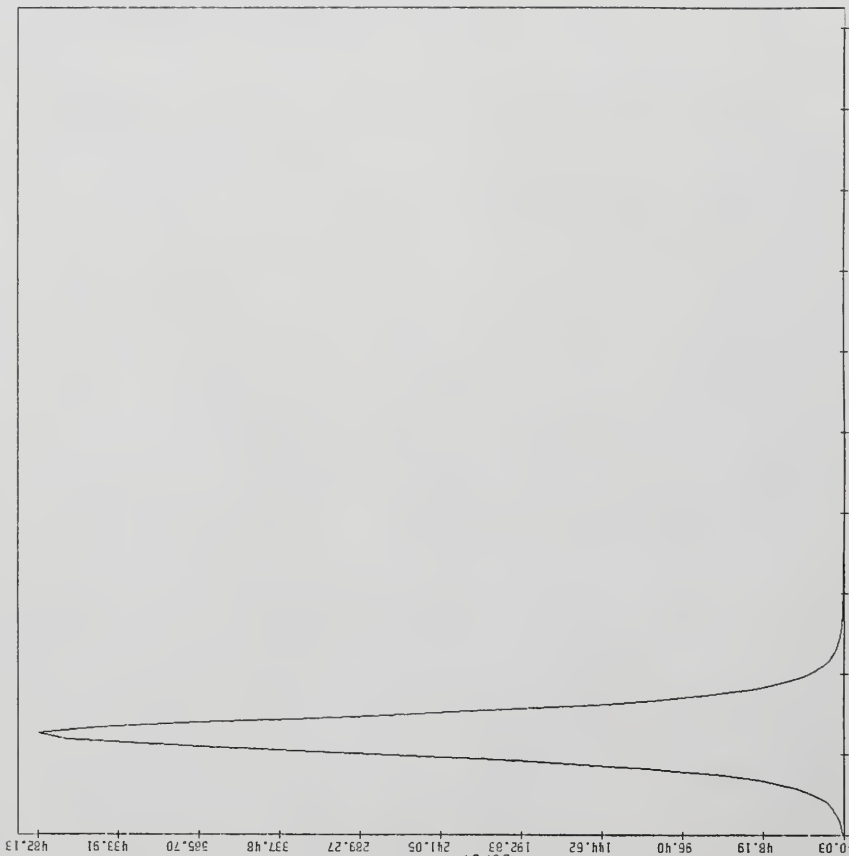

Figure 5-10: Thermal modes versus log(T) for the Cepheid model. These are the eigenvectors of AK2 and the individual modes are indistinguishable.

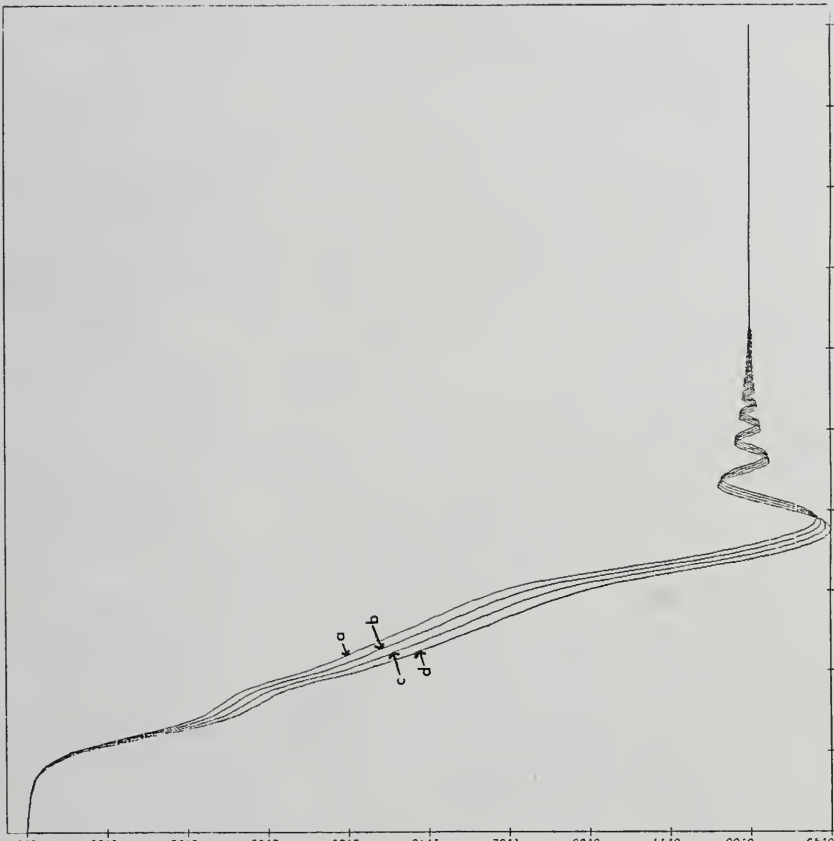

Figure 5-11: Luminosity variations associated with the thermal modes in Figure 5-10. The decay rates are (a)-8.93(-6), (b)-9.46(-6), (c)-1.00(-5) and (d)-1.06(-5).

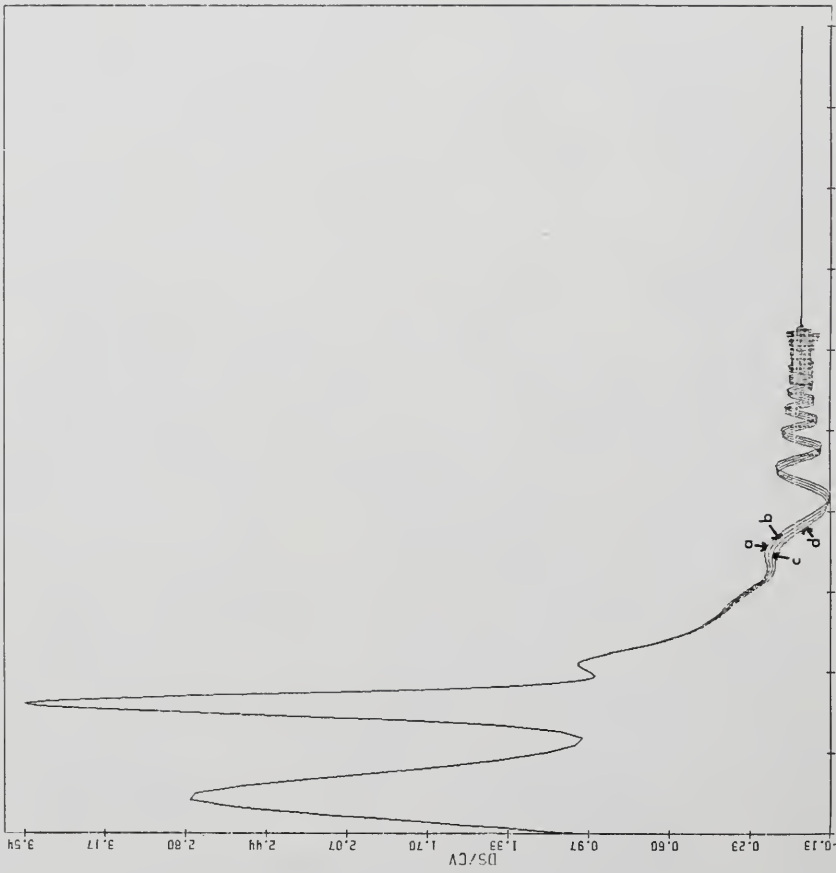

Figure 5-12: Thermal modes versus log(T) for the Cepheid model. These are the eigenvectors of D with decay rates (a)-8.93(-6), (b)-9.46(-6), (c)-1.00(-5) and (d)-1.06(-5).

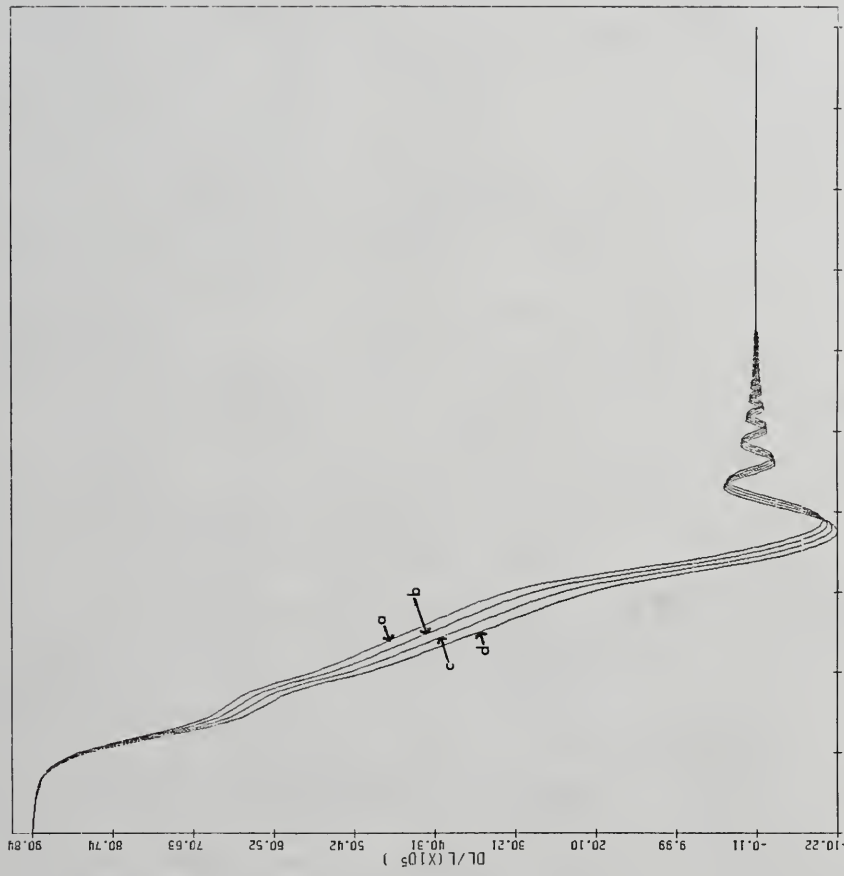

FIGURE 5-13

Figure 5-13: The luminosity variations associated with the thermal modes in Figure 5-12. The decay rates are (a)-8.93(-6), (b)-9.46(-6), (c)-1.00(-5) and (d)-1.06(-5).

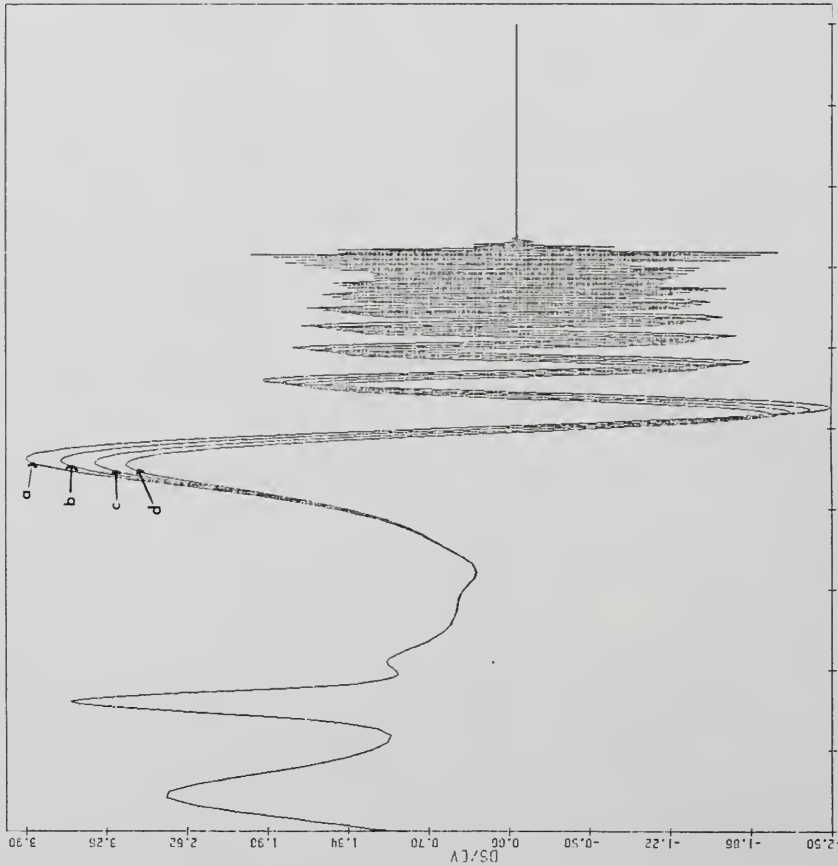

Figure 5-14: Thermal modes of the Cepheid model with decay rates approximately 1/10 of those in Figure 5-12. The decay rates are (a)-9.12(-7), (b)-9.77(-7), (c)-1.05(-6) and (d)-1.12(-6).

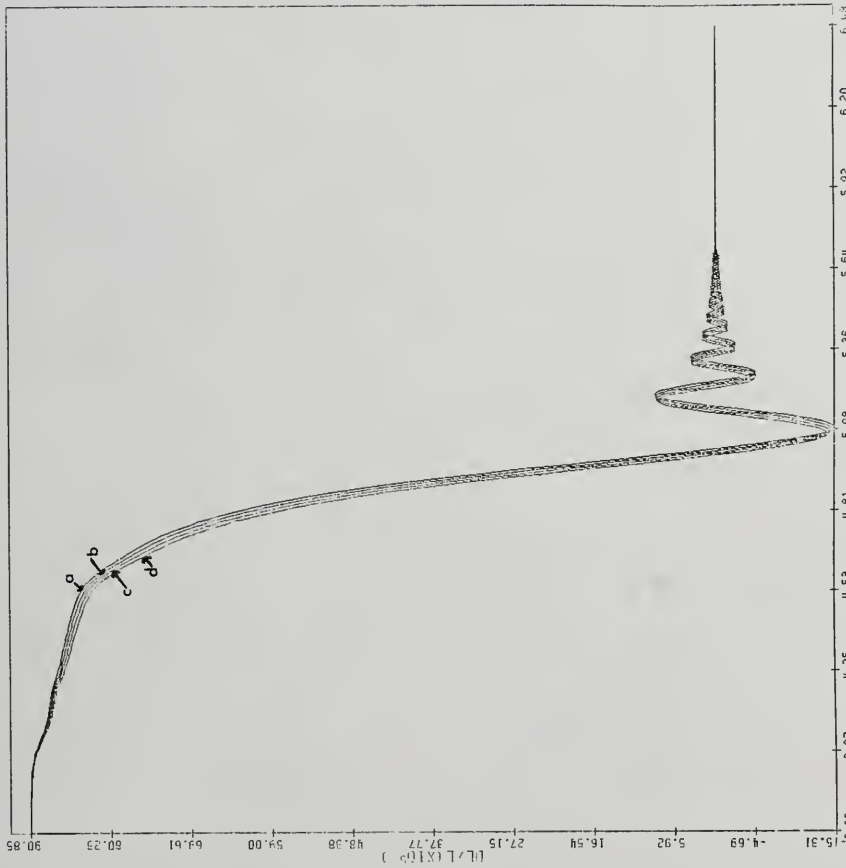

Figure 5-15: Luminosity variations associated with the thermal modes in Figure 5-14. The decay rates are (a)-9.12(-7), (b)-9.77(-7), (c)-1.05(-6) and (d)-1.12(-6).

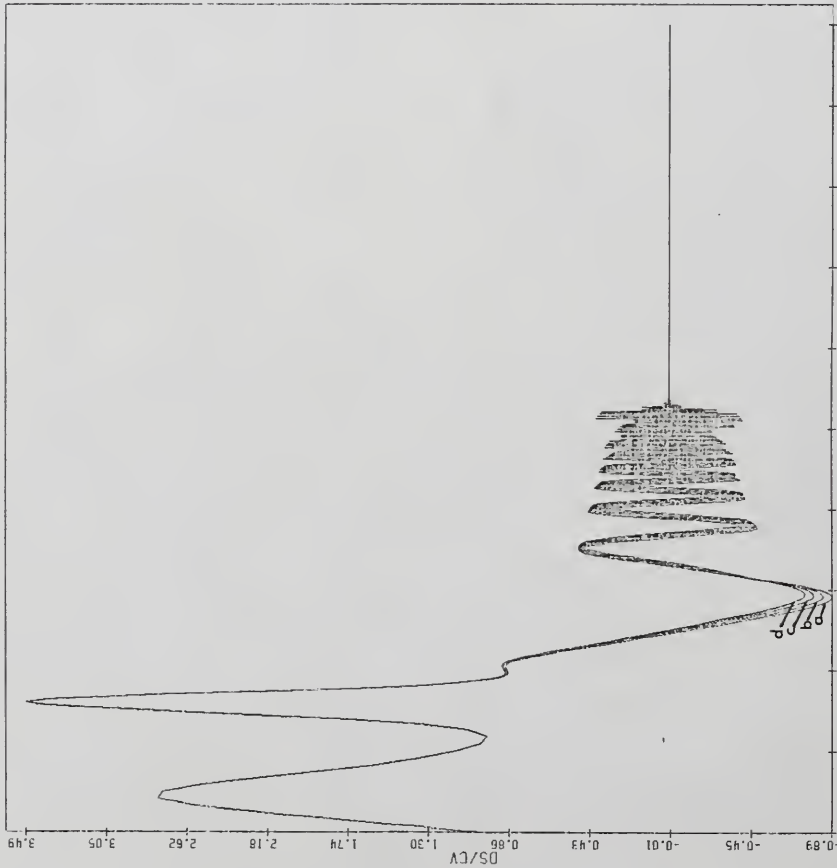

Figure 5-16: Thermal modes versus log(T) for the Cepheid model with decay rates 10 times those in Figure 5-12. The decay rates are (a)-8.77(-5), (b)-9.39(-5), (c)-1.01(-4) and (d)-1.08(-4).

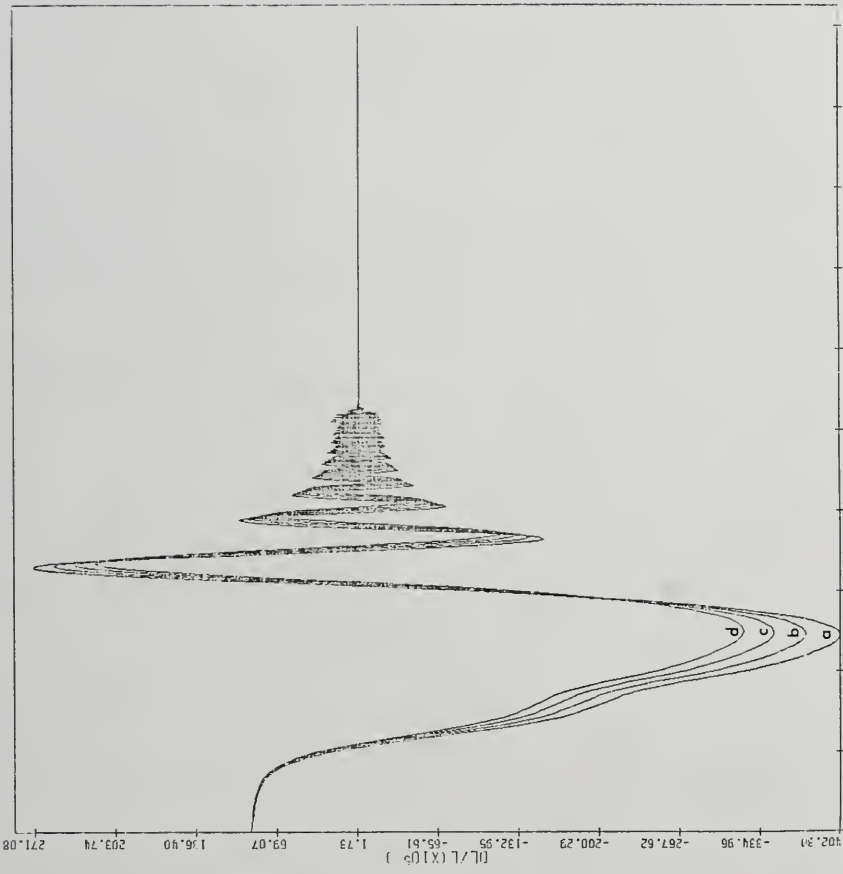

Figure 5-17: Luminosity variations associated with the thermal modes in Figure 5-16, the decay rates are (a)-8.77(-5), (b)-9.39(-5), (c)-1.01(-4) and (d)-1.08(-4).

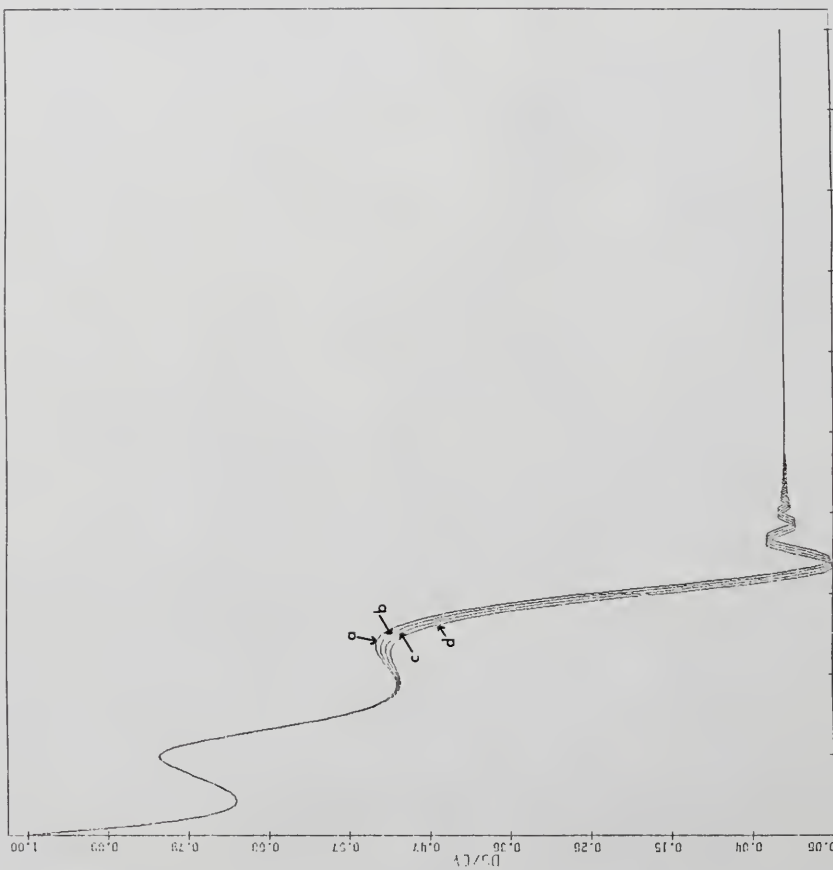

Figure 5-18: Thermal modes versus log(T) for BW Vulpeculae with decay rates approximately 10 times those in Figure 5-3. The decay rates are (a)-3.35(-3), (b)-3.73(-3), (c)-4.14(-3) and (d)-4.76(-3).

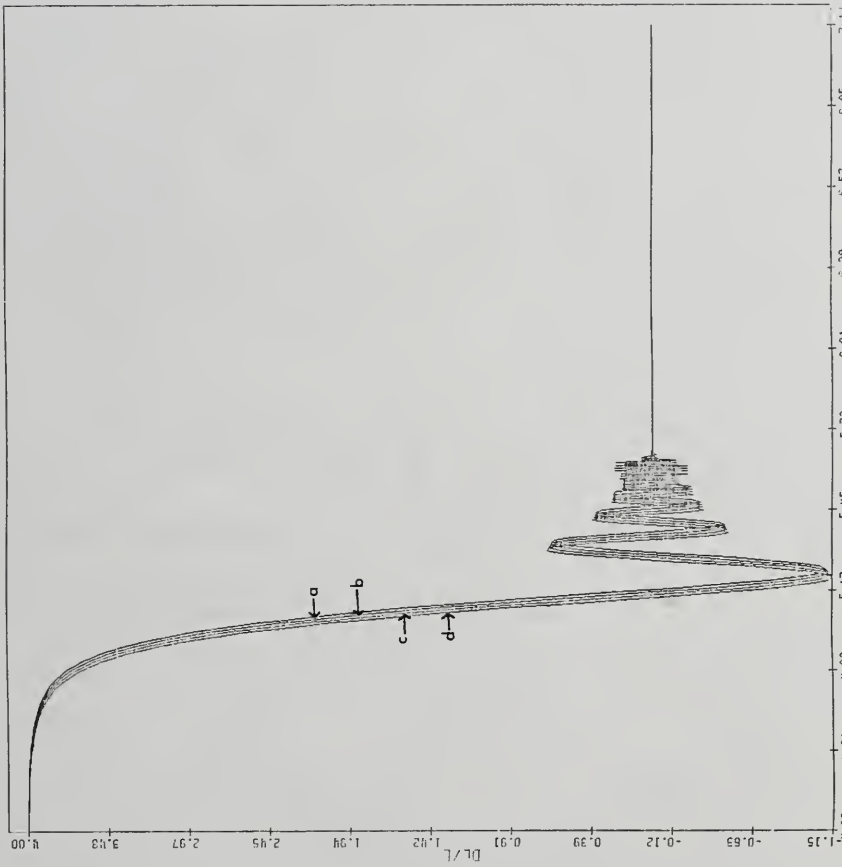

Figure 5-19: Luminosity variations associated with the thermal modes in Figure 5-18, with decay rates (a)-3.35(-3), (b)-3.73(-3), (c)-4.14(-3) and (d)-4.76(-3).

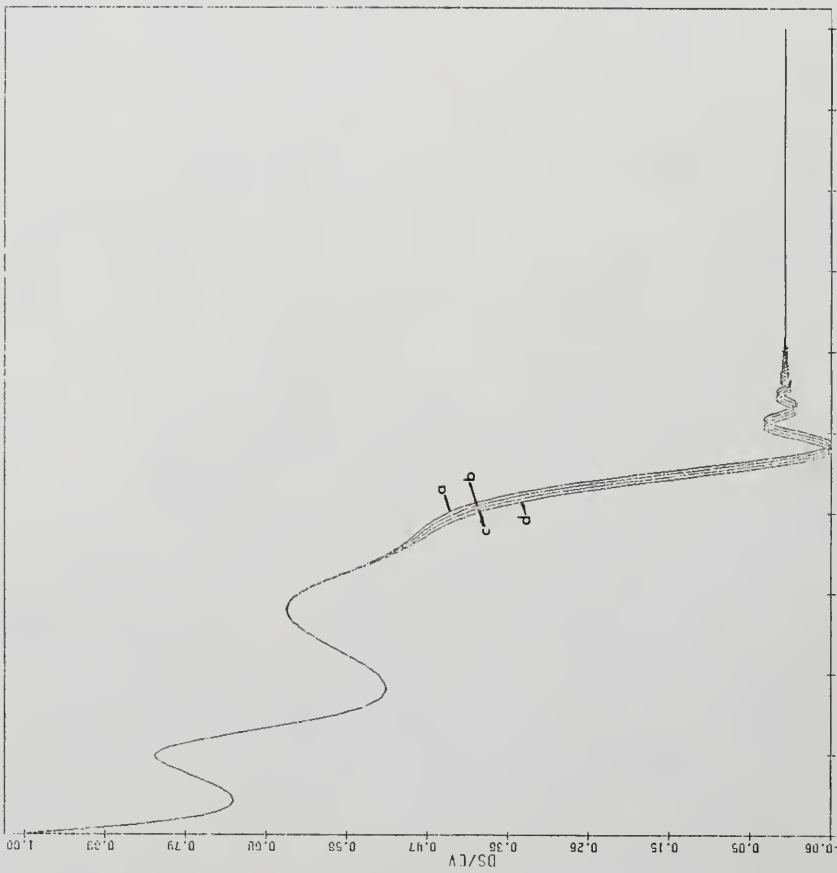

Figure 5-20: Thermal modes versus log(T) for BW Vulpeculae. The decay rates are approximately 1/10 those of Figure 5-3 and are (a)-3.40(-5), (b)-3.80(-5), (c)-4.26(-5) and (d)-4.76(-5).

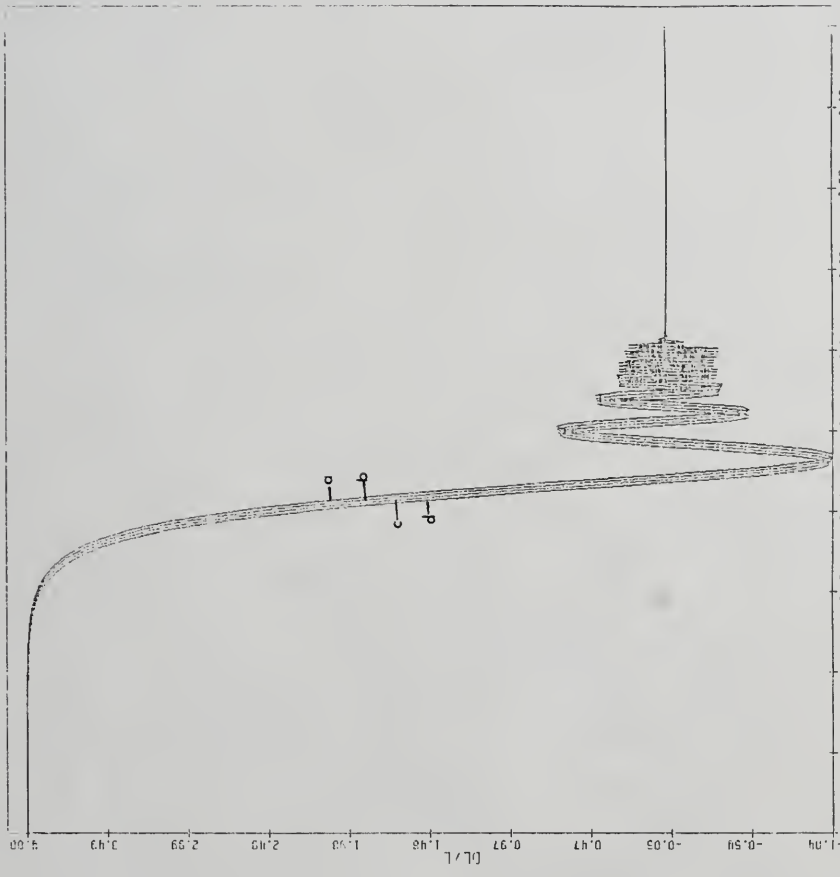

Figure 5-21: Luminosity variations associated with the thermal modes in Figure 5-20, with decay rates (a)-3.40(-5), (b)-3.80(-5), (c)-4.26(-5) and (d)-4.76(-5).

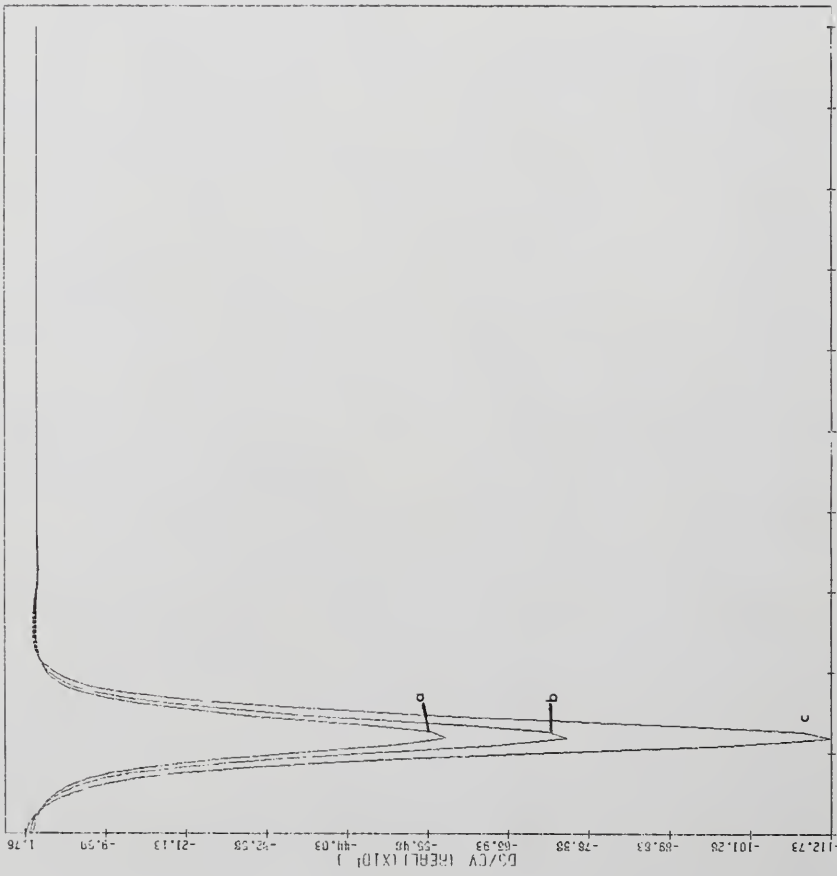

Figure 5-22: The real part of the pulsational $\delta S/C_v$ for the Cepheid model. These are the eigenvectors of AK2, (a) fundamental, (b) first and (c) second overtone.

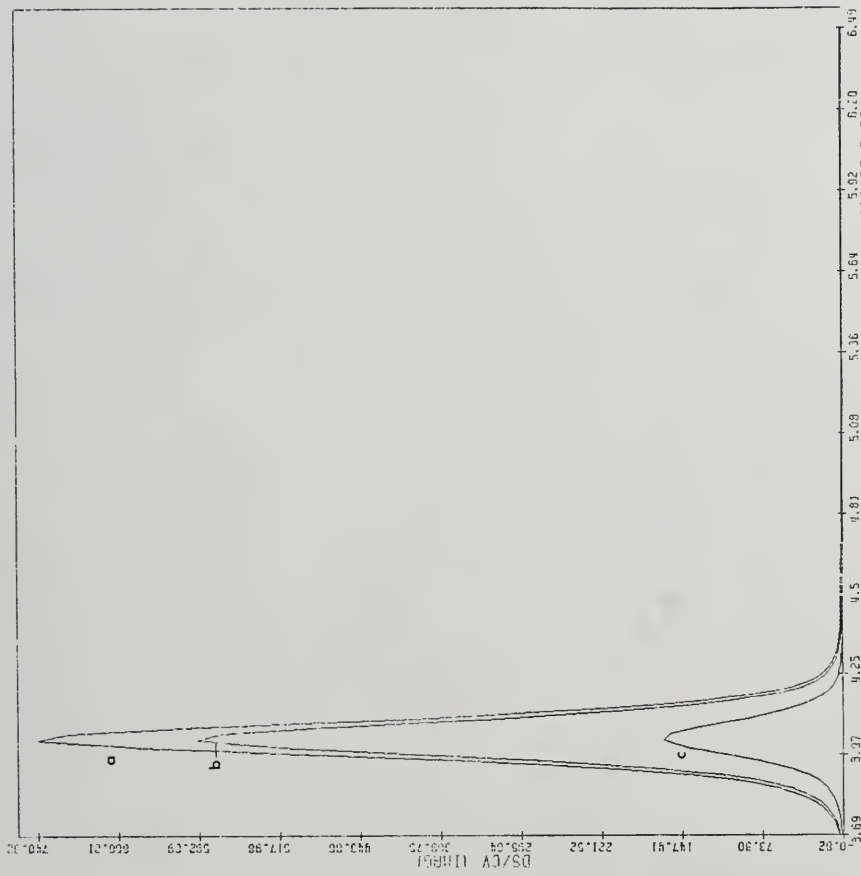

Figure 5-23: The imaginary part of the pulsational $\delta S/C_y$ for the Cepheid model. These are the eigenvectors of AK2, (a) fundamental, (b) first and (c) second overtone.

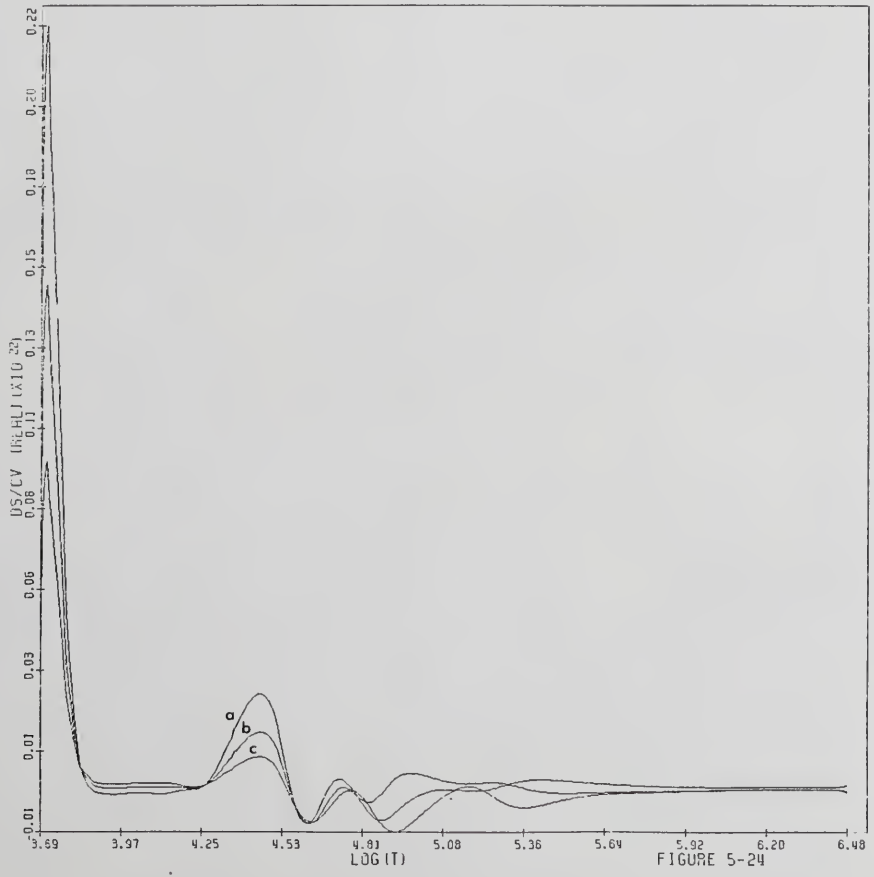

Figure 5-24: The real part of the pulsational $\delta S/C_v$ for the Cepheid model. These are the eigenvectors of D, (a) fundamental, (b) first and (c) second overtone.

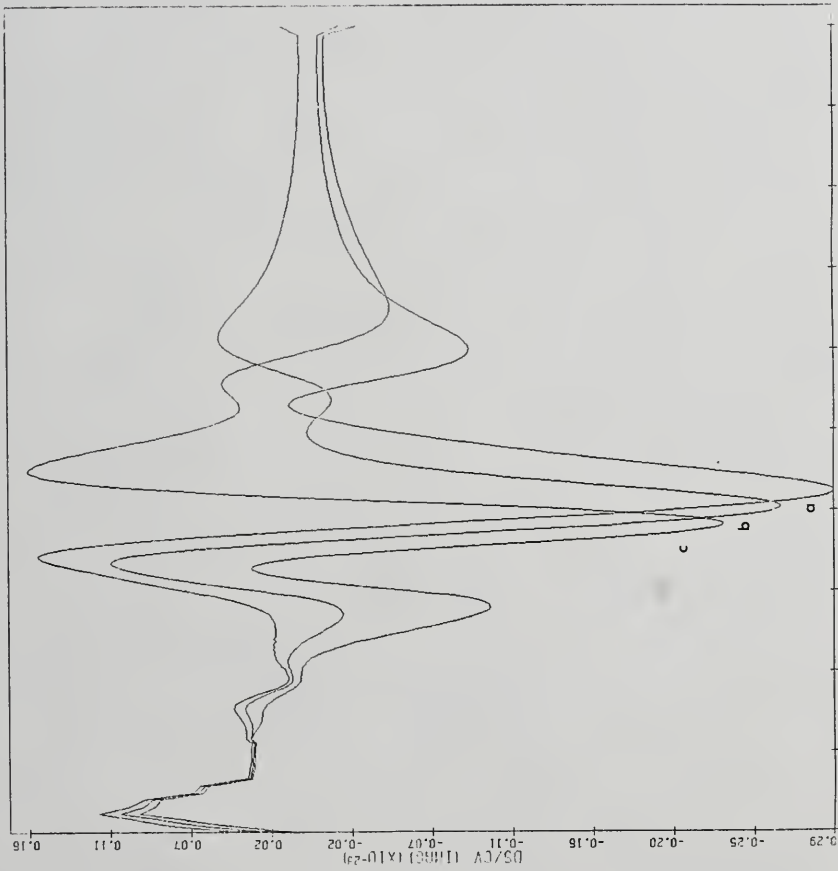

Figure 5-25: The imaginary part of the pulsational $\delta S/C_v$ for the Cepheid model. These are the eigenvectors of D, (a) fundamental, (b) first and (c) second overtone.

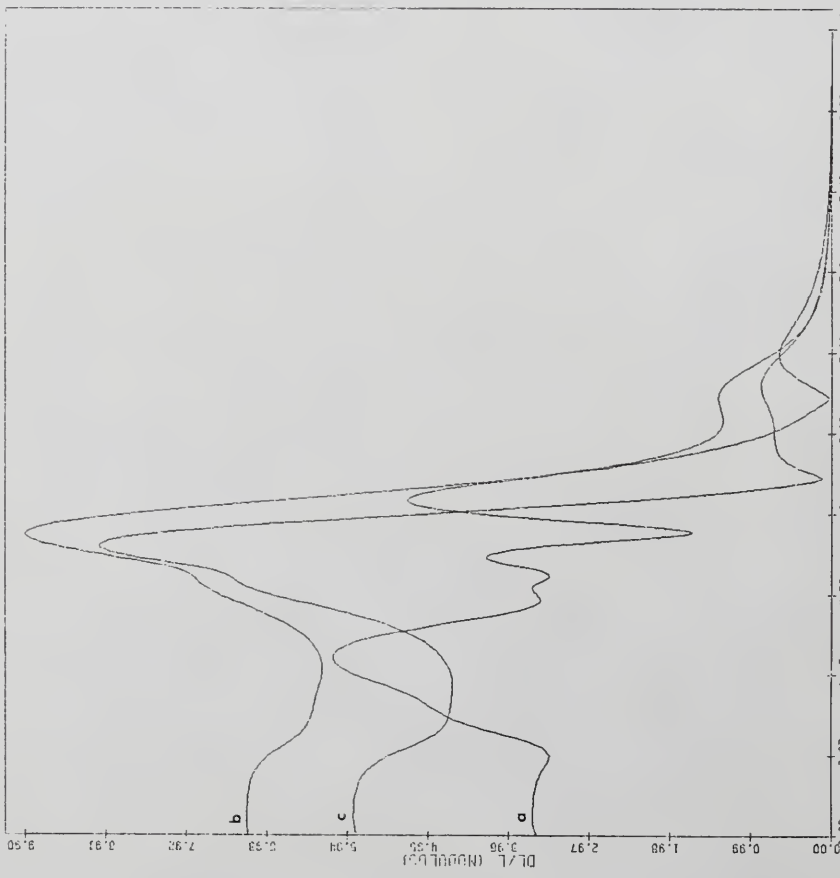

Figure 5-26: Modulus of the pulsational luminosity variations for the Cepheid model, (a) fundamental, (b) first overtone and (c) second overtone.

Table 5-1

BW Vulpeculae

$M=11.0\ M_{sun}$

$\log(L/L_{sun})=4.23$

$T_{eff}=25120$ K

$\Pi_0=0^d.193$, $\eta_0=-1.9 * 10^{-4}$

$\Pi_1=0^d.147$, $\eta_1=-2.3 * 10^{-3}$

$\Pi_2=0^d.118$, $\eta_2=-1.5 * 10^{-2}$

Composition X=0.70, Y=0.28, Z=0.02

Envelope mass = $5.02\ M_{sun}$

Table 5-2

DL Cassiopeiae

$M=5.69\ M_{sun}$

$\log(L/L_{sun})=3.57$

$T_{eff}= 5848\ K$

$\Pi_0= 7^d.87\ ,\ \eta_0 = 6.8 * 10^{-2}$

$\Pi_1= 5^d.64\ ,\ \eta_1= 1.9 * 10^{-1}$

$\Pi_2= 4^d.28\ ,\ \eta_2= 6.2 * 10^{-2}$

Composition X=0.70, Y=0.28, Z=0.02

Envelope mass = $2.76\ M_{sun}$

CHAPTER VI

DISCUSSION

To understand the utility of the thermal eigenvectors, we shall look at various forms that the linearized pulsation equations (3-5 and 3-6) acquire when the ξ_n's are used to expand them in the ratio of thermal time to pulsation period. Eliminating δS one can rewrite 3-5 and 3-6 as an integro-differential equation:

$$\omega^2 \, \delta r = \left(A + B \frac{1}{i\omega - D} C \right) \delta r. \qquad (6\text{-}1)$$

we have an eigenvalue problem for ω^2 and δr. Eliminating δr , 3-5 and 3-6 can be written in a form suitable for studying the secular behavior of a star:

$$i\omega\delta S = \left(D + G \frac{1}{\omega^2 - A} B\right) \delta S. \qquad (6\text{-}1a)$$

The $i\omega - D$ term is a resolvent that can be expanded in the complete set of eigenvectors of D. Adopting the Dirac (or bra-ket, see Davydov 1965, ch. 5) notation of quantum mechanics, this set is $\{ -\sigma_n , | \xi_n > \}$, and equation 6-1 becomes

$$\omega^2 \, \delta r = \left(A + \sum_n B \frac{| \xi_n \rangle\langle \xi_n |}{i\omega + \sigma_n} C \right) \delta r \, . \qquad (6\text{-}2)$$

Next, the mechanical eigenvector is expanded in the set of eigenvalues and eigenvectors of A, $\{ \omega_i^2 , | y_i \rangle \}$. We would like to examine the non-adiabatic effects on a mode that is primarily adiabatic, and this expansion will be written as

$$\delta r \equiv | y \rangle = | y_i \rangle + \sum_{j \neq i} \alpha_j | y_j \rangle$$

and

$$\omega = \omega_i + \Delta\omega$$

where

$$\omega_i^2 | y_i \rangle = A | y_i \rangle \, .$$

Inserting this expansion and multiplying eq. 6-2 by $\langle y |$ give

$$(1 + \sum_{j \neq i} |\alpha_j|^2) \, \omega^2 = \langle y_i | A | y_i \rangle +$$

$$\sum_n \frac{\langle y_i | B | \xi_n \rangle\langle \xi_n | C | y_i \rangle}{i\omega + \sigma_n} +$$

$$\sum_j \sum_n \left(\alpha_j^* \frac{\langle y_j | B | \xi_n \rangle\langle \xi_n | C | y_i \rangle}{i\omega + \sigma_n} + \right.$$

$$\frac{\langle y_i |B| \xi_n \rangle \langle \xi_n |C| y_j \rangle}{i\omega + \sigma_n} \alpha_j) +$$

$$\sum_k \sum_j \sum_n \alpha_k^* \frac{\langle y_k |B| \xi_n \rangle \langle \xi_n |C| y_j \rangle}{i\omega + \sigma_n} \alpha_j .$$

(6-3)

This expression is rather cumbersome, but following the normal quantum mechanical perturbation scheme, we evaluate the change in the eigenfrequency using the initial eigenvector. Choosing the adiabatic mode as the starting point, the quasi-adiabatic correction can be written as

$$\omega^2 - \omega_i^2 = \sum_n \frac{\langle y_i |B| \xi_n \rangle \langle \xi_n |C| y_i \rangle}{i\omega + \sigma_n} \qquad (6\text{-}4)$$

which is identical to equation (26) in Castor (1971). The normal quasi-adiabatic approximation is $\sigma_n/\omega_i \ll 1$, for all possible n, reducing 6-4 to

$$\omega^2 - \omega_i^2 = \frac{1}{i\omega_i} \langle y_i |BC| y_i \rangle \qquad (6\text{-}5)$$

as $\sum_n | \xi_n \rangle \langle \xi_n | = 1$.

This expression for the quasi-adiabatic correction can be further analyzed if $\Delta\omega/\omega \ll 1$. Then $\omega^2 \approx \omega_i^2 + 2\omega_i \Delta\omega$ and eq. 6-5 can be rewritten

$$\Delta\omega = -\frac{i}{2}\frac{1}{\omega_i^2} < y_i \,|BC|\, y_i >,$$

a result identical to the γ_i (equation 8, in Buchler 1983). Here, $\Delta\omega$ is purely imaginary, as all quantities on the right are real, and generally shows that the star is stable ($i\Delta\omega < 0$) as the diagonal elements of B are positive and the diagonal elements of C are negative.

This recapitulation of the quasi-adiabatic analysis serves to point out that by knowing the structure of the thermal modes, a better approximation can be made. Partitioning the thermal modes into two sets,

$$S_1 = \{ \sigma_n, \xi_n, n = 1, N_T : \sigma_n/\omega_i < 1 \}$$

and

$$S_2 = \{ \sigma_n, \xi_n, n = N_T + 1, N : \omega_i/\sigma_n < 1 \},$$

eq. 6-2 can be rewritten as an eigenvalue problem assuming an adiabatic starting point only to determine N_T

$$\omega^2 \,|\, y > = A|\, y > + \sum_{n=1}^{N_T} \frac{B|\, \xi_n >< \xi_n \,|C|\, y >}{i\omega + \sigma_n} + \sum_{n=N_T+1}^{N} \frac{B|\, \xi_n >< \xi_n \,|C|\, y >}{i\omega + \sigma_n}. \qquad (6\text{-}6)$$

The second term on the right is the quasi-adiabatic correction, now with an appropriate cutoff. However, the cutoff is not in the spatial

variable, as the integrals implied by the notation extend over the entire mass of the star. The correct cutoff is to stop the sum at the thermal eigenvalue whose magnitude is just below the pulsation frequency, as the sum over the set S_1 is doing. For this reason, the second term should be more correct in the calculation of this part of the stability coefficient.

The third term produces a correction in the lowest order, and therefore cannot be treated as a perturbation. To see this effect, the denominators of the sums are expanded in a binomial series and eq. 6-6 becomes

$$\omega^2 \mid y > = A \mid y > + \frac{1}{i\omega} \sum_{n=1}^{N_T} \frac{B \mid \xi_n >< \xi_n \mid C \mid y >}{1 + \sigma_n / i\omega} + \sum_{n=N_T+1}^{N} \frac{B \mid \xi_n >< \xi_n \mid C \mid y >}{\sigma_n (1 + i\omega/\sigma_n)} \qquad (6\text{-}7)$$

or

$$\omega^2 \mid y > = A \mid y > + \frac{1}{i\omega} \sum_{n=1}^{N_T} B \mid \xi_n > (1 - \frac{\sigma_n}{i\omega}) < \xi_n \mid C \mid y > + \sum_{n=N_T+1}^{N} B \mid \xi_n > (1 - \frac{i\omega}{\sigma_n}) < \xi_n \mid C \mid y >. \qquad (6\text{-}8)$$

The first term is the quasi-adiabatic correction already discussed and the second is the effect of the outer layers on the pulsation. The

expansion is in ω/σ_n, and in the limit ω/σ_n -->0, or very short thermal times; this sum becomes

$$\sum_{n=N_T+1}^{N} B|\ \xi_n >\frac{1}{\sigma_n}< \xi_n\ |C|\ y >.$$

This term represents a zero-order quantity and should not be neglected when the initial eigenvalue is calculated. If the thermal modes had a theta-function behavior at the transition zone, the set S_2 would form a complete set in and of itself for describing the thermal response of the outer layers of the star on time scales shorter than ω^{-1}. The actual eigenvectors have a fairly sharp fall at this point; so, a first try at including these terms is to write the sum over states as D'^{-1}, where D' is the outer $[(N - N_T)*(N - N_T)]$ submatrix of D that includes only those zones with $I > N_T$. Substituting D' for the second sum over states gives

$$\omega^2\ |\ y > = A|\ y > +$$

$$\frac{1}{i\ \omega}\sum_{n=1}^{N_T} B|\ \xi_n >< \xi_n\ |C|\ y > -$$

$$B|(D')^{-1}|C|\ y > + i\omega B|(D')^{-2}|C|\ y >. \quad (6\text{-}9)$$

This equation can be expanded in the ratio of the proper time scales; the second term on the right $\alpha_1 = \sigma/\omega_0$ and the last two in $\alpha_2 = \omega_0/\sigma$. Writing $\alpha=\alpha_1=\alpha_2$ to give the simplest expression and arranging the equations in a hierachy of terms by order in α give

$$\omega_0^2 \mid y_0 > = (A - B(D')^{-1}C)\mid y_0 > \qquad (6\text{-}10a)$$

$$\omega_0^2 \mid y_1 > + 2\omega_0\omega_1 \mid y_0 > = (A - B(D')^{-1}C)\mid y_1 > +$$

$$\frac{1}{i\omega_0} \sum_{n=1}^{N_T} B\mid \xi_n >< \xi_n \mid C\mid y_0 > +$$

$$i\omega_0 B(D')^{-2}C\mid y_0 >; \qquad (6\text{-}10b)$$

where

$$\mid y > = \mid y_0 > + \alpha \mid y_1 > + \alpha^2 \mid y_2 > + \ldots$$

and

$$\omega = \omega_0 + \alpha\omega_1 + \alpha^2\omega_2 + O(\alpha^3).$$

To eliminate secular terms in the equation for $\mid y_1 >$, the scalar product $< y_0 \mid y_1 >$ is set to zero. For convenience we shall set $<y_0|y_0>=1$. This gives the initial eigenvalue and the first order stability coefficient as

$$\omega_0^2 = < y_0 \mid A - B(D')^{-1}C\mid y_0 > \qquad (6\text{-}11a)$$

$$\omega_1 = - \frac{1}{2\omega_0^2} \sum_{n=1}^{N_T} < y_0 \mid B\mid \xi_n >< \xi_n \mid C\mid y_0 > +$$

$$1/2 < y_0 \mid B(D')^{-2}C\mid y_0 >. \qquad (6\text{-}11b)$$

At any point the matrix D' can be replaced by the sum over states that it approximates

$$\omega_0^2 = \langle y_0 \,|(A + \sum_{n=N_T+1}^{N} B|\ \xi_n > \frac{1}{\sigma_n} < \xi_n\ |C)|\ y_0 >, \quad (6\text{-}12a)$$

$$\omega_1 = -\frac{1}{2\omega_0^2} \sum_{n=1}^{N_T} < y_0\ |B|\ \xi_n >< \xi_n\ |C|\ y_0 > +$$

$$1/2 \sum_{n=N_T+1}^{N} < y_0\ |B|\ \xi_n > \frac{1}{\sigma_n^2} < \xi_n\ |C|\ y_0 >. \quad (6\text{-}12b)$$

Equations 6-11a and 6-11b agree with equations 25 and 39 respectively in Buchler and Regev (1982b), who derived them from physical arguments regarding the constant luminosity of the outer layers. It should be noted that the assumption of $\frac{d\ \delta L/L}{d\ m} = 0$ is not valid over the entire section of the Cepheid model above the transition zone. The sum over states is valid, and comparing the thermal mode $\delta L/L$ to that of the LNA analysis (Figure 5-16), we see that the functional dependence of the LNA $\delta L/L$ is reproduced by the thermal modes.

Using the infinitely sharp cutoff limit, the eigenvectors of 6-10a can be calculated in a straight forward way. Defining the error in $|y_0>$ as

$$E_y = \{ \sum_I |\ y(I) - \delta r(I)\ |^2 \}^{1/2},$$

where δr is the real part of the mechanical eigenvector given by the LNA stability analysis and both eigenvectors are normalized to unity in their respective scalar products. The error in the eigenfrequency is defined as

$$E_{\omega} = |\omega_0 - \omega_{LNA}|/\omega_{LNA}$$

These quantities are plotted in Figure 6-1 against the location of the transition zone, log(T_{trans}). A sharp minimum is seen at log(T_{trans}) = 5.23, corresponding to the location of the actual transition zone as predicted by the luminosity eigenvector plotted in Figure 5-6. In this model, the change is rather abrupt, falling a factor of 4 when log(T_{trans}) changes by -0.13 or +0.04 . The change ω_0 is not as dramatic, reflecting the "minimum" principle that a quasi-adiabatic oscillation will follow.

When the same quantities are plotted for the Cepheid (Figure 6-2), it is obvious that the agreement is not much better than using the adiabatic eigenvectors. The error is reduced at a point where the transition zone is located, but not by a factor of 10 as in BW Vul. This results from the more complicated behavior of $\delta L/L$ in the Cepheid (see Figure 5-16). The thermal modes have a large peak in the ionization zones due to the integrating factor's temperature dependence but do not have the rapid decrease inward of those in BW Vul. Therefore, the approximation of replacing the sum over states by the submatrix D' is not a good one for this class of star. As the sum over states contains the necessary information about the luminosity variations in the exterior, including the integrals as in 6-12a should give much closer agreement. This problem is discussed in Pesnell and Buchler (1983).

Comparing the initial eigensystem 6-12a to the adiabatic wave equation produces three differences:

1) There is, at present, no guarantee of either the reality or positivity of the eigenvalues of either 6-11a or 6-12a.

2) The eigenvectors $< y_0 |$ and $| y_0 >$ are not necessarily related by a transposition, much less being equal. The matrix $A - B(D')^{-1}C$ is not symmetric but is of an upper Hessenberg form whose only advantage is being diagonally dominant. The eigenvectors come as right and left hand vectors and must be calculated separately.

3) There is no proven relationship between the number of nodes in $| y_0 >$ and the numeric position of ω_0^2 in an increasing ordering of the spectrum of $A - B(D')^{-1} C$.

However, for stars which are predominantly adiabatic, as most pulsators are, the eigenvalues are close to the adiabatic frequencies, the second part of the operator having little or no effect on A. The transposed eigenvector has a serious numeric problem. In the region of the transition zone, the transposed matrix has a structure such that a discontinuity appears in $< y_0 |$. The use of eq. 6-12a instead of 6-11a will spread this feature over several zones, removing the discontinuity. When the transposed eigenvector is calculated using the LNA analysis, the feature is present but is much smoother. A change in the method of calculation is indicated, not a revision of 6-12a.

A final observation regarding 6-12a concerns the limit N_T -->0. As a normal star is almost adiabatic (N_T -->N), the opposite limit must describe an abnormal star. For the condition N_T -->0 to be satisfied, the non-adiabatic regions of the star must be extensive, covering all of the star that is oscillating. These conditions may be found in the R

Corona Borealis stars or other highly evolved stars where the envelopes are tenuous and have low gas to total pressure ratios. In these stars, trying to recover the adiabatic limit in one obvious way will lead to some rather strange behavior of ω^2.

Introducing an arbitrary scale factor, λ , into equations 3-5 and 3-6, which represents the ratio of the pulsation period to some overall thermal time, they become

$$\omega^2 \delta r = A \cdot \delta r + B \cdot \delta S \qquad (6\text{-}13a)$$

$$i\omega \delta S = \lambda (C \cdot \delta r + D \cdot \delta S). \qquad (6\text{-}13b)$$

For most stars, when $\lambda \to 0$ the adiabatic limit is recovered as δS is forced to 0. However, in the integro-differential form, splitting the thermal modes as before,

$$\omega^2 \, | \, y > = A | \, y > +$$

$$\frac{\lambda}{i\omega} \sum_{n=1}^{N_T} \frac{B | \, \xi_n > < \xi_n \, | C | \, y >}{1 \; + \; \lambda\sigma_n / i\omega} +$$

$$\lambda \sum_{n=N_T+1}^{N} \frac{B | \, \xi_n > < \xi_n \, | C | \, y >}{i\omega \; + \; \lambda\sigma_n} . \qquad (6\text{-}14)$$

The value of N_T may depend on λ for most stars, but for the radiation dominated atmospheres, the thermal response time is very short for all modes whose cutoff in amplitude is above the normal transition zone. Using the ideal gas as before, the atmosphere should have a low density

gradient and opacity gradient so that the diffusion length (4-15) is large. If the outer modes have $\sigma_n/\omega \gg 1$ for all $n > N_T$, then N_T is almost constant during this discussion.

In the limit of $\lambda \rightarrow 0$ (N_T constant), eq. 6-14 is expanded using the binomial theorem as before,

$$\omega^2 \mid y > = A \mid y > +$$

$$\sum_{n=N_T+1}^{N} B \mid \xi_n > \frac{1}{\sigma_n} < \xi_n \mid C \mid y > + O(\lambda) \ , \quad (6\text{-}15)$$

the $B(D')^{-1}C$ term does not disappear. For highly non-adiabatic envelopes, this term can dominate and change the spectrum so that it no longer reduces to the adiabatic case. This would, in part, explain the modes that have been named "strange" modes (King 1980; Saio and Wheeler 1982).

This explanation of the strange modes does not require that a mode be near (in some sense) to an adiabatic mode. There are no theorems that prove that all of the eigenvalues of 6-12a are real, and starting from an adiabatic mode, the non-adiabatic corrections could move the frequency far away from the initial value. It is interesting that if N_T can be considered constant, the adiabatic limit is never recovered in some models. This property is just what a strange mode shows.

Modes that possess the property of N_T being independent of λ shall be called "sudden" modes. They are characterized by a condition of thermal balance existing over a large fraction of the mechanical eigenvector's amplitude. The quasi-adiabatic stability coefficient would

be a poor approximation for these modes, as the second term in 6-12a will dominate ω_1. We must stress that the condition of thermal balance does not imply that the luminosity has a zero derivative in these modes.

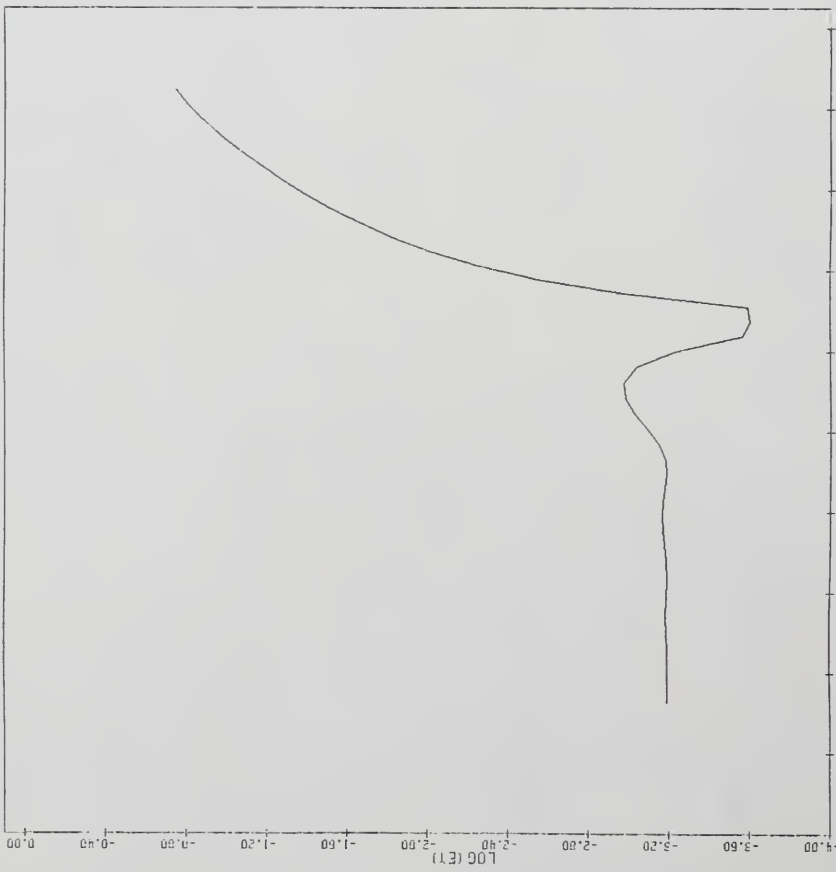

Figure 6-1: Logarithm of the error in the eigenvector versus the logarithm of the temperature of the transition zone for BW Vulpeculae.

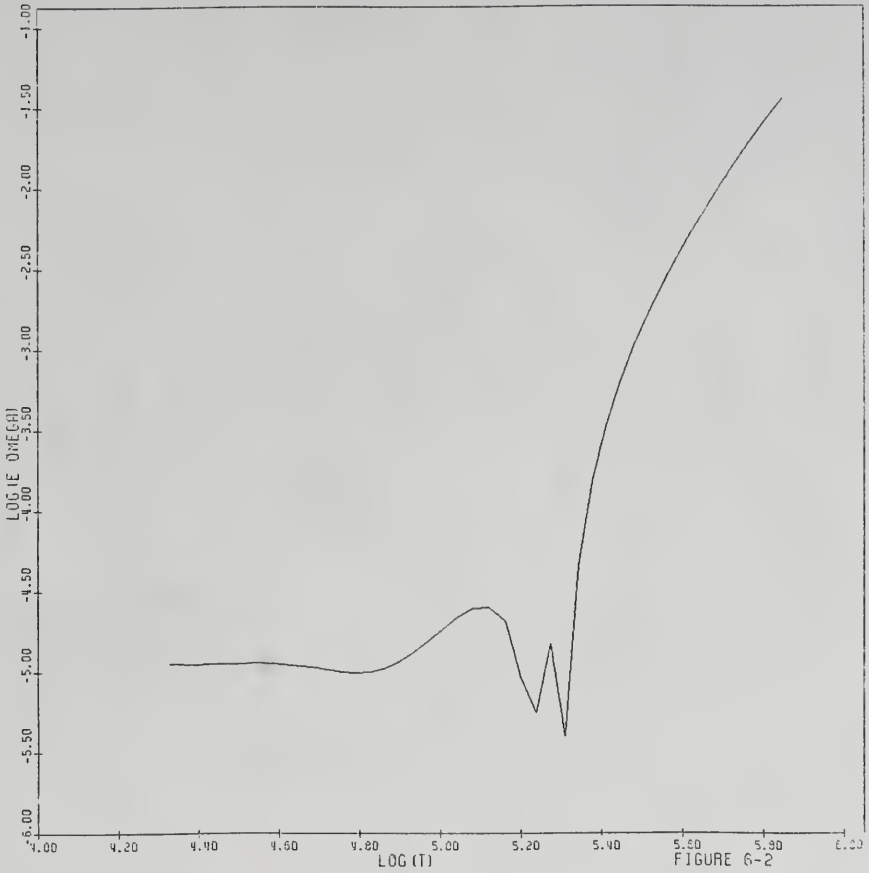

Figure 6-2: Logarithm of the error in the eigenvalue versus the logarithm of the temperature of the transition zone for BW Vulpeculae.

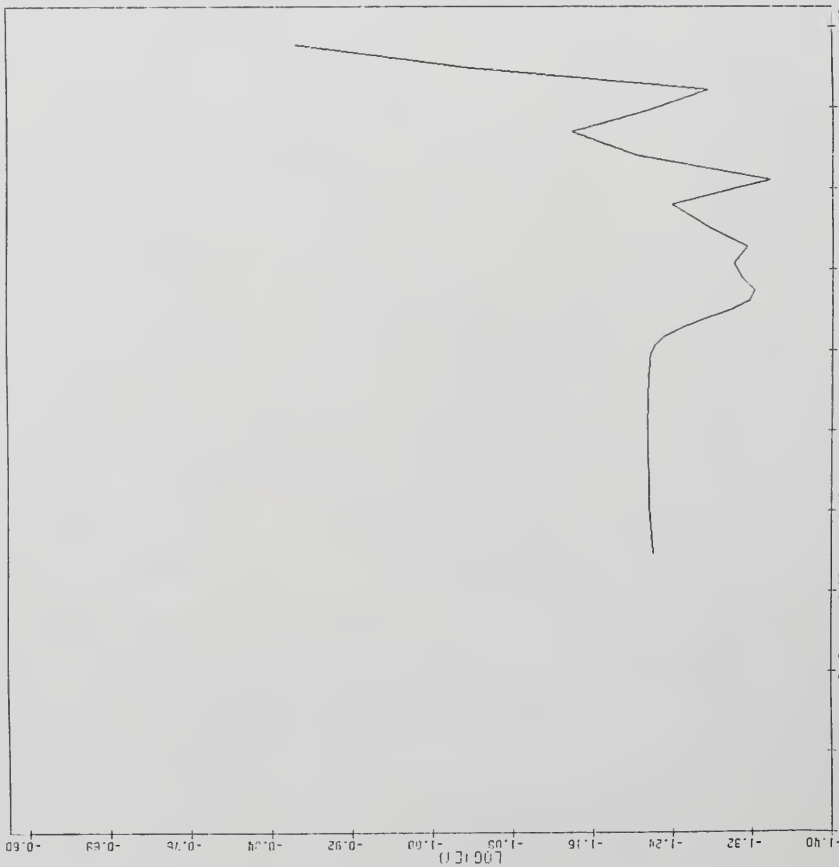

Figure 6-3: Logarithm of the error in the eigenvector versus the logarithm of the temperature of the transition zone for the Cepheid model.

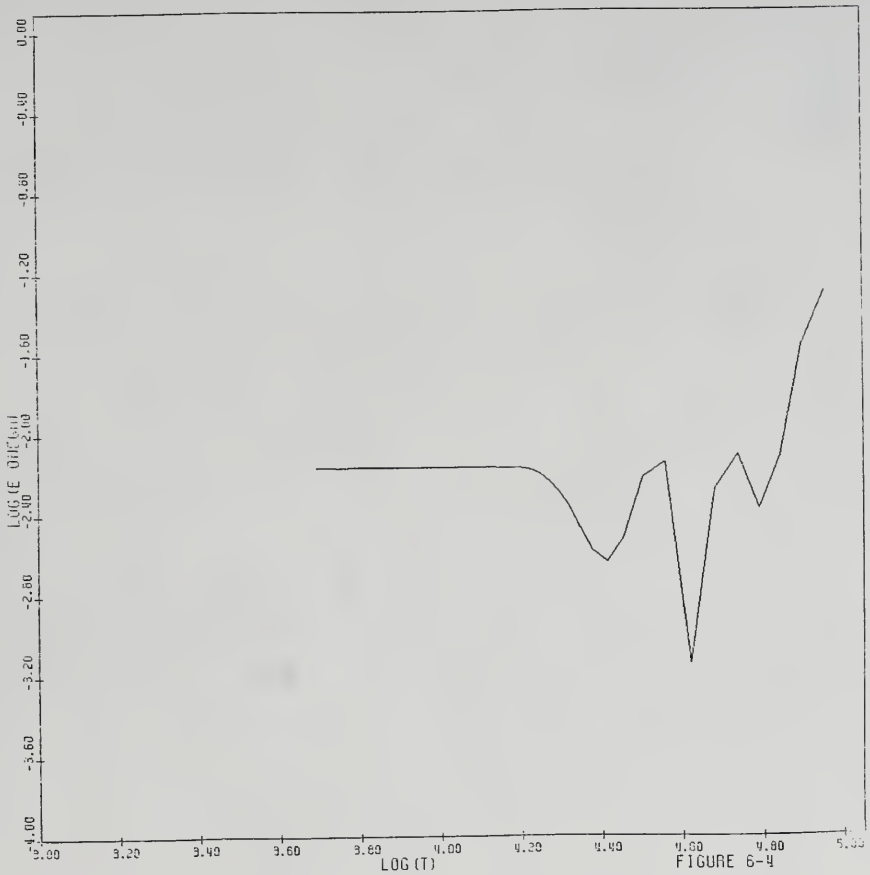

Figure 6-4: Logarithm of the error in the eigenvalue versus the logarithm of the temperature of the transition zone for the Cepheid model.

CONCLUSIONS

We have shown that the thermal structure of stellar pulsations can be represented by the eigenfunctions of the diffusion equation. As this equation is of second order in the spatial derivative, it can be mapped onto a Sturm-Liouville operator, with the concomitant theorems regarding the reality of the eigenvalues and the form of the eigenfunctions. This transformed operator defines a thermal time scale through a new independent variable with the units of $(\text{time})^{1/2}$. This time scale agrees with that of earlier authors in the interior and predicts the same location for the transition zone in a star.

The thermal modes that arise from the eigenvalue problem can be used to analyze the thermal effects in a first order perturbation expansion. The traditional adiabatic wave operator is replaced by an operator that includes the knowledge that the outer layers are in thermal balance, and that this does not imply that $\frac{d\ \delta L/L}{d\ m} = 0$ in these layers.

Partial spectra of the thermal modes are presented for two realistic stellar models, along with diagrams of the eigenvectors. Mathematically consistent expansions of the pulsation equations are presented that give the quasi-adiabatic stability coefficient and the

analogous expression when the outer layers are correctly accounted for. It is shown that a new type of mode, the "sudden", mode can be defined using these expressions.

The driving mechanism in Cepheids has features in the thermal modes that do not show up in a star of the Beta Cephei class. This casts doubt on the viability of ionization driving being responsible for these stars' variability.

In an aesthetic vein, a way of displaying the entropy or temperature variations for stars that normally have a "spike" in the hydrogen ionization zone is given, showing much of the detail in this region without the introduction of an arbitrary cutoff. This transformation also increases the numeric accuracy of solutions in the linear non-adiabatic pulsation stability analysis by limiting the variation of the elements of the coupling matrices.

APPENDIX A

THE ANALYTIC EQUATION OF STATE

For the purposes of these calculations, an equation of state has been developed, based in part on a routine supplied by Arthur Cox (Cox, A. N. 1980b). In this appendix the various formulae and constants used are discussed.

As our analysis requires the entropy of an ionizing gas, we first calculate the free energy (F) as a function of the specific volume (v), temperature (T), and composition (X,Y,Z). All thermodynamic functions can be evaluated by derivatives of F (Zel'dovich and Razier 1966, ch. III):

$$\text{entropy: } S = -\left(\frac{\partial F}{\partial T}\right)_{v,N}$$

$$\text{pressure: } P = -\left(\frac{\partial F}{\partial v}\right)_{T,N}$$

$$\text{internal energy: } E = -T^2\left(\frac{\partial (F/T)}{\partial T}\right)_{v,N}.$$

In order to calculate F, the approximation of an ideal, ionizing gas is adopted with the characteristics of the five species listed in Table A-1. Values for the mass weighting of the elements has been

adapted from Cox and Tabor (1976), and the atomic masses and ionization potentials are from Novotny (1973). For completeness, a term is added to include the effects of black body radiation. This is assumed to be that appropriate to isotropic radiation so that

$$F_{rad} = -\frac{a}{3} v T^4.$$

The ionized fraction of each element is determined by minimizing the free energy at the given temperature and specific volume. This procedure leads to a Saha equation that is solved using a Newton Method to a relative accuracy of 1 part in 10^{12} for the electron density. When the electron density is known, the reciprocal of the mean molecular weight (in moles/gram) is

$$n = 1/\mu = X/1.00797 + Y/4.0026 + Z/21.02447 + n_e.$$

The relative abundance of each ionization stage, n_i, is calculated from the ratios of the appropriate partition functions, and the free energy is written as a sum over these species.

$$F = -RT \{ \sum_i n_i \ln(m_i^{3/2} u_i / n_i) + n[-2.5048 + \ln(vT^{3/2})] \}$$

$$- \frac{a}{3} vT^4$$

where the constant term is:

$$1 + \frac{3}{2} \ln(2\pi m_p k) - \ln(N_A) - 3 \ln(h),$$

m_i is the species gram molecular weight, and u_i is the temperature independent partition function that is assumed to the ground state degeneracy.

The expressions for the entropy (ergs/gram/K), P (dynes/cm^2), and E (ergs/gram) are

$$S = R\{\sum_i n_i \ln(m_i^{3/2} u_i / n_i) + n[\, -1.0048 + \ln(vT^{3/2}) \,]\} + \frac{4a}{3} vT^3$$

$$P = nRT/v + \frac{a}{3} T^4$$

$$E = \frac{3}{2} nRT + avT^4 + \sum_i n_i \chi_i$$

Derivatives of the pressure and the internal energy are found by analytic differentiation of the above formulae.

The subroutine NEOS performs the calculations required to find the thermodynamic quantities as outlined above. A listing of this routine follows.

```
      SUBROUTINE NEOS(TIN,VIN,P,PV,PT,E,EV,ET,BP,BPV,BPT,
     &          OP,OPV,OPT,FRE,ENT,KUSE)
C
C     EQUATION OF STATE, OPACITY
C        FIRST ORDER ONLY
C     ARGUMENTS...TIN (DEGREES K), VIN=1/RHO (CM**3/GM)
C     METALS...
C        NA,AL ALWAYS IONIZED
C        MG,SI,FE INCLUDED AS SINGLE ELEMENT
C        ALL OTHERS IGNORED
C      KUSE=0, PRESSURE, INTERNAL ENERGY AND DERIVATIVES
C      KUSE=1, PRESSURE, INTERNAL ENERGY, OPACITY AND DERIVATIVES
C      KUSE=2, PRESSURE, INTERNAL ENERGY, ENTROPY AND DERIVATIVES
C      KUSE=3, PRESSURE, INTERNAL ENERGY, ENTROPY (WITH DERIVATIVES)
C              AND OPACITY (WITHOUT DERIVATIVES)
C      KUSE=4, OPACITY
C      KUSE=5, PRESSURE AND DERIVATIVES
C
C
C          TABLE OF RETURNED QUANTITIES.
C
C      FUNCTION        NAME   DERIVATIVE WITH RESPECT TO
C                                TEMP.        SP. VOL.
C-----------------------------------------------------*
C      PRESSURE      !    P !      PT       !     PV     *
C      INT. ENERGY   !    E !      ET       !     EV     *
C      OPACITY       !   OP !      OPT      !     OPV    *
C      MOLAR DENSITY !   BP !      BPT      !     BPV    *
C      ENTROPY       !  ENT !      ---      !     ---    *
C      FREE ENERGY   !  FRE !      ---      !     ---    *
C*****************************************************
C
      IMPLICIT REAL*8(A-H,O-Z)
C
C          X = HYDROGEN MASS FRACTION
C          Y = HELIUM MASS FRACTION
C          Z = METALLIC MASS FRACTION
C          PARGRM = MEAN MOLECULAR MOLAR DENSITY WITHOUT ELECTRONS
C
      COMMON/INHOM/  X,Y,Z,RMUC,PARGRM
      COMMON/CONST/  ZERO,ONE,TWO,THRE,FOR,TEN,AHF,QRT
C
C          R = GAS CONSTANT 8.31434E7
C          A = STEFAN-BOLTZMAN CONSTANT 7.56471E-15
C          BK = BOLTZMAN S CONSTANT 8.6170837E-5
C          AVAGD = AVAGADRO S NUMBER 6.02217E23
C          AD3 = A/3
```

```
C
      COMMON/THERMO/ R,A,BK,AVAGD,AD3
      DIMENSION CMASP(10),PARTN(10)
      DATA PARTN/ 10*0.0D0 /
      DATA CMASP/ 2.023958D0,1.011979D0,8.0078D0,16.015D0,
     &  8.0078D0,124.768D0,310.026D0,73.961D0,2.56984D-5,0.0D0 /
      DATA T3OUT,T4OUT/1.66579516 3D-25,3.802592017D-28/
      DATA T2OUT,T5OUT/ 5.347896D-35, 1.53021D-40 /
C
CC          IONIZATION POTENTIALS FOR HYDROGEN AND HELIUM
C
      DATA XH,XHE,XHE2/13.595D0,24.581D0,54.403D0/
      DATA C1,C2,C3,C4/4.0092926D-9,1.00797D0,4.0026D0,21.02447D0/
      DATA XM,CM,ZPZP/7.9D0,0.7D0,0.12014D0/
      DATA PREC / 1.D-12 /
      DATA ONHLF/1.5D0/
      V = VIN
      T = TIN
      IF( V .LE. ZERO ) GO TO 11
      IF( T .LE. ZERO ) GO TO 10
      FRE = ZERO
      ENT = ZERO
      RT = R*T
      TT4 = T**4
      TK = ONE/(T*BK)
      SQT = DSQRT(T)
C     C1=ORIGINAL(C1(0.33334622))/R
      T1 = V*SQT**3*C1
      T2 = T2OUT
      IF( T .GT. 2.D3 ) T2 = DEXP(-XH*TK)
      T3 = T3OUT
      IF( T .GT. 5.D3 ) T3 = DEXP(-XHE*TK)
      T4 = T4OUT
      IF( T .GT. 1.D4 ) T4 = DEXP(-XHE2*TK)
      T5 = T5OUT
      IF( T .GT. 1.D3 ) T5 = DEXP(-XM*TK)
      D = T1*T2
      B = FOR*T1*T3
      C = B*T1*T4
      DD = TWO*CM*T1*T5
      ZNA = Z*2.48D-3/24.969D0
      ZMG = Z*ZPZP/45.807D0
C
CC          CONVERGE ON ELECTRON DENSITY USING THE SAHA EQUATION.
CC
CC          GES IS THE MOLAR DENSITY OF ELECTRONS.
C
      GES = (X+Y*AHF)/(ONE+Y/(FOR*C))
```

```
      IF(GES.LT.X) GES = AHF*(DSQRT(D*(D+FOR*X))-D)
      IF( GES .LT. 1.D-6*Z ) GES = 1.D-6*Z
      XC2 = X/C2
      YC3 = Y/C3
C
CC
CC          NEWTON METHOD FOR ELECTRON DENSITY.
C
      DO 1 I=1,25
      T2 = C/GES+GES+B
      GEP = XC2*D/(GES+D)+YC3*(B+TWO*C/GES)/T2
     &   +ZMG*DD/(GES+DD) + ZNA
      T1 = ONE+XC2*D/(D+GES)**2+YC3/T2*
     &  (TWO*C/GES**2+(B+TWO*C/GES)*(ONE-C/GES**2)/T2)
     &  + ZMG*DD/(GES+DD)**2
      DGES = (GEP-GES)/T1
      GES = GES+DGES
      IF( DABS(DGES)/GES .LT. PREC ) GOTO 3
    1 CONTINUE
      GOTO 12
    3 CONTINUE
C
CC  ELECTRON PRESSURE
C
      PE = RT*GES/V
      IF( KUSE .EQ. 4 ) GOTO 5
C
CC     TOTLN = 1/MU = X/C2+Y/C4+Z/C3+GES
C
      TOTLN = PARGRM+GES
      XX = D/(GES+D)
      T2 = GES+B+C/GES
      YY = B/T2
      ZZ = C/(GES*T2)
      WW = DD/(GES+DD)
C
CC          DERIVATIVES OF THE SAHA EQUATION FOR THE PRESSURE AND
CC        INTERNAL ENERGY TEMPERATURE AND DENSITY DERIVATIVES.
C
      T1 = YC3*(B+TWO*C/GES)
      QC0 = ONE+XC2*XX/(GES+D)+ZMG*WW/(GES+DD)+YC3/T2*
     &     (TWO*C/GES**2+(B+TWO*C/GES)*(ONE-C/GES**2)/T2)
      QC1 = XC2*(ONE-XX)/(GES+D)
      QC4 = ZMG*(ONE-WW)/(GES+DD)
      QC2 = (YC3-T1/T2)/T2
      QC3 = (YC3*TWO-T1/T2)/(GES*T2)
      QGV = (QC1*D+QC2*B+QC3*TWO*C+QC4*DD)/(QC0*V)
      QP1 = D*(ONHLF+XH*TK)/T
```

```
      QP2 = B*(ONHLF+XHE*TK)/T
      QP3 = C*(THRE+(XHE+XHE2)*TK)/T
      QP4 = DD*(ONHLF+XM*TK)/T
      QGT = (QC1*QP1+QC2*QP2+QC3*QP3+QC4* QP4)/QC0
      IF( KUSE .EQ. 1 ) GOTO 5
C
C           PRESSURE DUE TO THE IDEAL GAS
C
      P = RT*TCTLN/V
      PT = P/T+RT*QGT/V
      PV = RT*QGV/V-P/V
C
C           BP IS R/MU
C
      BP = R*TCTLN
      BPV = R*QGV
      BPT = R*QGT
C
C            ADD THE RADIATION PRESSURE
C
      P = P+AD3*TT4
      PT = PT+FOR*AD3*TT4/T
      IF( KUSE .EQ. 5 ) RETURN
C
C           IONIZATICN ENERGY
C
      EI = (R/BK)*(XH*XX*XC2+YC3*(XHE*YY+(XHE+XHE2)*ZZ)
     &      +ZMG*XM*WW + ZNA*5.524D0 )
C           TOTAL INTERNAL ENERGY
      E = ONHLF*RT*TOTLN + A*V*TT4 + EI
      EV = T*PT-P
      QXT = ((CNE-XX)*QP1-XX*QGT)/(GES+D)
      DT2 = QGT*(ONE-C/GES**2)+QP2+QP3/GES
      QYT = (QP2-B*DT2/T2)/T2
      QZT = (QP3-C*QGT/GES-C*DT2/T2)/(T2*GES)
      QWT = ((CNE-WW)*QP4-WW*QGT)/(GES+DD)
      EIT = (R/BK)*(XH*QXT*XC2+YC3*(XHE*QYT+(XHE+XHE2)*QZT)+
     &      ZMG*XM*QWT)
      ET = ONHLF*R*(TOTLN+T*QGT)+FOR*A*V*TT4/T+EIT
      IF( KUSE .EQ. 2 ) GOTO 30
      IF( KUSE .EQ. 0 ) RETURN
C
C           OPACITY IS FROM A FIT BY STELLINGWERF AP. J. 195(441)1975
C       AND AP. J. 195(705)1975.
C
    5 CONTINUE
      I = 1
      GOTO 22
```

```
   23  GOTO (24,25,26),I
   24  OP = GKAP
       OPV = ZERO
       OPT = ZERO
       IF( KUSE .EQ. 4 ) RETURN
       IF( KUSE .EQ. 3 ) GOTO 30
       I = 2
       V = V*(ONE+1.D-8)
       GOTO 22
   25  CONTINUE
C     OPV=-D(LOG(KAPPA))/D(LOG(V))=D(LOG(KAPPA))/D(LOG(RHO))
       OPV = ONE-QGV*VIN/GES+(OP-GKAP)/OP*1.D8
       I = 3
       V = VIN
       T = T*(ONE+1.D-8)
       TT4 = TT4*1.0000004D0
       SQT = SQT*1.0000000005D0
       GOTO 22
   26  CONTINUE
C     OPT=D(LOG(KAPPA))/D(LOG(T))
       OPT = ONE+QGT*TIN/GES+(GKAP-OP)/OP*1.D8
       RETURN
C
C      GENERAL FIT TO KING OPACITY TABLES
C
   22  CONTINUE
       ZVAR1 = 21.D0*Z+0.979D0
       ZVAR2 = 105.D0*Z+0.895D0
       YVAR1 =-6.D-5*Y+6.294D-5
       YVAR2 = 4.53D6*Y-3.0447D5
       U = T*1.D-4
       U4 = TT4*1.D-16
       U6 = U4*U**2
       SQU = SQT*1.D-2
       UM8 = ONE/U4**2
       UM10 = ONE/(U4*U6)
       U25 = SQU*U**2
       U35 = U*U25
       UM45 = ONE/(U*U35)
       UM5 = U6/U
       V1 = V**0.35D0
       V2 = DSQRT(V1)
       T1 = 760.D0*UM5+316.D0/V2
       T1 = YVAR1*V1*U35+ONE/T1
       T1 = ONE/(TEN*U6+ONE/T1)
       T2 = ZVAR1*YVAR2*UM10+2.13D-3*V2*ZVAR2*UM45
C           OLD STELLINGWERF FORMULA
C       T2 = 1780.D0*U25/ZVAR1+ONE/T2
```

```
C              NEW STELLINGWERF FORMULA
       T2 = 513.4D0*U4/(ZVAR1*U) + ONE/T2
       T2 = 47.3D0*UM8+ONE/T2
       T2 = ONE/(4.D3+ONE/T2)
C   CPACITY
       GKAP = PE*(4.819D-13*V/U+T1+T2)
       GO TO 23
C
C              ENTROPY AND FREE ENERGY
C      SEE ZELDOVICH & RAZIER,PHYSICS OF SHOCK WAVES AND
C      HIGH TEMP. PHENOMENA,1966,PP. 192-197
C
   30  CONTINUE
C       7.76D11=SQRT(AVAGADRO S NUMBER)
       T32     = SQT**3*V/7.76026D11
       T32 = DLOG(T32)*TOTLN
       PARTN(2) = XC2*XX
       PARTN(4) = YC3*YY
       PARTN(5) = YC3*ZZ
       PARTN(6) = ZNA
       PARTN(7) = ZMG*WW
       PARTN(1) = XC2 - PARTN(2)
       PARTN(3) = YC3-PARTN(4)-PARTN(5)
       PARTN(8) = Z/C4-ZMG*WW-ZNA
       PARTN(9) = GES
       ENTX = 8.38508D0*TOTLN
       ETA = ONE
       DO 40 J=1,10
          IF( PARTN(J) .LE. ZERO ) GOTO 40
          ETA = ETA * (PARTN(J)/CMASP(J))**PARTN(J)
   40  CONTINUE
       ETA = DLOG(ETA)
       ENT = ((-ONE)*ETA+T32+ENTX+2.5D0*TOTLN)*R
      &       +(FOR*AD3)*V*T**3
C       FRE = (ETA-T32-ENTX-TOTLN)*R*T-AD3*V*T**4
       RETURN
C
C      DIAGNOSTICS
C
   10  WRITE(6,100) T,V
  100  FORMAT(1H0,27HNEGATIVE TEMP IN EOS      T=,1PD10.3,2X,2HV=,D10.3)
       STOP
   11  WRITE(6,101) T,V
  101  FORMAT(1H0,27HNEGATIVE DENSITY IN EOS   T=,1PD10.3,2X,2HV=,D10.3)
       STOP
   12  WRITE(6,102) T,V
  102  FORMAT(1H0,27HNO CONVERGENCE IN EOS     T=,1PD10.3,2X,2HV=,D10.3)
       STOP
```

TABLE A-1

PHYSICAL PROPERTIES OF THE COMPONENTS OF THE GAS

#	species	atomic weight	u	χ
		(gr/mole)		(eV)
1	Neutral Hydrogen	1.00797	2	13.595
2	Ionized Hydrogen	1.00797	1	---
3	Neutral Helium	4.0026	2	24.581
4	Ionized Helium (singly)	4.0026	4	54.403
5	Ionized Helium (doubly)	4.0026	2	---
6	Ionized metal	24.969	1	5.524
7	Ionizing metal (single stage)	45.807	1	7.900
8	Neutral metal	17.969	-	---
9	Electrons	5.486(-4)	2	---

APPENDIX B

THE INITIAL MODEL INTEGRATOR

For the present calculations, an initial envelope model gives an adequate description of the variation of the physical parameters as a function of position in a star. To construct an initial model we must solve the equations governing stellar structure with time derivatives set equal to zero. With the appropriate boundary conditions, a solution can be found by integrating inward from the surface until the desired envelope mass is reached. In this appendix, the equations, boundary conditions and integration techniques are discussed.

A spherically symmetric model in hydrostatic and thermal balance is governed by the equations

conservation of mass $$\frac{d\,r^3}{d\,m} = \frac{v}{4\pi/3} \qquad \text{(B-1)}$$

conservation of momentum $$\frac{d\,P}{d\,m} = -\frac{G\,M}{4\pi r^4} \qquad \text{(B-2)}$$

conservation of energy $$\frac{d\,L}{d\,m} = 0 \qquad \text{(B-3)}$$

energy transport $$L(m) = -(4\pi r^2)^2 \frac{ac}{3\kappa} \frac{d\,T^4}{d\,m} \qquad \text{(B-4)}$$

where they have been written in a Lagrangian form that uses the interior mass as the independent variable. The energy transport is assumed to be purely radiative and the opacity is a fit due to Stellingwerf (1975a,b).

We divide the model into N mass shells, or zones, with each variable assigned to the zone center or zone interface as shown in Figure B-1. The mass of shell I (zone-centered mass) is called DM1(I), and the mass associated with interface I is

$$DM2(I+1) = \tfrac{1}{2}(DM1(I)+DM1(I+1)).$$

A mass derivative of a zone-centered quantity (pressure etc.) is interface centered and vice-versa. All quantities are seen to be correctly centered with the exception of the opacity in equation B-8. The presence of the zone-centered opacity in the equation for the interface-centered luminosity necessitates the use of special interpolation schemes to correctly center the $\frac{1}{\kappa}\frac{d T^4}{d m}$ term. Several authors have published formulae for this purpose and we have chosen that of Stellingwerf (1975a) for our calculations. The specific form of the difference equations is such that they are compatible with the nonlinear hydrodynamic code developed at Los Alamos National Laboratory (King et al. 1964; Cox, Brownlee, and Eilers 1966). This work forms the basis for further work in nonlinear behavior of models and this compatibility enables us to compare our results with those of fully nonlinear models.

With this convention for the masses and derivatives, equations B-1 through B-5 can be written as

$$\frac{R(I+1)^3 - R(I)^3}{DM1(I)} = \frac{v(I)}{4\pi/3} , \qquad (B\text{-}5)$$

$$\frac{P(I+1) - P(I)}{DM2(I+1)} = - \frac{G\ M(I+1)}{4\pi\ R(I+1)^4} , \qquad (B\text{-}6)$$

$$\frac{L(I+1) - L(I)}{DM1(I)} = 0 , \qquad (B\text{-}7)$$

and

$$L(I+1) = -(4\pi R(I+1)^2)^2 \frac{ac}{3} \left\langle \frac{1}{\kappa} \frac{d\ T^4}{d\ m} \right\rangle . \qquad (B\text{-}8)$$

The boundary conditions at the surface are $P=P_0$ and $T=T_0=0.841T_{eff}$, where P_0 is the pressure due to an external atmosphere and T_{eff} is the effective temperature of the model. As these conditions are valid at a point beyond the actual model surface, they must be incorporated into the differenced equations by giving some elements of B-6 and B-8 special forms.

In the momentum equation (B-6), the pressure derivative is rewritten as

$$\frac{P(N+1) - P(N)}{DM2(N+1)} = - \frac{P(N)}{1/2\ f_A\ DM1(N)} . \qquad (B\text{-}9)$$

When $f_A = 1$ the outer pressure ($P(N+1)=P_0$) is zero, but there is a better approximation for f_A (see King et al. 1964). If one assumes that an infinite number of zones extends outward from the surface with each zone mass a constant fraction of the one interior, f_A can be written as

$$f_A = \frac{\alpha - 1}{\alpha + 1} \qquad (B\text{-}10)$$

where α = DM1(N)/DM1(N-1) is the constant mass ratio. Values for f_A are normally 0.1-0.2 . This modification moves the zero pressure boundary condition to the outermost zone as desired. For a consistent treatment, radiation pressure is added to this "atmospheric" contribution.

When the boundary condition $T = T_0$ is inserted into the luminosity equation (B-7), an analogous expression can be derived for the temperature of the outermost mass layer. Starting with equation B-4, and assuming the luminosity and radius are constant, a grey atmosphere relationship for T(N) is found:

$$T^4(N) = T_{eff}^4 \frac{3}{4} (\tau + 2/3) \qquad \text{(B-11)}$$

where

$$\tau = \int \kappa \, dm/4\pi R(N+1)^2 \qquad \text{(B-12)}$$

Given T_{eff} , DM1(N), R(N+1), and the opacity, T(N) can be evaluated so that the boundary condition is satisfied.

Along with the assumed form for the outermost mass shell, there are two additional relationships that need to satisfied to give a physical model. One of these is that the radius evaluated at the effective temperature be the photospheric radius given by the black body formula

$$L = 4\pi\sigma \, R_{photo}^2 \, T_{eff}^4 \, . \qquad \text{(B-13)}$$

This is satisfied by introducing an auxillary expression

$$R(N+1) = R_{photo}(1 + \beta) \qquad (B\text{-}14)$$

and varying β so that

$$R(T(m) = T_{eff}) = R_{photo} .$$

The second condition requires the optical depth of the outermost shell be at a chosen value, τ_0 , where $10^{-3} \leq \tau_0 \leq 10^{-2}$. This is achieved by varying the outer zone mass until τ(eq. B-12) = τ_0 . Both of conditions are satisfied to a relative accuracy of one part in one million.

Given eq. B-5 through B-8 and boundary conditions B-9, B-11, B-12, and B-14, we have a complete set of equations to describe the envelope. To integrate this set, the mass, luminosity, effective temperature, and composition are read in, guesses for DM1(N), f_A , and β are made, then values for P(N) and T(N) are found from B-9, B-6 and B-11. This zone is automatically in thermal balance and v(N) is changed to satisfy hydrostatic balance in a one dimension Newton method. The optical depth of the zone, $\tau(N)$, is compared to τ_0 , and if they do not agree, the mass of the zone is modified following another Newton method until $\tau(N) = \tau_0$ to the desired accuracy.

After the outer zone is converged, eq. B-5 is used to find the inner radius R(N). The mass for zone N-1 is a constant multiple of DM1(N), and this constant can be varied so that $T(N-1)/T(N) < \gamma$, where γ is normally 1.06. In a gas whose dominant component is hydrogen, the electron density changes rapidly during the ionization of hydrogen. This

increase in electrons corresponds to a rapid increase in the opacity as well. A star whose surface temperature is greater than 15,000 K will not have this difficulty as the ionization of helium does not produce as rapid an increase in the electron concentration. By limiting the temperature gradient as above, the opacity and opacity derivatives are not permitted to vary so much that they introduce further inaccuracies into the calculations.

Once DM1(N-1) is known, the hydrostatic pressure necessary to keep DM1(N) in suspension is given by eq. B-6. A first guess for T(N-1) and v(N-1) is made and they are corrected by a two dimension Newton method. Convergence of T and v to the desired accuracy ends the iteration in this zone. This process of guessing (if necessary) the mass ratio, evaluating the hydrostatic pressure and zeroing the functions

$$|P_{eos} - P_{hydro}| \text{ and } |L_{eq.B-8} - L_{star}|$$

is repeated for each succesive interior zone until the desired envelope mass has been integrated.

A subsidary loop controls the radius relationship. Using the initial guess for β , eq. B-5 to B-8 are integrated to a point where the temperature exceeds the effective temperature. By linear interpolation in the mass shells, the radius at T_{eff} is found and compared to R_{photo} . While the condition $| R(T_{eff}) - R_{photo}| / R_{photo} > 10^{-6}$ is true, β is changed using a secant method, R(N+1) is recalculated, and the integration restarted.

At the end of the integration, all equations are satisfied to the desired accuracy (here one part in one million.) This integration has been extremely stable for all physically viable models and no traps or inconsistencies are known to exist. The routine ATMHAT and support routines for the model builder are listed below.

```
      SUBROUTINE ATMHAT(ITITL)
      IMPLICIT REAL*8(A-H,O-Z)
C
C           ROUTINE FOR FINDING THE HYDROSTATIC EQUIL. MODEL
C     IN THERMAL BALANCE
C
      COMMON/PHYPAR/ RP(60),TP(60),VP(60),CV(60),DKDR(60),DKDT(60),
     &               DM1(60),AKAP(60),DM2(60),RM(60),RPPR(60)
      COMMON/BLK1/   IRAD,NFLAG,IR
      COMMON/BLK4/   PRESP(60),G1(60),G3M1(60),ENTPRY(60)
      COMMON/BLK5/   ALPHA,FSUBA,RAT,NRAT,MASOPT
      COMMON/BLK8/   G,AC3,SIGMA,PI,PI2,PI4,PI8,PI43
      COMMON/BLK17/  PFI,DTP,DVP,TTAU
      COMMON/CONST/  ZERO,ONE,TWO,THRE,FOR,TEN,AHF,QRT
      COMMON/OBSERV/ TEFF,RLUMGV,TOTMAS,RPHOTO,CORRAD
      COMMON/TAB/    ENVMAS,CORMAS,UMASS,RLUMX
      COMMON/CORRCT/ FRACS,FRACB,TTEST,VTEST,ITER
      COMMON/STORE/  DRAD(180),REN(60)
      COMMON/THERMO/ R,A,BK,AVAGD,AD3
      COMMON/INHOM/  X,Y,Z,RMUC,PARGRM
      DIMENSION ITITL(20)
C
C       A TWO DIMENSION NEWTON METHOD IS USED FOR THE SHELL INTEGRATION.
C
C          FLAGS AND COUNTERS:
C               MASCNT: COUNTS ITERATIONS WHEN CHANGING MASS OF NEW
C                       SHELL IN MASOPT=3 LOOP. ( MAXIMUM OF 30)
C
C               MASFLG: >0, ZONE MASS SUCH THAT TEMP. RATIO IS IN LIMITS
C                       SET BY TFACL AND TFACU.
C                       <0, STATIC MASS RATIO
C
C               KFLAG: COUNTER AND FLAG FOR PHOTOSPHERIC RADIUS LOOP.
C                      =>0, CONVERGING RFAC TO GIVE RP(IR+1)
C                       <0, CONVERGED RFAC.
C
C               ITAU: COUNTER FOR OPTICAL DEPTH OF OUTERMOST ZONE.
C                       (MAXIMUM OF 30)
C
C               IC: COUNTER FOR ACTUAL T,V ITERATIONS.
C                   MAXIMUM VALUE OF 30, FOR IC .GT. 10
C                   THE MAXIMUM FRACTIONAL CHANGE IN T AND V IS
C                   INCREASED FROM FRACS TO FRACB.
C
C                                                  2/16/83  WD PESNELL
C
      IC = 0
```

```
      ID = 0
C
C          DT AND DV ARE FRACTIONAL INCREMENTS IN T AND V FOR
C       EVALUATING THE NUMERIC DERIVATIVE OF THE LUMINOSITY EQUATION.
C
      DT = TEN**(-7)
      DV = TEN**(-7)
      IRP1 = IR + 1
      DELV = ZERO
      DELT = ZERO
      FRAC = FRACS
      UMASS = ZERO
      TAUWNT = 1.D-3
      CALL RADLUM(IR,-1)
      RPHOTO = DSQRT(RLUMGV/(PI4*SIGMA))/TEFF**2
      IF( DM1(IR) .LE. ZERO ) DM1(IR) = TWO*PI8*RPHOTO**2*TAUWNT/
     &                                                  AKAP(IR)
      TFACUS = 1.06D0
      TFACL = 1.002D0
      MASFLG =-1
      IF( MASOPT .EQ. 3 ) MASFLG = 1
C
C          THE DYNAMIC ZONING TO KEEP THE TEMPERATURE RATIO WITHIN
C       THE BOUNDS TFACU .GE. T(I)/T(I+1) .GE. TFACL IS STOPPED
C       WHEN T(I) .GT. TMAS3.
C
      TMAS3 = 1.5D4
C
C     START AT THE OUTER BOUNDARY
C
      CORMAS = TOTMAS-ENVMAS
      RM(IR+1) = TOTMAS
      UMASS = DM1(IR)
   20 CONTINUE
      ALPHA = RATMAS(MASOPT,IR)
      KFLAG = 0
      RFAC = 0.75D0
      RTEMP = 1.D17*DSQRT(RLUMGV)/(TOTMAS*TEFF)
      GOTO 40
C
C          SECANT METHOD TO FIND PHOTOSPHERIC RADIUS. RTEFF IS THE
C       VALUE OF THE RADIUS AT T=TEFF AS FOUND BY INTERPOLATION
C       IN THE SHELL MASSES.
C          THE OUTERMOST RADIUS IS GIVEN BY R=RPHOTO*(1+RFAC*RTEMP)
C       AND THE SECANT METHOD CHANGES RFAC TO CONVERGE ON R SUCH
C       THAT RTEFF = RPHOTO.
C                                                        10/17/82  WDP
```

```
   41  RTEFF = RPOFT(I,TEFF)
       RERROR = RTEFF/RPHOTO - ONE
       IF( MASOPT .EQ. 3 ) MASFLG = 1
       WRITE(11,1000) KFLAG,RERROR,RFAC,RTEFF,RPHOTO
       IF( DABS(RERROR) .LT. 1.D-6 ) GOTO 49
       KFLAG = KFLAG + 1
       IF( KFLAG .EQ. 1 ) GOTO 42
       RFAC2  = RFAC1
       RERRO2 = RERRO1
       RFAC1  = RFAC
       RERRO1 = RERROR
       RFAC = (RFAC2*RERROR-RFAC*RERRO2)/(RERROR-RERRO2)
       GOTO 40
   42  CONTINUE
       RFAC2  = ZERO
       RFAC1  = RFAC
       RERRO2 = ZERO
       RERRO1 = RERROR
       RFAC = RFAC*1.2D0
       IF( RTEFF .GT. RPHOTO ) RFAC = RFAC*0.75D0
       GOTO 40
   49  CONTINUE
C            CONVERGED ON RP(TEFF)=RPHOTO SET KFLAG=-1 AND DO MODEL
       KFLAG =-1
   40  CONTINUE
C
C          LAST ZONE IS CONVERGED TO BE AT AN OPTICAL DEPTH THAT IS
C        CONSISTENT WITH THE GREY ATMOSPHERE APPROXIMATION. THE MASS
C        OF THE LAST ZONE IS CHANGED TO GIVE AN OPTICAL DEPTH OF
C        TAUWNT IF MASOPT=3 IS CHOSEN.
CC
CC                                                        1/9/83 WDP
C
       RP(IR+1) = RPHOTO*(ONE+RFAC*RTEMP)
       ITAU = 0
   25  CONTINUE
       ITAU = ITAU + 1
       IF( ITAU .GT. 30 ) GOTO 100
       PRS = DM1(IR)*G*RM(IR+1)/(FSUBA*PI8*RP(IR+1)**4)
      &      +AD3*TP(IR)**4
       ID = 0
   21  CONTINUE
       DO 22 IC=1,25
       CALL STATE(IR,0)
       FV = PRESF(IR)-PRS
       DELV =-FV/DVP
       IF( DABS(DELV).GT.AHF*VP(IR) ) DELV = AHF*DSIGN(VP(IR),DELV)
       VP(IR) = VP(IR)+DELV
```

```
      IF( DABS(DELV)/VP(IR) .LT. VTEST ) GOTO 27
   22 CONTINUE
      PRSM = DM1(IR)*G*RM(IR+1)/(FSUBA*PI8*RP(IR+1)**4)
      PRS = PRSM+AD3*TP(IR)**4
         VP(IR) = R*TP(IR)/PRS
      IF( (RP(IR+1)**3-DM1(IR)*VP(IR)/PI43) .LT. ZERO )
     &    VP(IR) = AHF*PI43*RP(IR+1)**3/DM1(IR)
      GOTO 21
   27 CALL NEXTR(IR)
      CALL RADLUM(IR,0)
      ID = ID+1
      IF( ID .GT. 50 ) STOP
      DELT = TTAU-TP(IR)
      IF( DABS(DELT).GT.QRT*TP(IR) ) DELT = QRT*DSIGN(TP(IR),DELT)
      TP(IR) = TP(IR)+DELT
      IF( ID .GT. 10 ) WRITE(11,1000) ID,TP(IR),VP(IR),DELT
      IF( DABS(DELT)/TP(IR) .GT. TTEST ) GOTO 28
      IF( TP(IR) .LT. 5.D0*TEFF ) GOTO 29
      DM1(IR) = DM1(IR)*0.8D0
      GOTO 20
   28 CONTINUE
      PRSM = DM1(IR)*G*RM(IR+1)/(FSUBA*PI8*RP(IR+1)**4)
      PRS = PRSM+AD3*TP(IR)**4
         VP(IR) = R*TP(IR)/PRS
      IF( (RP(IR+1)**3-DM1(IR)*VP(IR)/PI43) .LT. ZERO )
     &    VP(IR) = AHF*PI43*RP(IR+1)**3/DM1(IR)
      GOTO 21
   29 CONTINUE
C
CC          CONVERGE THE LAST ZONE MASS SUCH THAT APPROXIMATE OPTICAL
CC        DEPTH IS GIVEN BY TAUWNT.
CC
CC                                                          1/9/83 WDP
C
      IF( MASOPT .NE. 3 ) GOTO 26
C3.18      FTAU = 0.75D0*TAUWNT-0.1875D0*AKAP(IR)*DM1(IR)/(PI4*RP(IRP1)**2)
      FTAU = TAUWNT-AKAP(IR)*DM1(IR)/(PI4*RP(IRP1)**2)
C3.18      DELM = PI4*FTAU*RP(IR+1)**2/(AKAP(IR)*0.1875D0)
      DELM = PI4*FTAU*RP(IR+1)**2/AKAP(IR)
      IF( DABS(DELM) .GT. DM1(IR)*QRT ) DELM = DSIGN(DM1(IR),DELM)*QRT
      DM1(IR) = DM1(IR) + DELM
      WRITE(11,1000) ITAU,FTAU,AKAP(IR),DM1(IR),DELM
      IF( DABS(FTAU) .GT. 1.D-6 ) GOTO 25
   26 CONTINUE
      UMASS = DM1(IR)
      DM2(IR+1) = PI4*RP(IR+1)**4*PRESF(IR)*FSUBA/(G*RM(IR+1))
C
C          ONCE THE OUTER MASS SHELL IS FOUND AND A GUESS ENTERED FOR
```

```
C       THE OUTER RADIUS, START INTEGRATING INWARD USING A DOUBLE
C       NEWTON-RAPHESON METHOD IN TEMPERATURE AND SPECIFIC VOLUME.
C       THE LUMINOSITY IS ASSUMED CONSTANT IN THIS VERSION OF CODE,
C       HOWEVER BY CHANGING THE VARIABLE RLUMX IN THE DESIRED FASHION
C       THE LUMINOSITY CAN BE CHANGED BY NUCLEAR ENERGY GENERATION OR
C       ANY ARBITRARY FUNCTION OF MASS.
C
C          THE COMPOSITION PROFILE IS CONSTANT IN MASS AS WELL. THIS
C       CAN BE REMEDIED BY CHANGING X, Y, AND Z IN A SUITABLE WAY.
C       THESE TWO CHANGES ARE COMPATIBLE WITH THE CODE AND SHOULD
C       REQUIRE VERY LITTLE MODIFICATION OF THE BASIC STRUCTURE OR
C       METHOD OF SOLUTION.
C
C                                                    2/21/83  WD PESNELL
C
      DO 10 II=2,IR
C
C          INTEGRATION IS FROM THE SURFACE INWARD.
C
           I = IR+1-II
           RLUMX = RLUMGV
           RM(I+1) = RM(I+2) - DM1(I+1)
C
C          PRSM IS THE HYDROSTATIC PRESSURE DUE TO ALL ZONES ABOVE
C       ZONE I EXCEPT FOR THE I+1 INTERFACE.
C
           PRSM = PRS
           TFACU = TFACUS
           IF( MASFLG .LE. 0 ) GOTO 12
           ALPHA = 1.3D0
           MASCNT = 0
C
C          ZONE MASS SUCH THAT TFACL<T(I)/T(I+1)<TFACU
C
           GOTO 12
   15  CONTINUE
           TRAT = TP(I)/TP(I+1)
           MASCNT = MASCNT + 1
           IF( MASCNT .GT. 30 ) GOTO 100
           IF( MASCNT .GT. 25 ) TFACU = TFACU + 0.01D0
           IF( TRAT .LT. TFACL ) GOTO 17
           IF( TRAT .LT. TFACU ) GOTO 19
           ALPHA = ALPHA*0.8D0
           GOTO 12
   17      ALPHA = ALPHA*1.25D0
   12  CONTINUE
           DM1(I) = DM1(I+1)*ALPHA
           IF( MASOPT .EQ. 2 ) DM1(I) = DM1(I+1)+ALPHA
```

```
            DM2(I+1) = AHF*(DM1(I)+DM1(I+1))
            PRS = PRSM+G*RM(I+1)*DM2(I+1)/(PI4*RP(I+1)**4)
            FRAC = FRACS
            IC = 0
            TP(I) = TP(I+1)*1.1D0
            VP(I) = VP(I+1)*0.9D0
   11   CONTINUE
            VPI = VP(I)
        TPI = TP(I)
        CALL NEXTR(I)
        IC = IC + 1
        IF( IC .GT. 30 ) GOTO 100
        IF( IC .GT. 10 ) FRAC = FRACB
        CALL STATE(I,0)
        CALL LUMEN(I,FT)
        FT = FT-RLUMX
        FV = PFI - PRS
C
CC       CALCULATE VOLUME AND TEMPERATURE DERIVATIVES
C
        DFVDV = DVP
        DFVDT = DTP
        TP(I) = TPI*(ONE+DT)
        CALL LUMEN(I,DFT)
        DFT = DFT-RLUMX
        DFTDT = (DFT-FT)/(TPI*DT)
        TP(I) = TPI
        VP(I) = VPI*(ONE+DV)
        CALL NEXTR(I)
        CALL LUMEN(I,DFT)
        DFT = DFT-RLUMX
        DFTDV = (DFT-FT)/(VPI*DV)
        DET = DFTDT*DFVDV-DFTDV*DFVDT
        DELV  = (FV*DFTDT-FT*DFVDT)/DET
        DELT  =-(FV*DFTDV-FT*DFVDV)/DET
C            LIMIT CORRECTIONS
        IF( DABS(DELV) .LT. FRAC*VPI .AND. DABS(DELT) .LT. FRAC*TPI )
     &                          GOTO 30
        XX = FRAC*DMIN1(VPI/DABS(DELV),TPI/DABS(DELT))
        DELT = DELT*XX
        DELV = DELV*XX
   30   TP(I) = TPI - DELT
        VP(I) = VPI - DELV
        IF( IC .GT. 20 )
     &    WRITE(11,1000) IC,TPI,DELT,VPI,DELV,FV,FT,I
 1000   FORMAT(I4,1P6D15.6,I4)
        IF( DABS(DELT)/TP(I) .GT. TTEST ) GOTO 11
        IF( DABS(DELV)/VP(I) .GT. VTEST ) GOTO 11
```

```
      CALL NEXTR(I)
      CALL STATE(I,0)
      CALL RADLUM(I,0)
      IF( (KFLAG.GE.0) .AND. (TP(I).GT.TEFF) ) GOTO 41
      IF( MASFLG .GT. 0 ) GOTO 15
   19 CONTINUE
            DM2(I+1) = AHF*(DM1(I)+DM1(I+1))
            UMASS = UMASS + DM1(I)
            IF( MASFLG .LE. 0 ) GOTO 10
      IF( TP(I) .GT. TMAS3 ) ALPHA = RATMAS(1,I)
      WRITE(11,1002) I,TP(I),VP(I),ALPHA
      IF( TP(I) .GT. TMAS3 ) MASFLG =-1
   10 CONTINUE
      DM2(1) = AHF*DM1(1)
      RM(1) = TOTMAS-UMASS
C
CCC    MODEL IS FINISHED, RETURN TO CODE
C
C         CORESV IS THE APPROXIMATE SPECIFIC VOLUME OF THE INERT
C       CORE UNDERLYING THE ENVELOPE. IF CORESV/VP(1) IS LESS THAN
C       0.1, THE ENVELOPE MASS SHOULD BE DECREASED OR THE NUMBER
C       OF ZONES INCREASED. THIS CONDITION NORMALLY MEANS THE THE
C       INNER RADIUS OF THE INNERMOST ZONE WAS FOUND TO BE NEGATIVE
C       AND WAS SET TO A SMALL VALUE.
C
C                                                    2/16/83  WDP
C
      CORESV = PI43*RP(1)**3/CORMAS
      WRITE(11,9001) (ITITL(I),I=1,20),IR
      WRITE(11,9002) RLUMGV,TOTMAS,TEFF,BPHOTO,RP(1),CORMAS,CORESV
      WRITE(11,9004) MASOPT,ENVMAS,UMASS,FSUBA,TFACU,TFACL,TTEST,VTEST
      WRITE(11,9003)
      DO 90 I=1,IR
      CALL NEOS(TP(I),VP(I),P1,P2,P3,E,E1,E2,B,B1,B2,O,O1,O2,F,S,2)
      REN(I) = S*RMUC/R
      WRITE(11,1002) I,RP(I+1),VP(I),TP(I),PRESF(I),REN(I),DM1(I)
   90 CONTINUE
      RETURN
  100 CONTINUE
C
C     LACK OF CONVERGENCE OVERALL
C
      WRITE(6,9000)
      STOP
 1002 FORMAT(I4,1P6D16.7)
 9000 FORMAT(25H NO CONVERGENCE IN ATMHAT    )
 9001 FORMAT(50H1 INITIAL MODEL IN HYDROSTATIC AND THERMAL BALANCE,//,
     &  20A4,I4,6H ZONES,/   )
```

```
9002  FORMAT(4X,18H TOTAL LUMINOSITY=,1PD11.4,12H TOTAL MASS=,D11.4,
     &  17H EFFECTIVE TEMP.=,D11.4,/,6X,21H PHOTOSPHERIC RADIUS=,D11.4,
     &   13H CORE RADIUS=,D11.4,11H CORE MASS=,D10.3,8H CORESV=,D10.3)
9003  FORMAT(4H  I ,5X,6HRADIUS,10X,10HSP. VOLUME
     &,5X,11HTEMPERATURE,6X,8HPRESSURE,9X,7HENTROPY,8X,9HZONE MASS)
9004  FORMAT(6X,8H MASOPT=,I2,15H ENVELOPE MASS=,1PD14.7,
     &   17H ENV. MASS CALC.=,D14.7,7H FSUBA=,D12.5,/,6X,7H TFACU=,
     &   D10.3,7H TFACL=,D10.3,7H TTEST=,D10.3,7H VTEST=,D10.3,//)
      END
      FUNCTION RPOFT(I,TOI)
      IMPLICIT REAL*8(A-H,O-Z)
C
CC       FINDS THE VALUE OF THE RADIUS AS A FUNCTION OF THE
CC     TEMPERATURE BY INTERPOLATION IN THE MESH.
CC        BASED ON THE INTERPOLATION SCHEME DEVELOPED FOR THE
CC      NON-RADIAL, NON-ADIABATIC CODE.
C                                                  10/14/82 WDP
C
      COMMON/PHYPAR/ RP(60),TP(60),VP(60),CV(60),DKDR(60),DKDT(60),
     &      DM1(60),AKAP(60),DM2(60),RM(60),RPPR(60)
      COMMON/BLK8/   G,AC3,SIGMA,PI,PI2,PI4,PI8,PI43
      COMMON/CCNST/  ZERO,ONE,TWO,THRE,FOR,TEN,AHF,QRT
      DATA ONTH/0.33333333333333D0/
      RPOFTI = (RP(I)**3+AHF*DM1(I)*VP(I)/PI43)**ONTH
      RPOTI1 = (RP(I+1)**3+AHF*DM1(I+1)*VP(I+1)/PI43)**ONTH
      RPOFT = RPOTI1-(RPOFTI-RPOTI1)*(TOI-TP(I+1))/(TP(I)-TP(I+1))
      RETURN
      END
      SUBROUTINE LUMEN(K,RL)
      IMPLICIT REAL*8(A-H,O-Z)
C
CC            RETURNS THE LUMINOSITY OUT OF ZONE K
C
      COMMON/BLK1/   IRAD,NFLAG,IB
      COMMON/BLK37/  RATIO(60),TP4(60),SPA1(480)
      COMMON/OBSERV/ TEFF,RLUMGV,TOTMAS,RPHOTO,CORRAD
      IF( K .EQ. IB ) GOTO 10
      CALL RADLUM(K,0)
      RL = (TP4(K)-TP4(K+1))*RATIO(K)
      RETURN
   10 CALL RADLUM(IB,-1)
      RL = RLUMGV
      RETURN
      END
      FUNCTION NODES(W,NZ,LOUT)
      IMPLICIT REAL*8(A-H,O-Z)
C FINDS NO. OF NODES(SIGN CHANGES) IN NZ ELEMENTS OF ARRAY W
      DIMENSION W(1),INODE(30)
```

```
      COMMON/CONST/  ZERO,ONE,TWO,THRE,FOR,TEN,AHF,QRT
      NODES=0
      NZ1=NZ-1
      DO 10 I=3,NZ1
      IF(W(I-1)*W(I).GE.ZERO) GO TO 10
C ZERO CROSSING FOUND. IS IT GENERAL ENOUGH TO BE A NODE?
      IF(W(I-2)*W(I-1).LT.ZERO) GO TO 10
      IF(W(I)*W(I+1).LT.ZERO) GO TO 10
      NODES=NODES+1
      INODE(NODES)=I-1
   10 CONTINUE
      INODE(NODES+1) = NZ
      IF(LOUT.EQ.0) RETURN
      WRITE(11,99) NODES
      IF(NODES.LT.1) RETURN
      WRITE(11,100) (INODE(I),I=1,NODES)
   99 FORMAT(/,1X,I2,12H NODES FOUND)
  100 FORMAT(7H NODES=,30I4)
      RETURN
      END
      BLOCK DATA
      IMPLICIT REAL*8(A-H,O-Z)
C        FUNDAMENTAL CONSTANTS ARE FROM NOVOTNY, INTRODUCTION TO
C     STELLAR ATMOSPHERES AND INTERIORS, 1973, APPENDIX II.
C                                                    2/16/83  WDP
      COMMON/CONST/  ZERO,ONE,TWO,THRE,FOR,TEN,AHF,QRT
      COMMON/BLK8/ GRAV,AC3,SIGMA,PI,PI2,PI4,PI8,PI43
      COMMON/THERMO/ R,A,BK,AVAGD,AD3
      DATA R,A,BK,AVAGD,AD3 / 8.31434D7,7.56471D-15,8.6170837D-5,
     &     6.02217D23,2.52157D-15 /
      DATA GRAV,AC3,SIGMA,PI,PI2,PI4,PI8,PI43/6.6726D-8,7.5595D-5,
     & 5.66961D-5,3.1415926536D0,6.283185307 2D0,12.56637061 44D0,
     & 25.1327412288D0,4.1887902048D0 /
      DATA ZERO,ONE,TWO,THRE,FOR,TEN,AHF,QRT  /
     &      0.0D0,1.0D0,2.0D0,3.0D0,4.0D0,10.0D0,
     &      0.5D0,0.25D0      /
      END
      SUBROUTINE NEXTR(I)
      IMPLICIT REAL*8(A-H,O-Z)
C
C        RETIURNS THE VALUE OF THE ZONES LOWER RADIUS
C
      COMMON/PHYPAR/ RP(60),TP(60),VP(60),CV(60),DKDR(60),DKDT(60),
     &               DM1(60),GKAP(60),DM2(60),GM(60),RPPR(60)
      COMMON/BLK1/   IRAD,NFLAG,IB
      COMMON/BLK8/   GRAV,AC3,SIGMA,PI,PI2,PI4,PI8,PI43
      DATA ONTH/0.3333333333333333D0/
      RADIUS = RP(I+1)**3 - DM1(I)*VP(I)/PI43
```

```
      IF( RADIUS .LE. 0.0D0 ) WRITE(11,1000) I
      IF( RADIUS .LE. 0.0D0 ) RADIUS = 1.0D-9*RP(IR+1)**3
      RP(I) = RADIUS**ONTH
      RETURN
      ENTRY ICCRER(I)
C
C          ENTER HERE FOR OUTER ZONE RADIUS
C
      RP(I+1) = (RP(I)**3+DM1(I)*VP(I)/PI43)**ONTH
      RETURN
1000  FORMAT(5H ZONE,I4,22H HAS A NEGATIVE RADIUS)
      END
      SUBROUTINE RADLUM(I,IOPT)
C
C     ******************************************************************
C      RADLUM CALCULATES THE RADIATIVE LUMINOSITY AND ROSSELAND OPACITIE
C     ******************************************************************
C
      IMPLICIT REAL*8(A-H,O-Z)
      COMMON/PHYPAR/ RP(60),TP(60),VP(60),CV(60),DKDR(60),DKDT(60),
     &      DM1(60),AKAP(60),DM(60),GM(60),RPPR(60)
      COMMON/OBSERV/ TEFF,RLUMGV,TOTMAS,RPHOTC,CORRAD
      COMMON/BLK1/   IRAD,NFLAG,IR
      COMMON/BLK17/  PFI,DTP,DVP,TTAU
      COMMON/BLK37/  RATIO(60),TP4(60),SPA1(480)
      COMMON/BLK8/   GRAV,AC3,SIGMA,PI,PI2,PI4,PI8,PI43
      COMMON/CONST/  ZERO,ONE,TWO,THRE,FOR,TEN,AHF,QRT
      DATA TOTH/0.666666666666667D0/
      VPI = VP(I)
      TPI = TP(I)
C  GET OPACITY ONLY IF IOPT=-1
      IF( NFLAG .NE. 3 ) GOTO 5
C
C
C      USE STELLINGWERF ANALYTIC OPACITIES
      KUSE = 4
      IF( IOPT .EQ. 1 ) KUSE = 1
      CALL NEOS(TPI,VPI,DUM1,DUM2,DUM3,DUM4,DUM5,DUM6,DUM7,DUM8,
     &      DUM9,AKAPI,DVR,DTR,F,E,KUSE)
      GOTO 10
C
C     TABULAR OPACITIES
C
   5  CALL INTERP(TPI,VPI,BB,AKAPI,DTR,DVR,IOPT,-1)
  10  CONTINUE
      AKAP(I) = AKAPI
      TP4(I)  = TPI**4
      IF(IOPT .EQ. -1) RETURN
```

```
      IF( IOPT .EQ. 0 ) GOTO 260
      DKDR(I)  = DVR
      DKDT(I)  = DTR
      RETURN
C
C       RATIO:=AC/3*(4PI*R(EFF)**2)**2/(KAPPA(EFF)*MASS(EFF))
C      SUCH THAT RATIO*(TP(I)**4-TP(I+1)**4)  = LUM.(I)
C        IF(IRAD=0)  SEE STOBIE MNRAS 144(1969)485
C        IF(IRAD=1)  SEE STELLINGWERF AP. J. 195(441)1975
C
 250  CONTINUE
C3.19       TAU = AKAPI*DM1(IR)/(FOR*PI4*RP(IR+1)**2)
      TAU = AKAPI*DM1(IR)/(PI4*RP(IR+1)**2)
      TTAU = TEFF*(.75D0*(TAU+TOTH))**QRT
      RETURN
 260  W   = TP4(I)
      IF( I .EQ. IR ) GOTO 250
      WP = TP4(I+1)
      IF( IRAD .EQ. 1 ) GOTO 270
      RPLUS =  QRT*(RP(I+2)+THRE*RP(I+1))
      RMIN =   QRT*(RP(I)+THRE*RP(I+1))
      RMIN=PI4*RMIN**2
      RPLUS=PI4*RPLUS**2
      RMIN = RMIN**2*W/(AKAP(I)*DM1(I))
      RPLUS =  RPLUS**2*WP/(AKAP(I+1)*DM1(I+1))
      RATIO(I) = AC3*(RPLUS+RMIN)/(W+WP)
      RETURN
 270  XLNW=DLOG(WP/W)
      XLNK=DLOG(AKAP(I+1)/AKAPI)
      C1 =-(PI4*RP(I+1)**2)**2*AC3/DM(I+1)
      C2 = WP/AKAP(I+1)  - W/AKAPI
      C3=C2/(ONE-XLNK/XLNW)
      RLUMP=C1*C3
      RATIO(I)=RLUMP/(W - WP)
      RETURN
      END
      SUBROUTINE STATE(I,IOPT)
C
C
C     ***************************************************************
C           STATE CALCULATES THE EQUATION OF STATE
C     ***************************************************************
C           REQUIRES THE ROUTINE NEOS FOR THE ANALYTIC EOS
C           REQUIRES THE ROUTINE INTERP FOR THE TABULAR EOS
C
C*****************************************************************
      IMPLICIT REAL*8(A-H,O-Z)
      COMMON/PHYPAR/ RP(60),TP(60),VP(60),CV(60),DKDR(60),DKDT(60),
```

```
     & DM1(60),AKAP(60),DM2(60),GM(60),RPPR(60)
      COMMON/BLK4/    PRESF(60),G1(60),G3M1(60),ENTPRY(60)
      COMMON/BLK17/   PFI,DTP,DVP,ITAU
      COMMON/SCRTCH/  CHR(60),CHIT(60),CP(60),DEL(60),DELAD(60)
      COMMON/THERMO/  R,A1,BK,AVAGD,AD3
      COMMON/CONST/   ZERO,ONE,TWO,THRE,FOR,TEN,AHF,QRT
      COMMON/BLK1/    IRAD,NFLAG,IR
      TPI = TP(I)
      VPI = VP(I)
      KUSE = 5
      IF( IOPT .EQ. 1 ) KUSE = 2
      IF( NFLAG .NE. 3 ) GOTO 10
C
CC          THE ANALYTIC EOS
C
      CALL NEOS(TPI,VPI,PFI,DVP,DTP,D4,DVE,DTE,BP,DBDV,
     & DBDT,D1,D2,D3,D6,ENT,KUSE)
      PRESF(I) = PFI
      IF( IOPT .NE. 1 ) RETURN
      DBDV = DEDV*VPI/BP
      DBDT = DEDT*TPI/BP
      BETAI = CNE-AD3*TPI**4/PFI
      CV(I) = DTE
C
CC          FIND THE ADIABATIC EXPONENTS
C
      G3M1(I) = DTP*VPI/DTE
      G1(I) = (TPI*DTP*G3M1(I)-VPI*DVP)/PFI
      DELAD(I) = G3M1(I)/G1(I)
C           EQUATION 27.28 COX & GIULI
      CHITI = FOR-THRE*BETAI+BETAI*DBDT
      CHIRHO = BETAI*(CNE-DBDV)
      CHR(I) = CHIRHO
      CHIT(I) = CHITI
      QI = CHITI/CHIRHO
      CON = PFI*VPI/TPI
C           EQUATION 9.86 COX & GIULI
      CP(I) = DTE+CON*CHITI*QI
      ENTPRY(I) = ENT
      RETURN
   10 CONTINUE
C
CC          TABULAR EOS
C
      CALL INTERP(TPI,VPI,BP,DTE,DBDT,DBDV,IOPT,1)
      PFI = BP*TPI/VPI*8.6167D8
      PFI = PFI+AD3*TPI**4
      PRESF(I) = PFI
```

```
      DVP = PFI/VPI*(DBDV-ONE)
      DTP = PFI/TPI*(DBDT+ONE)
      IF( IOPT .NE. 1 ) RETURN
      BETAI = CNE-AD3*TPI**4/PFI
C
CC       FIND THE ADIABATIC EXPONENTS
C
      CON = PFI*VPI/TPI
      CHITI = FOR+BETAI*(DBDT-THRE)
      CHRHO = BETAI*(ONE-DBDV)
      CHIT(I) = CHITI
      CHR(I) = CHRHO
      QI = CHITI/CHRHO
      CV(I) = 1.5D0*CON*(8.D0+BETAI*(DBDT-7.D0))+8.6167D8*DTE
      CP(I) = CV(I)+CON*CHITI*QI
      G3M1(I) = CON*CHITI/CV(I)
      G1(I)   = CHITI*G3M1(I)+CHRHO
      DELAD(I) = G3M1(I)/G1(I)
      RETURN
      END
      FUNCTION RATMAS(MASOPT,N)
      IMPLICIT REAL*8(A-H,O-Z)
C
C      GIVES THREE DIFFERENT WAYS OF ZONING A STAR
C       MASOPT:= 0   READ IN THE MASSES
C                1   MASS(I)=MASS(I+1)*B
C                2   MASS(I)=MASS(I+1)+B
C
C          A BRIEF DISCUSSION OF THE DIFFERENT MASSES USED.
C             RM = TOTAL MASS BELOW RADIUS R(OR BELOW INTERFACE I)
C             DM1 = ZONE MASS, FOR AN INTERFACE CENTERED QUANTITY
C          SUCH AS THE RADIUS D(RADIUS)/D(MASS)=(R(I+1)-R(I))/DM1(I)
C          AND GIVES A ZONE CENTERED QUANTITY.
C             DM2 = INTERFACE MASS = (DM1(I+1)+DM1(I))/2. FOR A ZONE
C          CENTERED QUANTITY SUCH AS TEMPERATURE D(T)/D(M) =
C          (T(I+1)-T(I))/DM2(I) AND GIVES AN INTERFACE CENTERED VALUE.
C                                                          12/30/82 WDP
C
      COMMON/PHYPAR/ RP(60),TP(60),VP(60),CV(60),DKDR(60),DKDT(60),
     &               DM1(60),AKAP(60),DM2(60),RM(60),RPPR(60)
      COMMON/CONST/  ZERO,ONE,TWO,THRE,FOR,TEN,AHF,QRT
      COMMON/TAB/    ENVMAS,CORMAS,UMASS,RLUMX
      DATA PREC/1.D-12/
      PN = DFLOAT(N)
C
CC    BEGIN THE CALCULATIONS
C
```

```
      BETA = 1.3D0
      GOTO (100,200,300),MASOPT
      READ(9,1000)  (DM1(I),I=1,N)
      BETA = ZERO
      GOTO 300
  100 CONTINUE
      ETA = (ENVMAS-UMASS+DM1(N))/DM1(N)
      BETA = THRE*QRT
      IC = 0
  110 FB   = (ONE-BETA**N)/(ONE-BETA)
      IC = IC+1
      IF( IC .GT. 30 ) GOTO 400
      DFDB = (FB-FN*BETA**(N-1))/(ONE-BETA)
      DBET = (FB-ETA)/DFDB
      IF( DABS(DBET) .GT. 0.1D0*BETA ) DBET=0.1D0*DSIGN(BETA,DBET)
      BETA = BETA-DBET
      IF( DABS(DBET)/BETA .GT. PREC ) GOTO 110
      WRITE(11,1000) BETA,ETA
      GOTO 300
  200 CONTINUE
      ETA = (ENVMAS-UMASS+DM1(N))/DM1(N)
      BETA = TWO*(ETA-FN)/(FN*(FN-ONE))*DM1(N)
      DO 220 I=2,N
           J = N-I+1
           DM1(J) = DM1(J+1)+BETA
  220 CONTINUE
C
CC          RETURN TO CODE
C
  300 CONTINUE
      RATMAS = BETA
      RETURN
  400 WRITE(6,4000)
      STOP
 4000 FORMAT(25H NO CONVERGENCE IN MASZON  )
 1000 FORMAT(1P4D18.10)
      END
```

FIGURE B-1

VARIABLE ASSIGNMENT IN THE MASS MESH

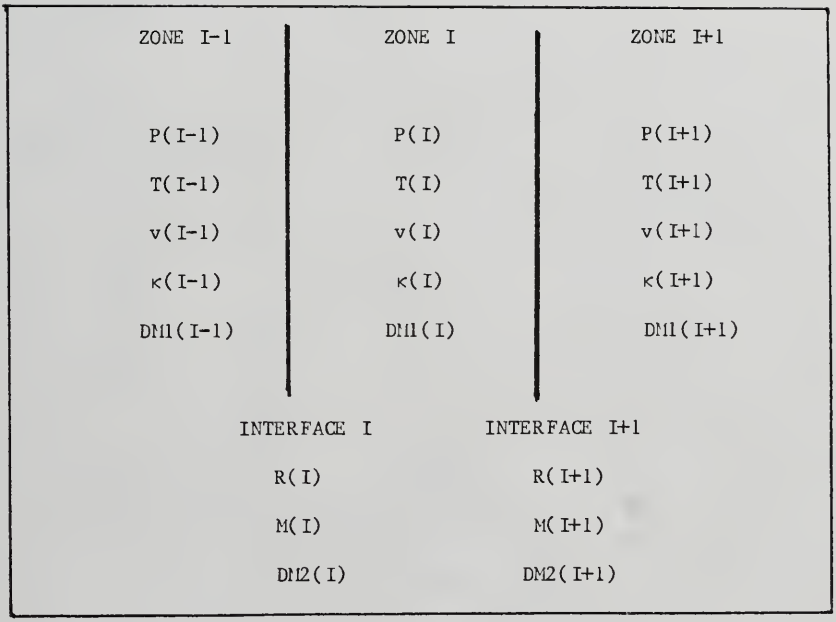

BIBIOGRAPHY

Aizenman, M. L. and Cox, J. P. 1975, Astrophysical Journal, **195**, 175.

Baker, N. H. and Kippenhahn, R. 1962, Zeitschrift fur Astrophysik, **54**, 114.

Baker, N. H. and Gough, D. O. 1979, Astrophysical Journal,**234**, 232.

Boyce, W. E. and DiPrima, R. C. 1969, Elementary Differential Equations and Boundary Value Problems (New York: John Wiley and Sons).

Buchler, J. R. 1978, in Nonlinear Equations in Physics and Mathematics ed. A. O. Barut and F. Calgero (Dordrecht: Reidel), p. 85.

Buchler, J. R. 1983, Astronomy and Astrophysics, **118**, 163.

Buchler, J.R. and Perdang, J. 1979, International Journal of Quantum Chemistry, Symposium **13**, 181.

Buchler, J.R. and Regev, O. 1982a, Astronomy and Astrophysics, **114**, 188.

Buchler, J. R. and Regev, O. 1982b, Astrophysical Journal, **261**, 301.

Butkov, E. 1968, Mathematical Physics (Reading, Massachusetts: Addison Wesley).

Castor, J. I. 1971, Astrophysical Journal, **166**, 109.

Chandrasekhar, S. 1967, An Introduction to the Study of Stellar Structure (New York: Dover Publications).

Christy, R. P. 1964, Reviews of Modern Physics, **36**, 555.

Christy, R. P. 1966, Astrophysical Journal, **144**, 108.

Clayton, D. D. 1968, Principles of Stellar Evolution and Nucleosynthesis (New York: McGraw-Hill).

Cole, J. D. 1968, Perturbation Methods in Applied Mathematics (Waltham, Massachusetts: Blaisdell).

Cox, A. N. 1980a, Annual Reviews of Astronomy and Astrophysics, **18**, 15.

Cox, A. N. 1980b, private communication.

Cox, A. N. and Tabor J. E. 1976, Astrophysical Journal Supplement, **31**, 271.

Cox, A. N., Brownlee, R. R. and Eilers, D. D. 1966, Astrophysical Journal, **144**, 1024.

Cox, J. P. 1958, Astrophysical Journal, **127**, 194.

Cox, J. P. 1960, Astrophysical Journal, **132**, 594.

Cox, J. P. 1980, Theory of Stellar Pulsations (Princeton, New Jersey: Princeton University Press).

Cox, J. P. and Giuli, R. T. 1968, Principles of Stellar Structure (New York: Gordon and Breach).

Cox, J. P., and Whitney, C. A. 1958, Astrophysical Journal, **127**, 561.

Davydov, A. S. 1965, Quantum Mechanics, 2nd edition, trans. D. ter Haar (Oxford, England: Pergamon Press Ltd.).

Gabriel, M. 1972, Astronomy and Astrophysics, **18**, 242.

Hansen, C.J. 1978, Annual Reviews of Astronomy and Astrophysics, **16**, 15.

Henyey, L. G. and Ulrich, R. K. 1972, Astrophysical Journal, **173**, 109.

Iben, I., Jr. 1965, Astrophysical Journal, **141**, 993.

King, D. S. 1980, Space Science Reviews, **27**, 519.

King, D. S., Cox, J. P., Eilers, D. D. and Davey, W. P. 1964, Astrophysical Journal, **182**, 859.

Kuzmak, G. E. 1959, Journal of Applied Mathematics and Mechanics, **23**, 730.

Ledoux, P. 1965, in Stellar Structure, ed. L. H. Aller and D. B. McLaughlin (Chicago: University of Chicago Press), p. 499.

Ledoux, P. and Pekeris, C. L. 1941, Astrophysical Journal, **94**, 124.

Ledoux, P. and Walraven, Th. 1958, Handbuch der Physik, **51**, 353.

Lesh, J. R. and Aizenman, M. L. 1978, Annual Reviews of Astronomy and Astrophysics, **34**, 203.

Lucy, L. B. 1976, Astrophysical Journal, **206**, 499.

Morse, P. M. and Feshbach, H. 1953, Methods of Theoretical Physics (New York: McGraw-Hill).

Novotny, E. 1973, Introduction to Stellar Atmospheres and Interiors (New York: Oxford University Press).

Osaki, Y. 1982, Proceedings of Pulsations in Classical and Cataclysmic Variable Stars, ed. C. J. Hansen and J. P. Cox (Boulder: University of Colorado and National Bureau of Standards), p. 303.

Pesnell, W. D. 1981, talk presented at Los Alamos National Laboratory, August 1981.

Pesnell, W. D. and Buchler, J. R. 1983, in preparation.

Pesnell, W. D., Regev, O. and Buchler, J. R. 1982, Proceedings of Pulsations in Classical and Cataclysmic Variable Stars, ed. C. J. Hansen and J. P. Cox (Boulder: University of Colorado and National Bureau of Standards), p. 216.

Ralston, A. 1967, Mathematical Methods for Digital Computers (New York: Wiley).

Regev, O. and Buchler, J. R. 1981, Astrophysical Journal, **250**, 769.

Saio, H. and Cox, J. P. 1980, Astrophysical Journal, **236**, 549.

Saio, H. and Wheeler, C. J. 1982, Proceedings of Pulsations in Classical and Cataclysmic Variable Stars, ed. C. J. Hansen and J. P. Cox (Boulder: University of Colorado and National Bureau of Standards), p. 327.

Saio, H., Winget, D. E. and Robinson, E. L. 1983, Astrophysical Journal, **265**, 982.

Shibahashi, H. and Osaki, Y. 1981, Publications of the Astronomical Society of Japan, **33**, 427.

Simon, N. R., Cox, A. N. and Hodson, S. W. 1980, Astrophysical Journal, **237**, 550.

Smith, B. T., Boyle, J. M., Dongarra, J. J., Garbow, B. S., Ikebe, Y., Klema, V. C. and Moler, C. B. 1976, Eispack Guide, 2nd edition (Berlin: Springer-Verlag).

Starrfield, S. G., Cox, A. N. and Hodson, S. W. 1980, Space Science Reviews, **27**, 621.

Starrfield, S. G. ,Cox, A. N., Hodson, S. W. and Pesnell, W. D. 1982, Proceedings of Pulsations in Classical and Cataclysmic Variable Stars, ed. C. J. Hansen and J. P. Cox (Boulder: University of Colorado and National Bureau of Standards), p. 78.

Starrfield, S. G., Cox, A. N., Hodson, S. W. and Pesnell, W. D. 1983, Astrophysical Journal, **268**, L27.

Stellingwerf, R. F. 1975a, Astrophysical Journal, **195**, 441.

Stellingwerf, R. F. 1975b, Astrophysical Journal, **195**, 705.

Stellingwerf, R. F. 1978, Astronomical Journal, **83**, 1184.

Stobie, R. S. 1969, Monthly Notices of the Royal Astronomical Society, **144**, 485.

Wilkinson, J. H. 1965, The Algebraic Eigenvalue Problem (Oxford, England: Clarendon Press).

Winget, D. E., Saio, H. and Robinson, E. L. 1982, Proceedings of Pulsations in Classical and Cataclysmic Variable Stars, ed. C. J. Hansen and J. P. Cox (Boulder: University of Colorado and National Bureau of Standards), p. 68.

Wood, P. R. 1976, Monthly Notices of the Royal Astronomical Society, **174**, 531.

Zel'dovich, Ya. B. and Razier, Yu. P. 1966, Physics of Shock Waves and High-Temperature Hydrodynamic Phenomena, ed. W. D. Hayes and R. F. Probstein (New York: Academic Press).

Zhevakin, S. A. 1963, Annual Reviews of Astronomy and Astrophysics, **1**, 367.

BIOGRAPHICAL SKETCH

The author was born on January 19, 1957, in Wilmington, Delaware. He attended Claymont High School and entered the University of Delaware in September, 1974, receiving a Bachelor of Science in physics in June, 1978. During this time, he held an Undergraduate Summer Research Grant from the National Science Foundation under the supervision of Dr. Harry Shipman.

In September, 1978, he entered graduate school at the University of Florida in the Department of Physics and began working under the direction of Dr. J. Robert Buchler. For three summers, 1980, 1981 and 1982, he was employed as a Summer Graduate Research Assistant at Los Alamos National Laboratory, where he worked with Arthur N. Cox. During his tenure at Florida, he has held a one-year research assistantship and taught undergraduate physics for four years.

I certify that I have read this study and that in my opinion it conforms to acceptable standards of scholarly presentation and is fully adequate, in scope and quality, as a dissertation for the degree of Doctor of Philosophy.

J. Robert Buchler, Chairman
Professor of Physics

I certify that I have read this study and that in my opinion it conforms to acceptable standards of scholarly presentation and is fully adequate, in scope and quality, as a dissertation for the degree of Doctor of Philosophy.

Thomas L. Bailey
Professor of Physics

I certify that I have read this study and that in my opinion it conforms to acceptable standards of scholarly presentation and is fully adequate, in scope and quality, as a dissertation for the degree of Doctor of Philosophy.

James W. Dufty
Professor of Physics

I certify that I have read this study and that in my opinion it conforms to acceptable standards of scholarly presentation and is fully adequate, in scope and quality, as a dissertation for the degree of Doctor of Philosophy.

James H. Hunter
Professor of Astronomy

I certify that I have read this study and that in my opinion it conforms to acceptable standards of scholarly presentation and is fully adequate, in scope and quality, as a dissertation for the degree of Doctor of Philosophy.

Pradeep Kumar
Assistant Professor of Physics

This dissertation was submitted to the Graduate Faculty of the Department of Physics in the College of Liberal Arts and Sciences and to the Graduate School, and was accepted as partial fulfillment of the requirements for the Doctor of Philosophy.

August 1983

Dean for Graduate Studies
and Research